

**Development of Alumina Modified Laterite Material for Fluoride
Removal from Contaminated Water**

By

KNUST

Juliet Osei

(BSc. Chemistry; M.Phil. Environmental Sciences)

**A Thesis submitted to the Department of Materials Engineering,
Kwame University of Science and Technology in partial fulfillment of the
requirements for the degree
of**

**DOCTOR OF PHILOSOPHY
(MATERIALS ENGINEERING)**

College of Engineering

©Department of Materials Engineering

August, 2016

CERTIFICATION

I hereby declare that this submission is my own work towards the PhD and that, to the best of my knowledge, it contains neither material previously published by another person nor material which has been accepted for the award of any other degree of the University, except where due acknowledgement has been made in the text.

Juliet Osei (PG7687512)
Student

.....

Signature

Date

Certified by:

Prof. F.W.Y. Momade

Supervisor

.....

Signature

Date

Certified by:

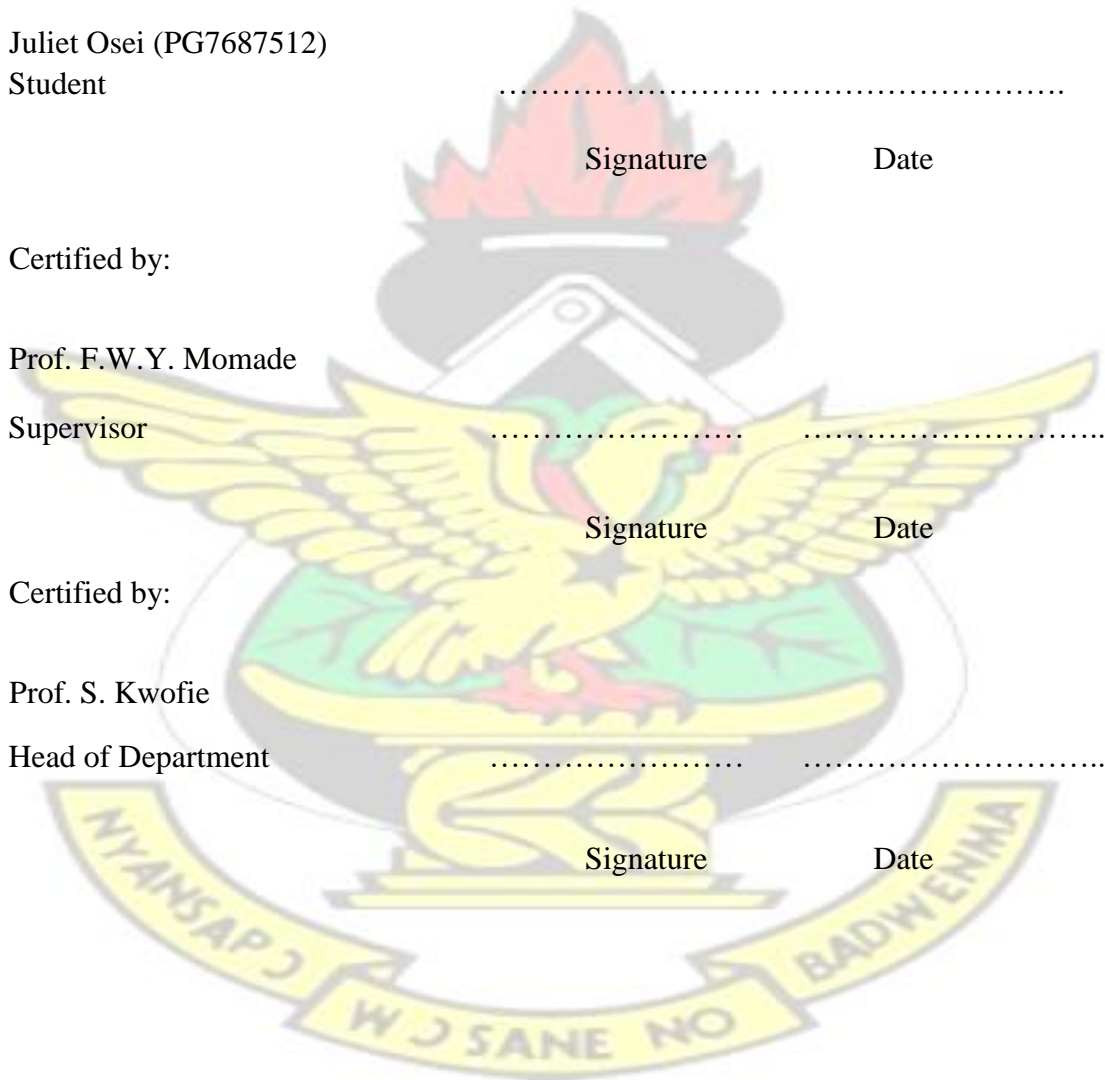
Prof. S. Kwofie

Head of Department

.....

Signature

Date



ABSTRACT

Fluoride in groundwater is a threat to the provision of potable water to our rural communities because continuous consumption of water contaminated with fluoride could lead to dental fluorosis or even in extreme cases, skeletal fluorosis. Many fluoride removal techniques have been suggested but most of them have been found not to be practical and sustainable in Ghana as they are either expensive or need highly skilled personnel to operate. The need for a local adsorbent which is less expensive and effective for fluoride removal is of much relevance. Laterite has been identified as a local adsorbent which is readily available and not expensive. However, there have been debates among researchers about the effectiveness of laterite to remove fluoride. This study investigated the characteristics of three (3) laterites from three locations of the Upper East Region for fluoride removal. These areas are Agamolga, Balungu and Dua. Chemical and mineralogical analyses performed using X-Ray Fluorescence (XRF) and X-Ray Diffraction (XRD) methods showed varying amounts of iron oxide/hydroxide (goethite/hematite), silica and kaolinite. Scanning Electron Microscopy (SEM) combined with Energy Dispersive X-ray (EDX) showed that the minerals are intimately associated. Isoelectric Point (IEP) value was influenced by the mineral composition with the larger IEP value corresponding to higher iron oxide/hydroxide content.

The study measured the responses of the different laterites to fluoride uptake under different conditions of pH, temperature, particle size of adsorbent and initial concentration of fluoride solution. The responses showed that Agamolga and Balungu laterites could remove fluoride better than Dua laterite mainly due to the chemical and mineralogical constituents of these two laterites as compared to Dua laterite which has

high silica content. To improve the adsorption capacity of the laterite for fluoride uptake, an alumina modified laterite (AML) was developed using Balungu laterite. The effect of treatment temperature and application to different conditions of fluoride uptake was investigated including adsorbent dosage, initial fluoride concentrations, solution pH and fluoride uptake in the presence of other competing anions. The response of AML to the different experimental conditions shows that the material is capable of removing fluoride to a level below the WHO recommended limit of 1.5 mg/L. At a dosage of 4% solids, AML could remove fluoride from 10 ± 0.2 to 0.42 mg/L without any pH adjustment within 35 minutes. The results indicated that the adsorption characteristics of AML were not significantly affected in the pH range of 6-9 and this means pH adjustment of the raw water is unnecessary. The results also showed that there was an improvement on the adsorption capacity as the raw laterite assumed an adsorption capacity of 0.55 mg/g whereas the AML material assumed a value of 0.69 mg/g. The results also showed little or no significant change in fluoride adsorption by AML in the presence of other competing ions such as chloride, sulphate, phosphate, bicarbonate and nitrates.

TABLE OF CONTENT

CERTIFICATION.....	ii
ABSTRACT	iii
TABLE OF CONTENT	iv
LIST OF TABLES.....	x
LIST OF FIGURES.....	xi
LIST OF ABBREVIATIONS	xii
ACKNOWLEDGEMENTS	xiii

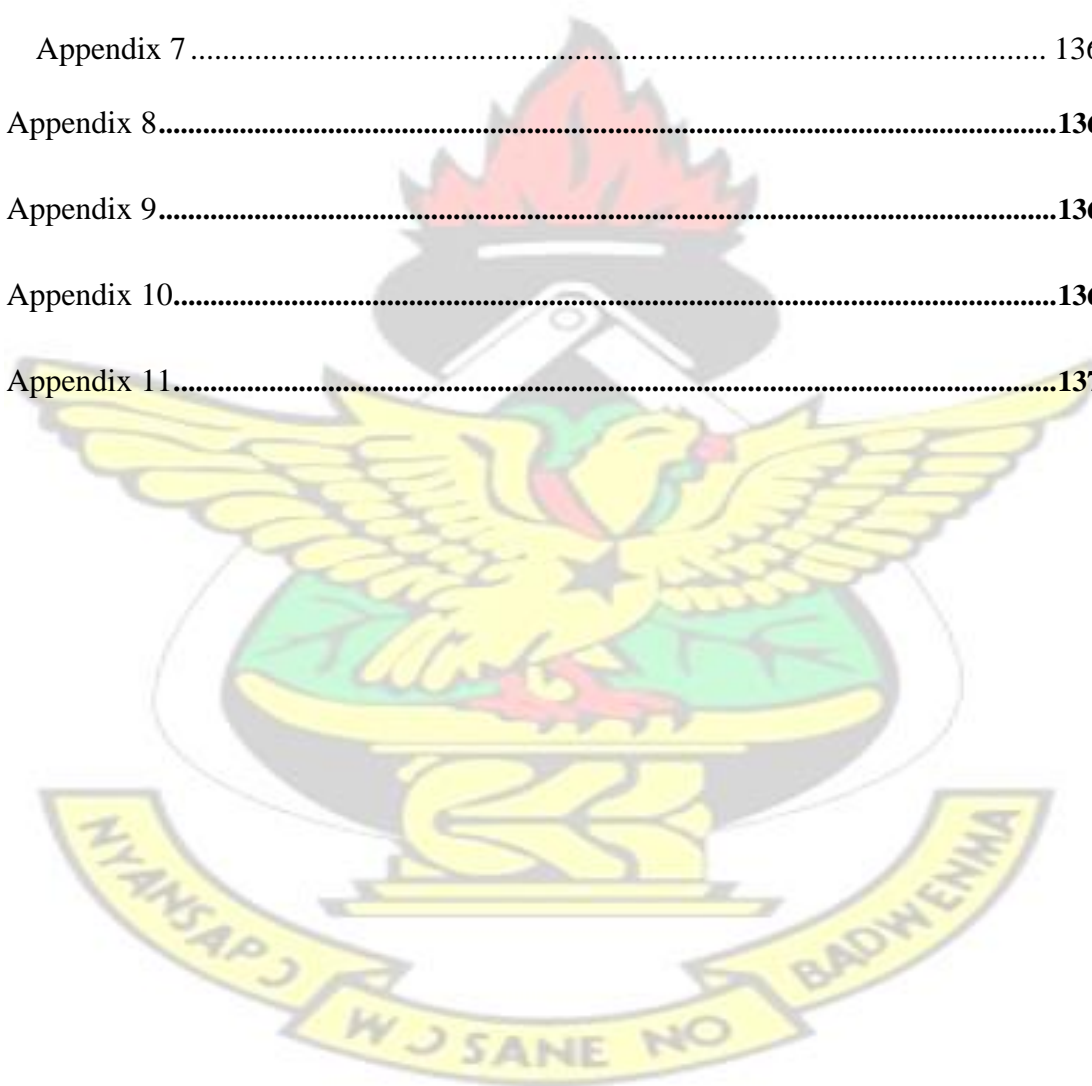
DEDICATION	xiv
CHAPTER ONE	1
INTRODUCTION	1
1.1 Background	1
1.2 Fluoride-contaminated groundwater in Ghana.....	2
1.3 Defluoridation techniques	5
1.4 Statement of problem	6
1.5 Objectives of the study.....	8
1.6 Hypothesis.....	9
1.7 Significance of the study.....	9
1.8 Scope.....	9
CHAPTER TWO.....	11
LITERATURE REVIEW	11
2.1 Introduction to chapter	11
2.2 Geochemistry and environmental occurrence of fluoride.....	11
2.2.1 <i>Distribution and sources of fluoride groundwater</i>	12
2.2.2 <i>Occurrence of fluoride in groundwater</i>	13
2.3 Fluoride and human health.....	16
2.3.1 <i>Fluorosis</i>	17
2.3.2 <i>Dental fluorosis</i>	18
2.3.3 <i>Skeletal fluorosis</i>	20
2.4 Management of fluoride-containing drinking water using defluoridation techniques	21
2.4.1 <i>Defluoridation of water using coagulation-precipitation method</i>	21
2.4.2 <i>Defluoridation of water by ion exchange method</i>	23
2.4.3 <i>Defluoridation of water using membrane-based processes</i>	24
2.4.4 <i>Defluoridation of water using adsorption technique</i>	25

2.4.4.1 Activated Alumina (AA).....	27
2.4.4.2 Ceramic adsorbent	30
2.4.4.3 Crushed limestone.....	30
2.4.4.4 Hydrous ferric oxide (HFO).....	31
2.4.4.5 Synthetic hydrated iron (III)-aluminum (III)-chromium ternary mixed oxide (HIACMO).....	31
2.4.4.6 Bone char	32
2.4.5 Water defluoridation using clay adsorption techniques.....	32
2.5 Laterite and its use as adsorbent for fluoride removal.....	35
2.5.1 Laterite as a geomaterial	35
2.5.2 Laterite definition and classification.....	37
2.5.3 Chemical and mineralogical character of laterite	38
2.5.4 Use of laterite in water treatment studies.....	39
2.5.5 Modification of laterite for use in water treatment	40
2.6 Adsorption mechanism and kinetic considerations.....	41
2.6.1 Adsorption models/isotherms	41
2.6.2 Limitations of the Freundlich and Langmuir models	43
2.6.3 Sorption dynamics.....	44
2.6.3.1 Reaction-based models	44
2.6.3.2 Diffusion models.....	45
2.6.4 Mechanism for fluoride uptake.....	46
2.7 Analytical procedures for the determination of fluoride concentration in solutions	47
2.8 The role of Total Ion Solution Adjustment Buffer (TISAB) solutions in fluoride determination	47
CHAPTER THREE.....	48
MATERIALS AND METHODS	48
3.1 Materials.....	48
3.1.1 Selection of laterite and sample preparation	49
3.1.2 Alumina samples	51
3.2 METHODS	52
3.2.1 Characterization of laterite samples	52
3.2.1.1 XRF analysis.....	52

3.2.1.2 XRD analysis	52
3.2.1.3 SEM analysis	53
3.2.1.4 Electrophoretic studies	53
3.2.2 Heat treatment.....	54
3.2.3 Preparation of fluoride solution.....	54
3.2.4 Preparation of TISAB.....	54
3.2.5 Analysis of fluoride solutions	55
3.2.6 Adsorption tests with laterite.....	56
3.3 Alumina modified laterite (AML) material.....	56
3.3.1 Preparation of AML.....	56
3.3.2 Characterization of AML	57
3.3.3 Batch adsorption studies with AML	57
3.3.4 Competitive uptake of anions experiments	58
CHAPTER FOUR	59
RESULTS	59
4.1 Tests with laterite materials	59
4.1.1 Chemical characterization of raw laterite samples.....	59
4.1.2 Phase/mineralogical composition of the raw laterite samples.....	63
4.1.3 Effect of particle size on fluoride uptake by Balungu laterite material	65
4.1.4 Adsorption tests with the raw and laterite heat-treated at 400°C	65
4.1.5 Effect of initial pH of solution on fluoride uptake by laterites heat-treated at 400°C	66
4.1.6 Contact time and initial fluoride concentration	71
4.2 Tests with alumina modified laterite (AML)	71
4.2.1 Micro-structural characterisation of AML.....	71
4.2.2 Adsorption responses of AML material treated at various temperatures.....	72
4.2.3 Fluoride adsorption at different laterite-alumina ratios	73
4.2.4 Fluoride adsorption at various initial solution pH	73
4.2.5 Effect of sorbent dosage and initial fluoride concentration	75
4.2.6 Effect of initial fluoride concentration on fluoride adsorption by AML.....	75
4.2.7 Adsorption in the presence of competing anions.....	76
CHAPTER FIVE	77

DISCUSSION.....	77
5.1 Characterization of laterite	77
5.1.1 Chemical characteristics of laterite	77
5.1.2 Mineralogical characteristics	78
5.1.3 SEM analysis.....	79
5.1.4 Implications of characteristics of laterite and its use as an adsorbent for fluoride removal	80
5.1.5 Effect of heat-treatment on the mineralogy of laterites.....	80
5.2 Fluoride adsorption tests with laterite	82
5.2.1 Fluoride uptake by raw and heat-treated laterites.....	82
5.2.2 Solution pH during fluoride adsorption	84
5.2.4 Effect of particle size on fluoride uptake.....	89
5.2.4 Equilibrium adsorption by Balungu laterite at different initial fluoride concentrations	90
5.3 Mechanism and kinetics considerations.....	91
5.4 Micro-structural Characterization of AML.....	96
5.5 Fluoride adsorption tests	99
5.5.1 Heat-treatment temperature in preparation of AML and fluoride adsorption	99
5.5.2 AML composition and fluoride adsorption.....	101
5.5.3 Effect of solution pH on fluoride adsorption by AML.....	102
5.5.4 Adsorbent dosage and fluoride uptake by AML	104
5.5.5 Initial fluoride concentration and fluoride uptake by AML.....	105
5.6 Equilibration isotherms and sorption kinetics.....	106
5.7 Fluoride adsorption in the presence of co-existing anions.....	111
CHAPTER SIX.....	114
SUMMARY, CONCLUSIONS AND RECOMMENDATIONS	114
6.1 Summary	114
6.2 Conclusions	115
6.3 Recommendations	116
REFERENCES	117

Appendix.....	134
Appendix 1	134
Appendix 2	134
Appendix 3	134
Appendix 4	135
Appendix 5	135
Appendix 6	135
Appendix 7	136
Appendix 8.....	136
Appendix 9.....	136
Appendix 10.....	136
Appendix 11.....	137



LIST OF TABLES

Table 2.1: Fluoride levels in different types of rocks (Source: Jha <i>et al.</i> , 2011).	14
Table 2.2: Countries where the fluoride levels in water exceed 1.5mg/L (Fawell <i>et al.</i> , 2006).	18
Table 4.1: Composition of the major elements in the raw laterite samples. .	59
Table 4.2: Composition of minor elements in the raw laterite samples.	60
Table 4.3: Point of zero charge (pH_{pzc}) results of Agamolga, Balungu and Dua laterite.	63
Table 4.4: Effect of particle size of Balungu laterite on fluoride adsorption.	63
Table 4.5: Fluoride uptake by raw and heat treated (HT) laterites at 400°C.	64
Table 4.6: Changes in solution pH during adsorption of fluoride by Agamolga, Balungu and Dua laterites.	64
Table 4.7: Effect of initial pH on fluoride adsorption by Agamolga laterite	65
Table 4.8: pH changes at different time intervals after pH adjustment at varying starting pH by Agamolga laterite	65
Table 4.9: Effect of initial pH on fluoride adsorption by Balungu laterite. ..	65
Table 4.10: Variation of solution pH during adsorption with Balungu laterite after initial pH adjustment.	66
Table 4.11: Effect of initial pH on fluoride adsorption by Dua laterite.	67
Table 4.12: pH at different time intervals after pH adjustment at varying starting pH using Dua laterite.	67
Table 4.13: Amount of fluoride adsorbed by Balungu laterite at different initial fluoride concentrations.	68
Table 4.14 Effect of heat treatment on adsorption efficiency by AML.	69
Table 4.15: Effect of different ratios of alumina modified laterite on fluoride uptake.	70
Table 4.16: Effect of initial pH of fluoride solution on fluoride uptake by AML.	71
Table 4.17: Solution pH during adsorption by AML in acidic and alkaline pH ranges.	71
Table 4.18: Effect of adsorbent dosage on fluoride uptake by AML.	72
Table 4.19: Effect of initial concentration of fluoride solution on fluoride uptake by AML.	72
Table 4.20: Effect of other anions on F ⁻ adsorption by AML.	73

LIST OF FIGURES

Figure 1.1: Spatial distribution of fluoride in groundwater in the Bongo district of the Upper East Region of Ghana (Source; WRC, 2014)	5
Figure 2.1: Severe case of dental fluorosis in Bongo, Ghana (Courtesy of Cumberbatch, 2008).	19
Figure 2.2: A case of dental fluorosis (source: Avishek <i>et al.</i> , 2010).	19
Figure 2.3: A case of children suffering from skeletal fluorosis. (Source; Mjengera & Mkongo, 2003)	21
Figure 3.1: General analytical scheme.	50
Figure 3. 2: A map showing locations (underlined) where laterite samples were collected.	51
Figure 4.1: X-ray diffraction pattern of Agamolga laterite sample.	61
Figure 4.2: X-ray diffraction pattern of Balungu laterite sample.	61
Figure 4.3: X-ray diffraction pattern of Dua laterite sample.	61
Figure 4.4 : SEM image of Agamolga, Balungu and Dua laterite.	62
Figure 4.5: SEM image showing overlay of elements in AML of composition of (a) 10 g laterite plus 1 g alumina and (b) 10 g laterite plus 3 g alumina.	69
Figure 5.1: XRD pattern of the Agamolga, Balungu and Dua laterite samples.	75
Figure 5.2: A comparison of x-ray diffraction peaks of the raw and heat-treated Balungu laterite between $2\theta=20-22$	78
Figure 5.3: Fluoride removal from water by raw and heat-treated (HT) laterite (400°C).	80
Figure 5.4: Change in solution pH during fluoride adsorption by raw and heat-treated (HT) laterites.	81
Figure 5.5: Change in fluoride concentration and solution pH during adsorption at various initial pH media for the heat-treated Balungu laterite (pH6.05* means pH of solution without adding an acid or base).	83
Figure 5.6: Change in fluoride concentration and solution pH during adsorption at various initial pH media for the heat-treated Agamolga laterite (pH6.02* means pH of solution without adding an acid or base).	84
Figure 5.7: Change in fluoride concentration and solution pH during adsorption at various initial pH media for the heat-treated Dua laterite (pH6.13* means pH of solution without adding an acid or base).	85
Figure 5. 8: Effect of particle size of laterite on fluoride removal.	86
Figure 5.9: A plot of fluoride adsorption at different initial concentrations.	

.....	87
Figure 5.10: Langmuir (a) and Freundlich (b) plots of equilibrium adsorption data for Agamolga and Balungu laterites.	90
Figure 5.11: Pseudo-first order plots of adsorption data.	92
Figure 5.12: Pseudo-second-order plots of adsorption data.	93
Figure 5.13: SEM image (a) and EDX spectra (b) of AML (3 g alumina: 10 g laterite) taken at different phases on the surface of the AML.	94
Figure 5.14: Schematics showing AML synthesis.	95
Figure 5.15: SEM image indicating aluminum build-in in the iron oxide surface.	96
Figure 5.16: Effect of heat treatment temperature on adsorption efficiency by AML.	97
Figure 5.17: A plot of adsorption efficiency vs. heat treatment temperature at 20 and 35 minutes contact time.	97
Figure 5.18: Rate of fluoride adsorption by different ratios of AML.	99
Figure 5.19: (a) Effect of initial pH on the adsorption of fluoride and (b) solution pH after adsorption by AML in acidic media.	100
Figure 5.20: (a) Effect of initial pH on the adsorption of fluoride and (b) solution pH after adsorption by AML in basic media.	101
Figure 5.21: Adsorbent dosage vs. percentage of fluoride adsorption by AML (initial concentration of fluoride solution=10 mg/L).	103
Figure 5.22: Fluoride removal by AML at various initial fluoride concentrations.	104
Figure 5.23: Langmuir (a) and Freundlich (b) isotherms of fluoride adsorption by AML at room temperature (adsorbent dosage= 4g/100mL, pH=6±0.2).	105
Figure 5.24: Pseudo-first-order (a) and pseudo-second-order(b) plots of the adsorption data for AML	107
Figure 5.25: A plot of q_t against $t^{1/2}$ for (c_1 -10mg/L) by AML.	108
Figure 5.26: Effect of (a) PO_4^{3-} , NO_3^- , HCO_3^- and (b) Cl^- , SO_4^{2-} in solution on fluoride uptake by AML.	110

LIST OF ABBREVIATIONS

EPA Environmental Protection Agency

FTIR Fourier Transfer Infrared Spectroscopy

AML Alumina Modified Laterite

LOI Loss on Ignition

NGO Non-Governmental Organization

SEM-EDX Scanning Electron Microscopy-Energy Dispersive X-ray Spectroscopy

WHO World Health Organization

XRD X-ray Diffraction

XRF X-ray Fluorescence

KNUST

ACKNOWLEDGEMENTS

I appreciate the able supervision of my supervisor, Prof. F.W.Y. Momade who tirelessly took me through this educational journey. I could not have imagined a better supervisor for my PhD work.

I am very grateful to all the lecturers and staff of Materials Engineering Department, KNUST, especially Dr. A.A. Adjaottor and Mr. Felix Ati for the support they offered to me throughout my study. Your commendations and criticisms pushed me to the limits to achieve excellence.

I am highly indebted to Profs. Patrick Mensah and Samuel Ibekwe of Southern University and AM College for their support to a conference in Oklahoma, USA through US National Science Foundation under NSF-NEXTGENC 3(Grant # HRD 0932300) and NSF-SUIRES (Grant # IIA 1358204) projects. I am very thankful to Ghana Grid Company (GRIDCo) for the financial support I received to do so this

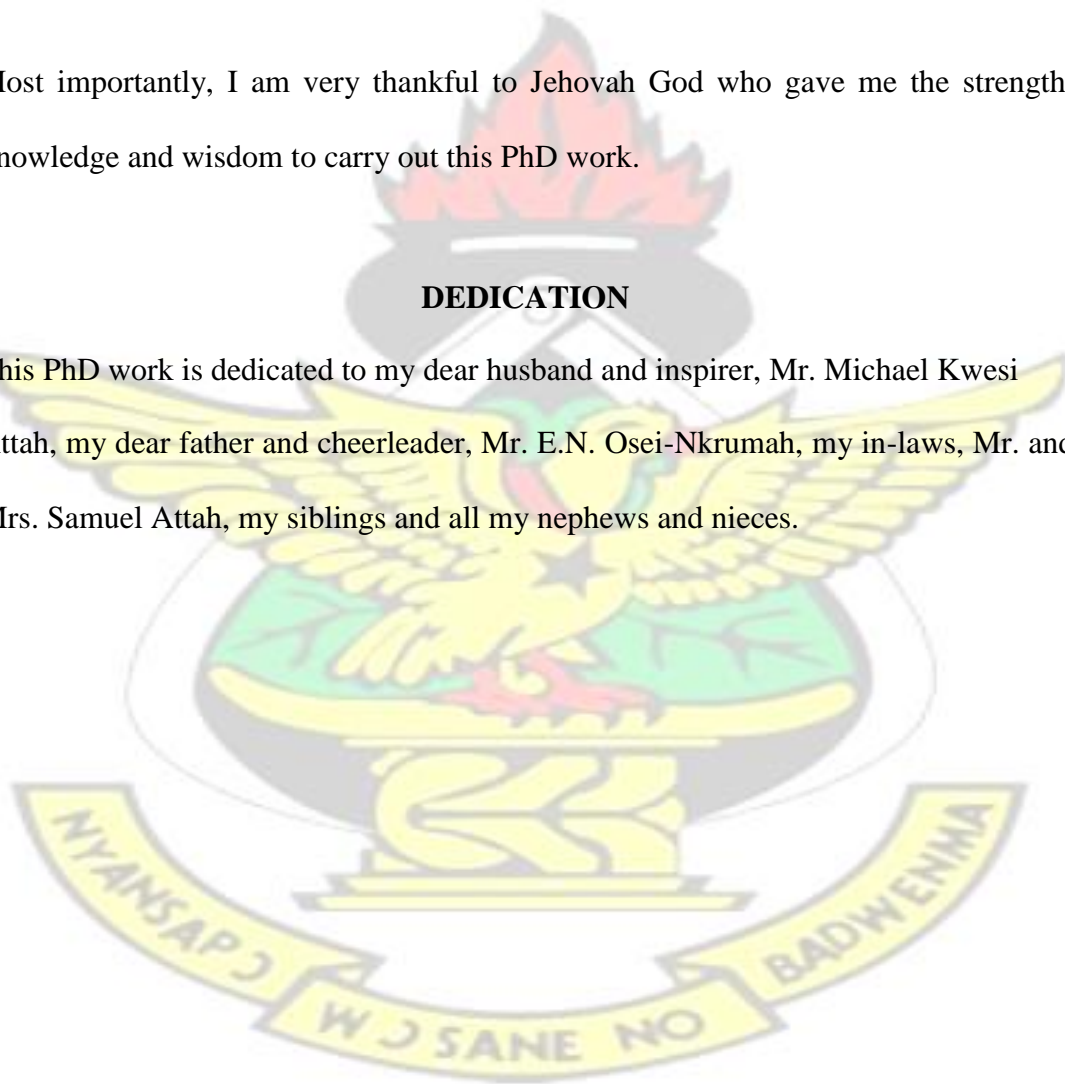
work. I am grateful to Dr. K. Mensah-Darkwah who did some of the SEM analyses for me at North Carolina State University.

As a matter of fact, there are many people whose names are worth mentioning but I cannot forget the help I received from Dr. Adolf Awuah who helped in editing my work. My gratitude to Prof. Shiloh Osae, Prof. Richmond Fianko, Dr. Samuel Afful, Dr. D.K. Adotey and all staff of Ghana Atomic Energy Commission. I appreciate the love and support of my Lab mates at the Inorganic Lab of GAEC.

Most importantly, I am very thankful to Jehovah God who gave me the strength, knowledge and wisdom to carry out this PhD work.

DEDICATION

This PhD work is dedicated to my dear husband and inspirer, Mr. Michael Kwesi Attah, my dear father and cheerleader, Mr. E.N. Osei-Nkrumah, my in-laws, Mr. and Mrs. Samuel Attah, my siblings and all my nephews and nieces.



CHAPTER ONE

INTRODUCTION

1.1 Background

Fluoride contamination of drinking water is a global problem and excess intake of fluoride can be toxic to the human body (Fan *et al.*, 2003). Although very low levels of fluoride in drinking water cause dental caries, widespread occurrence of fluoride above the WHO recommended limit of 1.5 mg/L in water meant for human consumption can cause multidimensional health problems such as dental and skeletal fluorosis (Vuhahula *et al.*, 2009). Waters contaminated with high fluoride concentrations are seen in large and extensive geographical belts. The most severe problems associated with high fluoride waters occur in China (Wang *et al.*, 2002), India (Agarwal *et al.*, 2003), Sri Lanka (Chernet *et al.*, 2002) and Rift Valley countries in Africa (Vuhahula *et al.*, 2009).

Fluoride in groundwater is mostly of geogenic origin resulting from the breakdown of rocks containing fluoride ions. Also, human induced activities such as the application of fertilizers to the soil for vegetable cultivation and liquid wastes from industries add fluoride ions to groundwater. Fluoride levels of between 1.5-5 mg/L in water can result in dental fluorosis whilst fluoride levels between 5-40 mg/L could result in skeletal fluorosis (Fordyce *et al.*, 2007). Dental fluorosis is a development disturbance of dental enamel caused by successive exposures to high concentrations of fluoride during tooth development, leading to enamel with lower mineral content and increased porosity (Alvarez *et al.*, 2009). This condition leads to a permanent discoloration of teeth of affected persons and normally attacks children between 20 and 30 months of age who

are exposed to fluoride. The critical age for development of dental fluorosis is between 1 and 4 years, at 8 years old the child would not be at risk (Alvarez *et al.*, 2009).

High fluoride concentration in water is also linked with skeletal fluorosis (Ghorai & Pant, 2005). For tropical and warmer countries, a level of 1.0 mg/L has been suggested in drinking water (Jha *et al.*, 2011; Biswas *et al.*, 2010; Sujana *et al.*, 2009). People from the tropical countries tend to perspire more due to the warmer climate and therefore tend to drink water frequently to avoid dehydration, hence the fluoride content in the water supply should be reduced to prevent excessive fluoride consumption (Agarwal *et al.*, 1999).

The problem with high fluoride concentrations in water is not only a local one but also a global issue. In countries such as Germany, China, Mexico, India and some parts of Africa, high fluoride concentrations have been reported in their waters (Wakgari *et al.*, 2011; Armienta *et al.*, 2008; Qinghai *et al.*, 2007; Msonda *et al.*, 2007; Gunnar *et al.*, 2005; Queste *et al.*, 2001).

1.2 Fluoride-contaminated groundwater in Ghana

In Ghana, the occurrence of high fluoride concentration in groundwater causing fluorosis has become one of the most important health related geo-environmental issues. Some parts of the Northern and Upper Regions of Ghana have been identified for high fluoride concentrations in their ground waters (WRC, 2014; Anim-Gyampo *et al.*, 2012; Atipoka, 2010; Apambire *et al.*, 1997). The work of Rossiter *et al.* (2010) for example shows that some groundwater resources in Ghana are not of the standard required to be potable. In the Northernmost part of Ghana, availability of and access

to potable water remains a challenge in the rural communities. This is due to the relatively long dry seasons experienced in the area. There is the competition for available surface water resources by both humans and animals especially in the dry season as streams dry out (Anim-Gyampo *et al.*, 2012). The Government of Ghana and its development partners in response to this challenge have provided boreholes to help alleviate water scarcity in many areas including the Bongo District

; *et al.*, 2009; Pelig-Ba, 1998; Apambire *et al.*, 1997; Shier *et al.*, 1996).

et al., 2009; Atipoka, 2010). One major concern in the Bongo District is the high levels of fluoride found in some of their groundwater systems and the origin of these ions has been attributed to the chemical nature of the aquifer host rock of the area (Apambire *et al.*, 1997). It is estimated that 62% of the total population of school children in the Bongo District suffer from dental fluorosis (Apambire *et al.*, 1997), a disease which attacks the teeth rendering them permanently brownish. The problem with fluoride contamination is not limited to these regions only but also other parts of the country such as the north of Obuasi, Accra and some locations along the coast (*fer et al.*, 2009).

According to Ayamseigna *et al.* (2008), out of over 600 boreholes located in the Northern Region of the country, one hundred and fifty one (151) of them have been found to contain fluoride levels greater than the safe limit of 1.5 mg/L recommended by the World Health Organization (WHO) and 1.0mg/L for tropical countries like Ghana (Biswas *et al.*, 2010). According to Atipoka (2010), among the 335 boreholes that were drilled in the seven areas of the district, 35 have been capped due to high fluoride content and 25 are non-functional due to faulty parts. Some of the boreholes

in use contain fluoride levels in the range of 1.7-4.0 mg/L. These values are very high with respect to the WHO recommended level of 1.5 mg/L of fluoride in drinking water. The WHO safe limit of 1.5 mg/L is based on a daily water consumption rate of 2 Litres/day for adult body mass, and a standard diet containing 0.2-0.5 mg fluoride (Apambire *et al.*, 1997). According to Apambire *et al.* (1997), out of the 371 wells or boreholes sampled in the Upper Regions of Ghana, 23% of them have fluoride concentrations above 1.5 mg/L.

Recent data from Water Resources Commission (2014) show some groundwater systems with fluoride levels above the WHO recommended limit of 1.5 mg/L (Figure 1.1). Apambire *et al.* (1997) traced the origin of fluoride in groundwater in the Bongo District of the Upper East Region of Ghana to the underlying rocks of the Bongo granitic suite comprising coarse grained hornblende granite grading towards its outer contacts into biotite and hornblende syenite phases. Abugri and Pelig-Ba (2010) measured the fluoride content of soils in the Bongo district and found elevated fluoride levels (range between 219.26 and 1163.01 mg/kg dry weight). They however, concluded that high concentrations of fluoride found in groundwater in the area may have a relation with the fluoride content in the surrounding soil.

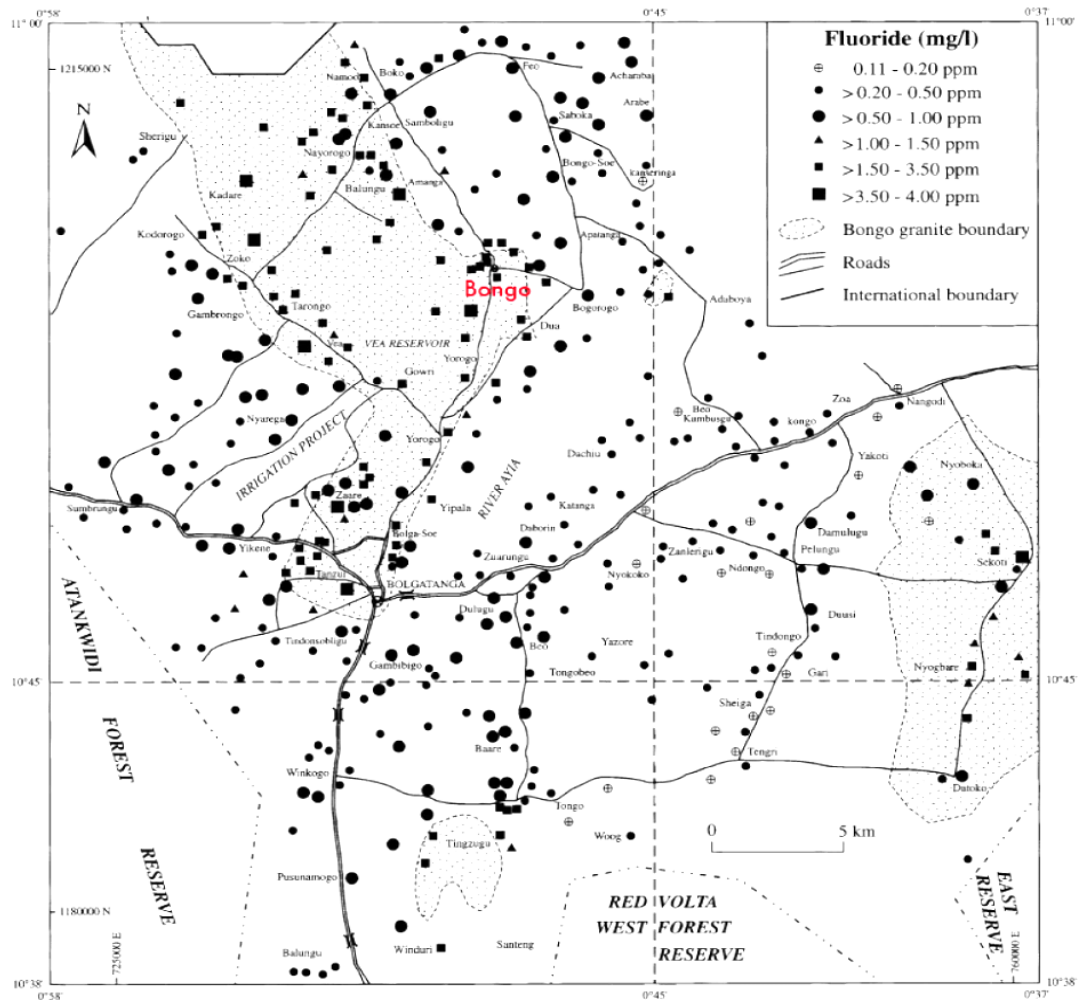


Figure 1.1: Spatial distribution of fluoride in groundwater in the Bongo district of the Upper East Region of Ghana (Source; WRC, 2014)

1.3 Defluoridation techniques

There are several defluoridation techniques that have been developed or show potential for the removal of fluoride from contaminated water. These techniques include among others, coagulation/precipitation (Zhu *et al.*, 2007; Hu *et al.*, 2005), the use of membranes (Sehn, 2008; Tahaikt *et al.*, 2007), ion exchange (Meenakshi & Viswanathan, 2007; Kir & Alkan, 2006), and adsorption (Gomoro *et al.*, 2012; Wambu *et al.*, 2012; Tor, 2006; Karthikeyan *et al.*, 2005; Moges *et al.*, 1996; Hauge *et al.*, 1994). The choice of treatment method has been influenced by factors such as

the amount of the ions in source water, the type of chemical species in source water, the available treatment processes, cost of treatment, handling of residues or waste generated and versatility of a given technique. However as result of limitations in cost of the treatment method, production of enormous waste and difficulty in end-use applications of some of the above treatment techniques, an environmentally benign, robust and low-cost technique is required for treatment of contaminated water.

Adsorption technology is touted as efficient among other defluoridation techniques by many researchers mainly due to the fact that the technique is economical and efficient and produces high-quality water (Lunge *et al.*, 2011; Sarkar *et al.*, 2006; Ghorai & Pant, 2005). A lot of studies have been geared towards the removal of fluoride using various adsorbents (Biswas *et al.*, 2010; Nath & Dutta, 2010; Wu *et al.*, 2007; Sarkar *et al.*, 2006; Ghorai & Pant, 2005; Dey *et al.*, 2004; Jamode *et al.*, 2004; Chidambaram *et al.*, 2003; Agarwal *et al.*, 1999; Srimurali *et al.*, 1998; Zevenbergen *et al.*, 1996). More importantly, adsorption technique is of wide usage and can be used in large-scale central water treatment systems and in the development of a small-scale Point-Of-Entry (POE) or Point-Of-Use (POU) system (Onyango & Matsuda, 2006). The various defluoridation techniques have both advantages and disadvantages. For example, adsorption technique has been highly rated to be effective for treating water contaminated with fluoride due to its simplicity of operation and availability of a wide range of adsorbents. However, the disadvantage of this technique is peculiar to the adsorbent involved.

1.4 Statement of problem

The management and maintenance of current and proposed defluoridation technologies (coagulation followed by precipitation, ion exchange, electrochemical

degradation and membrane-based processes) require expensive chemicals and /or a high level of technological skill and can be applied only in centralized systems. Adsorption is a robust technique for removing ions in drinking water. The literature abounds with reports on various adsorbents that have been used for fluoride removal from drinking water (Biswas *et al.*, 2010; Nath & Dutta, 2010; Wu *et al.*, 2007; Sarkar *et al.*, 2006; Ghorai & Pant, 2005; Dey *et al.*, 2004; Jamode *et al.*, 2004; Chidambaram *et al.*, 2003; Agarwal *et al.*, 1999; Srimurali *et al.*, 1998; Zevenbergen *et al.*, 1996). These studies have been conducted mainly because of the need to have alternative adsorbents that are low in cost, could be available locally, do not need much processing and could remove the fluoride well. Some researchers in Ghana have successfully investigated a variety of local adsorbents such as bauxite (Craig *et al.*, 2015; Ayamsega, 2008), high aluminum content bauxite ore, activated neem seeds and zeolites (Buamah *et al.*, 2013) in removing fluoride from contaminated water.

Laterite is also a local adsorbent which is found almost everywhere of the country. This material has been identified as a possible adsorbent probably because it consists of alumina and metal oxides (Sarkar *et al.*, 2006), which are oxides that are known to remove fluoride from water. Availability of laterite in the country makes its use as an adsorbent very recommendable in terms of cost and sustainability. However, reports on the use of laterite as an adsorbent for fluoride removal shows variability in its performance (Ayamsega *et al.*, 2008). The variability in its performance has mainly been influenced by its chemical and mineral compositions (Osei *et al.*, 2015). Sarkar *et al.* (2006) report high performance of laterite for fluoride removal and attribute the high performance to the iron oxide phase in the material. Craig *et al.* (2015) in

evaluating the performance of laterite in relation to activated alumina and bauxite, report of low performance of laterite in fluoride uptake as compared to bauxite and alumina. This project seeks to investigate the adsorptive properties of some local laterites for fluoride removal and modify the laterite to enhance its adsorptive properties for efficient removal of fluoride.

KNUST

1.5 Objectives of the study

The main objective of this project is to develop an alumina modified laterite with properties capable of removing or minimizing the amount of fluoride in a contaminated water to levels, that is below the WHO recommended limit of 1.5 mg/L.

The specific objectives are:

- To select, characterize and test local laterite materials for their fluoride adsorption properties;
- To improve the fluoride removal efficiency of the selected laterite material through modification of the laterite with alumina;
- To examine the effects of the following parameters on the fluoride removal efficiency of laterite:
 - pH, Heat treatment temperature, Particle size;
 - Initial fluoride concentration, Adsorbent dosage;
 - Alumina: Laterite ratio, Contact time; and,
 - Competitive anions (Cl^- , SO_4^{2-} , NO_3^- , PO_4^{3-}).
- To determine the model of uptake of fluoride using the Langmuir and Freundlich isotherms through the study of the mechanism and kinetics (1st and 2nd Order) of fluoride uptake.

1.6 Hypothesis

The research work is based on the following hypotheses;

1. By immersing laterite particles in finely pulverized and pulped alumina, the particles will be coated with alumina, which on heat treatment; will adhere not only physically but also chemically to the laterite (especially the iron oxide-hydroxide particles).
2. Chemical adhesions will be by diffusion of Al into the surface structure of the Fe-oxides.
3. The adhesion will result in the formation of a stable composite that will improve the adsorption properties of the modified laterite.

1.7 Significance of the study

The study would

- 1) provide knowledge on characteristics of laterites and modified laterites in fluoride adsorption performance.
- 2) argue for the use of locally available material for low cost and sustainable fluoride de-contamination systems.

1.8 Scope

The scope of the study will be limited to:

1. Desk study and literature survey on fluoride occurrence in groundwater and mitigation measures.

2. Selection and testing of local laterite to determine its chemical and mineralogical characteristics in relation to its use as fluoride adsorbent.
3. Modification of selected laterite to improve fluoride adsorption characteristics.

KNUST



CHAPTER TWO

LITERATURE REVIEW

2.1 Introduction to chapter

This chapter gives an overview of fluoride occurrence in the environment. It discusses the impact of fluoride on health and a number of defluoridation techniques that have been employed in recent past to tackle the issue of high fluoride in water, taking into consideration their advantages and disadvantages of their applications. The chapter closes with discussion on the need for a cost effective and sustainable adsorbent which can be used to remove fluoride from drinking water.

2.2 Geochemistry and environmental occurrence of fluoride

Fluoride is an ion of the chemical element fluorine. Fluorine exists as a diatomic gas in its elemental form and is the lightest member of the group of halogens. In some respects, its chemical behaviour is different from other members of the halogen group and some of these differences are evident in its behaviour in natural water. It is the most electronegative of all the elements. It has an oxidation state of -1 and occurs in both organic and inorganic compounds. Fluorine does not exhibit any taste, smell or colour and so when present in water, it cannot be determined physically. Its presence can only be determined by chemical means. Combined chemically in the form of fluorides, fluorine ranks 17th “ representing about 0.06- . 9% “ M *et al.*, 2007). Minerals such as fluorspar, cryolite, mica, hornblende, rock phosphate, among others contain significant amount of fluoride (Murray, 1986, cited in Fawell *et al.*, 2006). Minerals of fluoride of commercial interest

are cryolite and rock phosphates. The common mineral of fluoride, fluorite (CaF_2) has low solubility and occurs in both igneous and sedimentary rocks. Volcanic activity and fumarolic gases evolve with fluoride.

Thermal waters with high pH are reported to be rich in fluoride (Edmunds and Smedley, 1996, cited in Fawell *et al.*, 2006).

2.2.1 Distribution and sources of fluoride groundwater

The abundance of fluoride in the earth crust makes its presence in all natural water possible. Seawater contains about 1 mg/L of fluoride while rivers and lakes show levels of less than 0.5 mg/L (Fawell *et al.*, 2006). However, in groundwater, the concentrations of fluoride, either low or high depend on the nature of the rocks and the occurrence of fluoride-bearing minerals with which the water is in contact.

Water with high fluoride concentrations occur in large and extensive geographical belts associated with;

- a) Volcanic rocks.
- b) Granitic and gneissic rocks.
- c) Sediments of marine origin in mountainous areas.

Areas documented to have high fluoride levels associated with volcanic activity trace from the East African Rift system and the Jordan valley down through Sudan, Ethiopia, Uganda and Kenya (Mondal *et al.*, 2009; Msonda *et al.*, 2007). Elevated levels of fluoride in groundwater which have been associated with igneous and metamorphic rocks such as granites and gneisses have been found in areas such as India, Pakistan, West Africa, Thailand, China, Sri Lanka and Southern Africa

(Abugri and Pelig-Ba, 2011; Mondal *et al.*, 2009; Azhar *et al.*, 2006; Fawell *et al.*, 2006; Apambire *et al.*, 1997). Areas where fluoride concentrations have been associated with sediments of marine origin include Iraq, Iran through Syria and Turkey to the Mediterranean region, and hence from Algeria to Morocco (Fawell *et al.*, 2006).

2.2.2 Occurrence of fluoride in groundwater

The occurrence of fluoride in groundwater could be high or low depending on the nature of rocks and occurrence of fluoride bearing minerals. Fluoride concentrations in groundwater are limited by its solubility (affected by Ca presence e.g. 40 mg Ca/L max 3.1 mg fluoride/L). High fluoride concentration is normally found in calcium-poor groundwater in fluoride bearing minerals (Fawell *et al.*, 2006).

The presence of fluoride in groundwater could result due to both natural and human-induced processes. The geochemistry of groundwater plays an important role in controlling the composition and movement of dissolved constituents of groundwater. Fluoride has an ionic radius similar to that of hydroxide ion and substitutes readily in hydroxyl positions during magmatic differentiation (Naseem *et al.*, 2010). Therefore fluorides can substitute the hydroxide ion (OH⁻) in certain minerals such as muscovite $(K_2Al_4)(Si_6Al_2O_{20})(OH,F)_4$ which is in the mica group and amphiboles such as amosite $(FeMg)_7(Si_4O_{11})_2(OH)_4$ and also in hornblende $(Ca,Na)_{23}(Mg,Fe,Al)_5(Si,Al)_8O_{22}(OH)_2$ (Msonda *et al.*, 2007).

Fluorine is naturally found in combined forms in rocks and soil in a wide variety of minerals such as fluorapatite or fluorite (CaF₂), fluorapatite (Ca₁₀(PO₄)₆F₂) and micas in

granites, cryolite (Na_3AlF_6), apatite ($\text{Ca}_5(\text{PO}_4)_3\text{F}$) and some silicates such as topaz ($\text{Al}_2\text{SiO}_4(\text{F},\text{OH})_2$) (Jha *et al.*, 2011; Fantong *et al.*, 2010; Guo *et al.*, 2010; G.-T Chae *et al.*, 2007; Msonda *et al.*, 2007; Apambire *et al.*, 1997). In some waters with high pH, mineral surfaces are capable of absorbing anions, and if such surfaces carry fluoride ions, they could be available for release by substitution of hydroxide ions (Hem, 1970). High fluoride concentrations in groundwater might result from such effect. Fluorite (CaF_2), commercially known as fluorspar has usually been considered as a dominant source of groundwater fluoride (49% fluorine) and has normally been associated with quartz, calcite, dolomite or barite (Jha *et al.*, 2011; Chae *et al.*, 2007). It is mostly found in granites as an accessory mineral (Reddy *et al.*, 2010). Fluorine may occur in limestone that is accompanied with tremolite, actinolite and pyroxene, where fluoride levels may go as far as 0.4-1.2% (Jha *et al.*, 2011). Dissolution of volcanic acid rocks also contributes to the fluoride levels in groundwater (Armentia and Segovia, 2008). The levels of fluoride in different rock particles are presented in Table 2.1 below:

Table 2.1: Fluoride levels in different types of rocks (Source: Jha *et al.*, 2011).

Rocks	Fluoride range (ppm)	Average
Basalt and gneisses	20-1060	360
Shales and clays	20-2700	870
Limestone	10-7600	800
Sandstones	0-1200	220
Phosphorite	10-880	180
(ash)	2400-41500	3100
	40-480	80

The levels of fluoride in a geological terrain are influenced by the hydrological conditions pertaining in that area. Some of these conditions include neutral to alkaline pH, low calcium concentrations, high sodium and bicarbonate

concentrations of groundwater (Brindha & Elango, 2011; Garcia *et al.*, 2011).

Concentration of fluoride in groundwater is also dependent on the contact times with aquifer minerals. High fluoride concentration can be built up in groundwaters which have long residence times in the aquifer. Such groundwaters are usually associated with deep aquifer systems and a slow groundwater movement. Shallow aquifers which contain recently infiltrated rain usually have low fluoride. Exceptions can occur in shallow aquifers situated in active volcanic areas affected by hydrothermal alteration. Under such conditions, the solubility of fluoride increases with increasing temperature and fluoride may be added by dissolution of HF gas (Frencken, 1992).

Climate also plays an important role in the occurrence of fluoride in groundwater. Arid regions are prone to high fluoride concentrations. Under such climate, groundwater flow is slow and the reaction times with rocks are therefore long. The fluoride contents of water may increase during evaporation if solution remains in equilibrium with calcite and alkalinity is greater than hardness. Dissolution of evaporative salts deposited in arid regions may be an important source of fluoride. Fluoride increase is less pronounced in humid tropics because of high rainfall inputs and their diluting effect on groundwater chemical composition.

Anthropogenic addition of fluoride to water results from air emissions such as coal combustion, waste production by various industries, including steel, aluminum, copper and nickel smelting and the production of glass, phosphatic fertilizers, brick and tile (Farooqi *et al.*, 2007). Fertilizers containing phosphate most especially the super-

phosphates, are perhaps the single most important sources of fluoride contamination to agricultural lands. A repeated application of rock phosphate that contains several percent of fluoride was shown to significantly elevate the fluoride content of soils (Jha *et al.*, 2011). Leachates from landfill could also add to the fluoride contents of soils (Sunil & Ramanathan, 2008).

KNUST

2.3 Fluoride and human health

Among the major sources of ingested fluoride are water, air and other dietary sources (including food, tea, drinks prepared with fluoridated water), fluoride tablets and dental care products such as toothpaste. Drinking water is considered as the largest single contributor to daily fluoride intake (Fawell *et al.*, 2006). However, this is not true in all cases. For a given person, exposure to fluoride (mg kg^{-1} of body weight per day) through drinking water is determined by the fluoride level in the water and the daily water consumption (liters per day). A number of factors including age, type of fluoride compound, pH conditions, the concentrations of magnesium and calcium affect the amount of fluoride absorbed by a given individual (Harrison, 2005).

Fluoride in drinking water can be either beneficial or detrimental to health depending on its concentration. It is estimated that about 60% of fluoride taken into the body is retained whilst the rest is primarily removed through urine (Fawell *et al.*, 2006).

Fluoride at low concentrations (about $<1.0 \text{ mg/L}$) in drinking water has mitigating effect on dental caries. Fluoride modifies the process of tooth decay by; improvement of the chemical structure of the enamel during development, making it more resistant to acid attack; the encouragement of remineralization with an improved quality of

enamel crystals and reduction of the ability of plaque bacteria to produce acid (Harrison, 2005).

On the other hand, high concentrations of fluoride (>1.5 mg/L) in drinking water could give rise to adverse effect, ranging from mild dental fluorosis to crippling skeletal fluorosis over prolonged exposure when water is consumed over an extended period of time (Hussain *et al.*, 2010). Fluorine is a highly electronegative element and has the tendency to be attracted by positively charged ions like calcium (Ozsvath, 2008). Fluoride ions displace hydroxide ions from hydroxyapatite ($\text{Ca}_5(\text{PO}_4)_3\text{OH}$), the principal mineral constituent of teeth especially the enamel and bones, to form the harder, tougher and more stable fluorapatite ($\text{Ca}_5(\text{PO}_4)_3\text{F}$). A small amount of this mineral strengthens the enamel. However, fluorapatite is an order of magnitude less soluble than hydroxyapatite and at high fluoride concentration the conversion of a large amount of the hydroxyapatite into fluorapatite makes the teeth and (after prolonged exposure) the bones denser, harder and more brittle (Dissanayake and Chandrajith, 2009). Thus, a large amount of fluoride gets bound in these tissues and only a small amount is excreted through sweat, urine and stool. The intensity of fluorosis is not merely dependent on the fluoride content in water, but also on the fluoride from other sources, physical activity and dietary habits.

2.3.1 Fluorosis

The fluorosis problem is found in countries where their fluoride concentrations in water exceed 1.5 mg/L. The problem is more pronounced in these areas (Table 2.2).

Table 2.2: Countries where the fluoride levels in water exceed 1.5mg/L (Fawell *et al.*, 2006).

Continent	Countries
Africa	Ethiopia, Sudan, Kenya, Tanzania, Egypt, South Africa, Nigeria, Senegal, Algeria, Uganda, Ghana.
Asia	India, China, Korea, Thailand, Sri Lanka, Indonesia, Yemen, Pakistan
Latin America	Greece, Finland, Sweden, Great Britain, Poland, Moldavia, Ukraine

2.3.2 Dental fluorosis

Dental fluorosis is a form of developmental defect of enamel. It is visible by white, yellow and brown streaks on the teeth. The damage to the teeth is more than cosmetic, as it is associated with painful cavity-like feelings. Fluorosis occurs during the period of tooth formation when fluoride is incorporated in the crystalline structure of tooth enamel in such a way as to increase its porosity (EPA, 1997). The severity of dental caries depends on when and for how long the overexposure to fluoride occurs, the individual response, weight, degree of physical activity, nutritional factors and bone growth. The risk period for aesthetic changes in permanent teeth is between 20 and 30 months of age (Alvarez *et al.*, 2009). The teeth are not discolored at the time of eruption, but subsequently become stained and discolored as a consequence of the increased porosity. In its mild form, dental fluorosis is characterized by white, opaque areas on the tooth surface and in its severe form; it is manifested as yellowish brown to black stains and severe pitting of the teeth. Usually, the extent of dental fluorosis is dependent on the level of fluoride exposure up to the age of 8-10 years, as the effect of fluoride is seen only in the developing teeth while they are being formed in the jawbones and are still under the gums (Jha *et al.*, 2011). The effect of dental fluorosis may not be apparent if the teeth are already fully grown prior to the fluoride over

exposure. Therefore, the fact that an adult shows no signs of dental fluorosis does not necessarily mean that his or her fluoride intake is within the safe limit.



Figure 2.1: Severe case of dental fluorosis in Bongo, Ghana (Courtesy of Cumberbatch, 2008).



Figure 2.2: A case of dental fluorosis (source: Avishek *et al.*, 2010).

There are also social stigmas against sufferers of dental fluorosis. While all the teeth are affected, the incisors especially the maxillary incisors and permanent molars are often the teeth most affected by fluorosis. This is because these are the teeth that are first to develop.

2.3.3 Skeletal fluorosis

Skeletal fluorosis affects people of all ages. The disease is manifested in the affected individual when it has reached an advanced stage. Fluoride is deposited in the joints of neck, knee, pelvic and shoulder bones and makes movement of the hands and legs difficult (Jha *et al.*, 2011). Some of the early symptoms include sporadic pain, back stiffness, burning like sensation, prickling and tingling in the limbs, muscle weakness, chronic fatigue, abnormal calcium deposits in bones and ligaments (Bhardwaj, 2008; Shashi *et al.*, 2008). At the advanced stage of osteoporosis, long bones and bony outgrowths may occur. Vertebrae may fuse together and eventually the victim may be crippled. This may even lead to a rare bone cancer; osteosarcoma and finally spine, major joints, muscles and nervous system get damaged. Fluorosis is non-curable, thus efforts should be directed toward prevention and attempting to alleviate some of the symptoms (Jha *et al.*, 2011).



Figure 2.3: A case of children suffering from skeletal fluorosis. (Source; Mjengera & Mkongo, 2003)

Excessive consumption of fluoride could also lead to many other disease manifestations; neurological manifestations, depression, gastrointestinal problems, urinary tract malfunctioning, nausea, abdominal pain, tingling sensation in fingers and toes, muscle fiber degeneration, low hemoglobin levels, excessive thirst, headache, skin rashes, nervousness, reduced immunity, repeated abortion, male sterility, reduced intelligence etc.(Jha *et al.*, 2011).

2.4 Management of fluoride-containing drinking water using defluoridation techniques

A lot of research works have been carried out on various methods of removing fluoride from fluoride contaminated drinking water. These defluoridation methods are mainly based on the principles of precipitation, membrane separation processes, ion- exchange and adsorption.

2.4.1 Defluoridation of water using coagulation-precipitation method

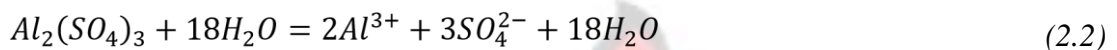
A popular technique that employs the principle of coagulation followed by precipitation is the Nalgonda method developed by Bulusu *et al.* (1988) of National Environmental Engineering Research Institute (NEERI) in India. This technique has been successfully implemented in Tanzania, China, and India for the removal of fluoride in water for domestic and community purposes. In this method as described by Meenakshi and Maheshwari (2006), two chemicals, alum (aluminum sulphate or potassium aluminum sulphate) and lime (calcium oxide) are rapidly mixed with the fluoride-contaminated water. As lime is added, it leads to the precipitation of fluoride as insoluble calcium fluoride and raises the pH value of water up to 11-12.



As lime leaves a residue of 8.0 mg F⁻/L, it is used only in conjunction with alum treatment to ensure the proper fluoride removal.

As a first step, precipitation occurs by lime dosing which is followed by a second step in which alum is added to cause coagulation. When alum is added to water, two reactions take place.

Alum dissolution



Aluminum precipitation (Acidic)



In the second reaction, Al (OH)₃ reacts with fluoride ions present in water.

Co-precipitation (non-stoichiometric, undefined product)



The optimum pH range for fluoride removal is 5.5-7.5. Although the Nalgonda technique is an efficient technique for removal of fluoride, Mohapatra *et al.* (2009) and Meenakshi and Maheshwari (2006) identified the following as the shortcomings with this method;

- i. A large space is needed for drying the sludge.
- ii. The technique cannot be automated. It requires a regular attendance during treatment process.
- iii. The technique requires regular analysis of feed and treated water in order to calculate the correct dose of chemicals that has to be added since the water matrix changes with time and season.
- iv. The taste of the treated water makes it unattractive.
- v. The defluoridation process is temperature dependent.

- vi. The technique is affected by silicates.
- vii. The levels of SO_4^{2-} ion from aluminum sulphate coagulants reaches high levels and in few cases exceeds the maximum permissible limit of 400 mg/L.
- viii. The amount of aluminum remaining in excess of 200 ppb in treated water is believed to cause dementia and also affect musculoskeletal, respiratory and cardiovascular systems.
- ix. Only a smaller portion of fluoride (18-33%) in the form of precipitate is removed and converts a greater portion of ionic fluoride (67-82%) into soluble $\text{Al}^{3+}\text{-F}^-$ complex ions which are toxic.

2.4.2 Defluoridation of water by ion exchange method

The use of ion exchange resins for removal of fluoride in water has been well studied in many places in the world. Fluoride removal from water supplies could be done with a strongly basic anion-exchange resin containing quaternary ammonium functional groups. The fluoride is removed based on the following reaction;



Chloride ions of the resin are replaced by fluoride ions. The process is repeated until all the sites on the resin are occupied. The resin is regenerated by backwashing with water that is supersaturated with sodium chloride salt. The fluoride ions are replaced with new chloride ions and the process could be started again.

It has been observed that anion-exchange resins are prone to interference from other anions such as sulphate, carbonate and phosphate than cation-exchange resins (Ku *et*

al., 2002; Lopez *et al.*, 1992). The order of selectivity of anions on Amberlite IRA410 was: $\text{SO}_4^{2-} > \text{Cl}^- > \text{HCO}_3^- > \text{OH}^- > \text{F}^-$ (Lopez *et al.*, 1992).

Ion- exchange resins are efficient in removing about 90-95% of fluoride and maintaining the taste and colour of fluoride contaminated water.

However, there are a number of setbacks associated with this method:

- i. The technique is expensive because of the cost of resin, pre-treatment required to maintain the pH, regeneration and waste disposal.
- ii. Regeneration of resin is a problem because it leads to fluoride rich waste, which has to be treated separately before final disposal.
- iii. Efficiency is reduced in presence of other ions like sulphate, carbonate, phosphate and alkalinity.
- iv. The resulting treated water has high levels of chloride and very low pH.

2.4.3 Defluoridation of water using membrane-based processes

Membrane-based processes such as dialysis, electro-dialysis, nanofiltration and reverse osmosis have been successfully used for the removal of fluoride from drinking water (Richards *et al.*, 2010; Zakia *et al.*, 2001; Lhassani *et al.*, 2000). Reverse osmosis (RO) has emerged as a preferred alternative to provide safe drinking water (Sehn, 2008). It is a physical process in which the contaminants are removed by applying pressure on the feed water to direct it through a semipermeable membrane. The process is a reverse of natural osmosis as a result of the applied pressure to the concentrated side of the membrane, which overcomes the natural osmotic pressure. RO membrane rejects ions based on size and electrical charge. RO produces high purity water. The factors influencing the membrane selection are cost, recovery rejection, raw water characteristics and pre-treatment. Efficiency of the process is governed by different

factors such as pressure, temperature, raw water characteristics and regular monitoring and maintenance. The membrane-based processes present some advantages as compared to other fluoride removal methods;

1. The membranes provide a barrier to suspended solids, all inorganic pollutants, organic micro pollutants, pesticides and microorganisms.
2. The process allows the removal and disinfection of water in one step.
3. No chemicals are used and very little maintenance is needed.
4. The membranes work within a wide pH range.
5. Interference by competing ions is avoided.
6. Life span of membrane is relatively long so regeneration of membrane is of little concern.
7. The process is automated.

However, there are a number of challenges with this process;

1. The process removes all the ions present in water although some of these ions are essential to health. Thus remineralization is required after the process.
2. The process is expensive.
3. pH adjustment is required as the water produced is acidic.
4. Lots of water is wasted as brine and disposal of the brine is difficult.

2.4.4 Defluoridation of water using adsorption technique

Adsorption of a solute from its solution to the adsorbent phase is an equilibrium process (Sarkar *et al.*, 2006). Removal of fluoride by adsorption technique is carried out using the adsorption capacity of the material used (Jayantha *et al.*, 2004). Normally the material that is used as adsorbent has greater surface area and has the ability to

adsorb fluoride. Adsorption is considered as one of the most widely used and effective techniques for fluoride removal in drinking water (Meenakshi and Maheshwari, 2006). The parameters specific to a particular system are generally defined by the properties of the solute, the solution conditions and nature of adsorbent.

Adsorption technique is very important in defluoridation research because of its lower cost and high efficiency. The technique has the advantage of generating lesser quantity of sludge and regeneration of spent adsorbent. The technique is also efficient in removing fluoride from water when fluoride concentrations exist in low concentrations. Efficiency of the technique depends on nature of adsorbent, initial fluoride concentration, temperature, adsorbent dosage, pH and agitation time (Osei *et al.*, 2015; Salifu *et al.*, 2013; Gomoro *et al.*, 2012; Vithanage *et al.*, 2012; Sujana *et al.*, 2011). The process of adsorption occurs through many techniques depending on the material (adsorbent) which includes ion exchange, complexation, coordination, precipitation, and physical adsorption. The principle behind adsorption technique is captured in three phases (Mohapatra *et al.*, 2009; Onyango & Matsuda, 2006; Fan *et al.*, 2003);

- 1) Fluoride ion is transported by the process of diffusion from the bulk solution across the boundary layer surrounding the adsorbent particle, called external mass transfer.
- 2) Adsorption of the fluoride ion onto particle surface.
- 3) The adsorbed fluoride ions may exchange with the structural elements inside the adsorbent particles depending on the chemistry of solids, or the adsorbed fluoride ions are transferred to the internal surfaces of porous materials (intra particle diffusion).

In the evaluation of the adsorbents for fluoride removal, consideration is given to its availability, acceptability, cost implication, performance and regenerability. However, there are many raw/treated natural and synthetic materials which have shown potential for fluoride adsorption. Overviews of a few of these adsorbents that have been reported in literature are discussed in this work.

2.4.4.1 Activated Alumina (AA)

Activated Alumina (AA) is the granular form of Aluminum (III) oxide (Al_2O_3) with a very high internal surface area, usually in the range of $200\text{-}300\text{m}^2/\text{g}$. The high surface area gives the material a very large number of sites where adsorption could likely take place. Four different kinds of AA could be identified depending on the pH in water (Onyango and Matsuda, 2006). They are; acidic ($\text{pH } 4.5\pm 0.5$), weakly acidic ($\text{pH } 6.0\pm 0.5$), neutral ($\text{pH } 7.5\pm 0.5$) and basic ($\text{pH } 9.5\pm 0.5$) activated alumina.

In an aqueous environment at pH values below its point of zero charge (pH_{pzc}), AA forms protonated ($=\text{Al-OH}_2^+$) and neutral ($=\text{Al-OH}$) aluminol sites, which are responsible for the binding of fluoride ions by the formation of inner-sphere complexes. Based on the good performance of AA, it has been used as an adsorbent for fluoride removal by many researchers under different conditions (Camacho *et al.*, 2010; Stewart, 2009; Tang *et al.*, 2009; Tripathy *et al.*, 2006; Ghorai & Pant, 2005; Ku and Chiou, 2002). Normally the ability of AA to remove fluoride on the first adsorption cycle is low unless it is treated first.

Ku and Chiou (2002) have shown that the removal efficiency of fluoride using AA is influenced significantly by solution pH and the optimum operating pH was found to be in the range of 5 to 7. For neutral and acidic solutions, the adsorption capacity of fluoride by AA was interfered by the presence of sulphate ions.

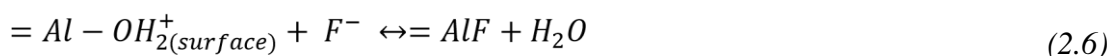
The selectivity sequence of anion adsorption on activated alumina in the pH range of 5.5-8.5 (Johnston & Heijnen, 2002):

$\text{OH}^- > \text{H}_2\text{AsO}_4^- > \text{Si}(\text{OH})_3\text{O}^- > \text{HSeO}_3^- > \text{F}^- > \text{SO}_4^{2-} > \text{CrO}_4^{2-} > \text{HCO}_3^- > \text{Cl}^- > \text{NO}_3^- > \text{Br}^- > \text{I}^-$ The performance of AA to remove fluoride is reduced when bicarbonate ion content is increased. This is because bicarbonate ions buffer water pH at higher values therefore decreasing the number of active sites on AA available for binding fluoride ions (Onyango and Matsuda, 2006).

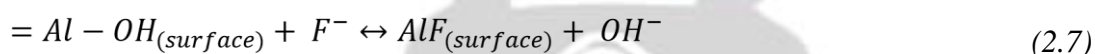
The pH of the solution could inhibit fluoride uptake since solution pH determines the speciation of fluoride, the number and distribution of active sites on AA. In the acidic medium where the pH of solution is below 3.2, the fluoride uptake by AA usually decreases. This is due to the fact that HF is weakly ionized and this results in the formation of soluble alumino-fluoro complexes due to the presence of aluminum ions in solution. As a result, the number of active sites for available for fluoride adsorption is reduced (Onyango and Matsuda, 2006).

Fluoride uptake is maximum at an almost neutral pH of the solution. For example at almost neutral pH when the pH_{pzc} of AA is about 8-9, the probable active sites would include $=\text{Al}-\text{OH}_2^+$ (protonated) and $=\text{Al}-\text{OH}$ (non-protonated) aluminol-sites. The interaction between the protonated aluminol sites ($=\text{Al}-\text{OH}_2^+$) and fluoride would lead

to the formation of inner-sphere complexes and the elimination of water. The reaction is represented by;



The protonated aluminol sites are normally responsible for the rapid kinetics as a result of the coulombic attraction between the positively charged sites and the negatively charged fluoride species (Onyango and Matsuda, 2006). For the nonprotonated aluminol sites (=Al-OH), the reaction involves ligand exchange and forming inner sphere complexes with fluoride. There is also the release of hydroxyl ions and the reaction is slow which is characterized by higher activation energy. The reaction is represented as;



When the pH is increased beyond the pH_{pzc} , it is expected that the electrostatic shielding of the active sites would be enhanced and this would reduce the number of active sites and activity. This argument is the reason why AA performs badly at $pH > pH_{pzc}$ (Onyango and Matsuda, 2006).

There are many shortcomings in the use of AA for fluoride adsorption. It is expensive as it is a synthetic material and may not be readily available in all regions which have high fluoride levels in their waters. Its performance is affected by the presence of co-ions such as silicates, sulphates, bicarbonates and phosphates in water.

According to Agarwal *et al.* (1999), regeneration of filter material is difficult as it involves treatment of the adsorbent bed by acid and alkali and it can be done only with the help of trained persons, who are generally not available in most of our villages. The process also results in moderately high residual aluminum in output water ranging

from 0.1 ppm to 0.3 ppm and it is relevant to note that aluminum is a neurotoxin and a concentration as low as 0.08 ppm of aluminum in drinking water is reported to have caused Alzheimer's disease (Agarwal *et al.*, 1999). The health implications associated with the use of alumina as adsorbent also include severe neuro-degenerative disease known as Amyotrophic Lateral Sclerosis and Parkinsonism Dementia (Dey *et al.*, 2004).

2.4.4.2 Ceramic adsorbent

Chen *et al.* (2010) presented studies with the use of ceramic adsorbent for the removal of fluoride in drinking water. The adsorbent has a high fluoride removal efficiency and sufficient mechanical strength to retain its physical integrity after long time adsorption. They are prepared by cost effective mixture of materials consisting of Kanuma mud, which is widespread in Japan with zeolites, starch and $\text{FeSO}_4 \cdot 7\text{H}_2\text{O}$. Experimental results show that the material adsorbs at a maximum capacity of 2.16 mg/g. The adsorbent was found to adapt to a wide pH range of 4-11 for fluoride adsorption. In the use of this adsorbent however, the presence of competing anions such as phosphate, sulphate and carbonate interfered with fluoride adsorption.

2.4.4.3 Crushed limestone

In the use of crushed limestone for removing fluoride in drinking water, Nath & Dutta (2010) used two methods. First by the method of precipitation and then followed by adsorption. The process starts by pre-treatment of water containing fluoride with citric and acetic acids. Fluoride is precipitated as CaF_2 followed by the adsorption of fluoride on limestone. The addition of acid before treatment with crushed limestone enhanced

fluoride adsorption. Although crushed limestone has shown to be a good adsorbent, removal of fluoride with the same lot of limestone chips decreased the adsorption efficiency of the limestone chips.

2.4.4.4 Hydrous ferric oxide (HFO)

Dey *et al.* (2004) used a synthesized hydrous ferric oxide material as adsorbent for the removal of fluoride in drinking water. The advantages of using this material are that it does not leach out on prolonged contact with water and regeneration (73-75%) of fluoride-rich HFO is possible with 1.0 M NaOH solution. However, the disadvantage with its use is that the pH at which there is optimum adsorption is narrow. Maximum adsorption of fluoride is at pH4. There is also the negative effect of competitor ions such as arsenite, arsenate, phosphate and sulphate on fluoride adsorption onto HFO.

2.4.4.5 Synthetic hydrated iron (III)-aluminum (III)-chromium ternary mixed oxide (HIACMO)

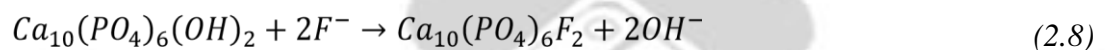
Biswas *et al.* (2010) experimented with the use of hydrated iron (III) aluminum (III) chromium ternary mixed oxide for removal of fluoride in water. In the study, HIACMO was found to be highly efficient in removing fluoride in water. Another advantage with its use is the regeneration of fluoride adsorbed material up to 90±0.2% with 0.5 M NaOH.

The disadvantage of this method includes the fact that it works in a narrow pH range of 4.0-7.0. The cost of producing HIACMO is estimated to be US \$28 per kilogram of material.

2.4.4.6 Bone char

Bone char is produced in granules by ashing animal bones which consist of 10% carbon and 90% calcium phosphate (Mirna *et al.*, 2014). The main constituent of bones is hydroxyapatite ($\text{Ca}_{10}(\text{PO}_4)_6(\text{OH})_2$) and in the presence of fluoride, the hydroxides are replaced by fluoride forming the insoluble fluorapatite ($\text{Ca}_{10}(\text{PO}_4)_6\text{F}_2$). Fluorapatite can react with caustic soda and hydroxyapatite is again formed. Based on this phenomenon, bone char has been used in water treatment.

Bone char reacts with fluoride in solution by ion exchange between the fluoride in solution and hydroxide from the hydroxyapatite. According to Kaseva (2006), the reaction can be represented by;



Bone char has the potential to remove fluoride from water. Kaseva (2006) also made use of bone char by optimizing regenerated bone char for fluoride removal. His work was based on heat regeneration of exhausted bone char. The results of his work showed that regeneration of bone char was most practical at temperature of 500°C and at particle size of 0.5-1.0 mm. The time for pyrolysis was 120 minutes and the removal capacity of the regenerated bone char was 0.55 mg F/g of bone char.

2.4.5 Water defluoridation using clay adsorption techniques

The first reported study on the use of soil to remove fluoride was published in 1967 (Bower and Hatcher, 1967). There has also been a number of studies involving the use of Ando soil of Kenya (Zevenbergen *et al.*, 1996), fired clay/soil (Bardsen and Bjorvatn, 1997), fired clay chips in Ethiopia (Moges *et al.*, 1996), amended clay

(Agarwal *et al.*, 2003), montmorillonite (Tor, 2006; Karthikeyan *et al.*, 2005), laterite (Sarkar *et al.*, 2006) and acid treated clay (Wambu *et al.*, 2012).

Bower and Hatcher (1967) had showed that fluoride adsorption onto minerals and soil was accompanied by the release of OH⁻ ions. It was also discovered that the adsorption of fluoride was dependent on the concentration of the fluoride solution and the adsorption could be explained by the Langmuir adsorption isotherm.

An improvement in the use of clay in defluoridation studies was the use of fired clay (Moges *et al.*, 1996; Bjorvatn *et al.*, 1997; Hauge *et al.*, 1994). Bjorvatn and his group indicated that pre-drying of clay at 50°C resulted in a similar efficiency as preheating at 250°C. Although Moges and his group did not show the effect of firing on the efficiency of adsorbent to adsorb fluoride, Hauge and his group indicated the optimum temperature at which maximum efficiency of adsorption could occur was at 600°C. At temperatures above 700°C, the fluoride adsorption capacity of the clay decreased and clay fired at 900°C and beyond seemed incapable of removing F⁻ from water. Therefore, fluoride adsorption with fired clay was found to be temperature dependent.

Modification of the adsorptive surface of clay is necessary to enhance fluoride removal from water. The structure of clay plays a significant role in determining the charge on the clay surface and type of exchange that can occur with ions in solution (Mohapatra *et al.*, 2009). Sorption of the negatively charged fluoride is better as the surface becomes more positive. Adsorption is strongly affected by the pH of the fluoride solution because pH modifies the charges on edge positions in

phyllosilicates and also those of variably charged minerals such as gibbsite, hematite and goethite. In acidic medium, the charges are positive whereas in the basic or alkaline medium the charges are negative. The specific pH range for positive and negative surface charge would be determined by the pKa values of the conjugate acids of the metal hydroxides.

Researchers have also experimented with soil as a potential adsorbent for fluoride removal in fluoride contaminated water. (Wang *et al.*, 2002; Zevenbergen *et al.*, 1996; Bjorvatn *et al.*, 1997). A study conducted on soils from the Highland areas of Addis Ababa, Ethiopia could reduce fluoride content of water at an initial fluoride concentration of 15 mg/L to 1 mg/L at a soil dosage of 100 g/L (Bjorvatn *et al.*, 1997). Availability and low cost of operation of soil for fluoride removal makes its use as an adsorbent for fluoride removal very good. Zevenbergen *et al.*(1996) worked on Ando soil, a relatively young black soil prevalent in Kenya. This soil is derived from the volcanic ash which in part has weathered to yield active aluminum in various forms, notably in allophane and complexed by organic matter. The soil exhibits high porosity and has a distinct visual difference between the topsoil and the subsoil. In the study (Zevenbergen *et al.*, 1996), the use of Ando soil was found to be very efficient in removal of fluoride in water due to its high active aluminum content and acidic character. However, Ando soil can be used on a small scale basis in rural areas of Kenya and other regions along the Rift zone.

Defluoridation study involving the use of montmorillonite which has been treated with hydrochloric acid was conducted by Tor (2006). The study was conducted by batch

equilibrations. Effect of pH, contact time, initial fluoride concentration and adsorbent dosage on the adsorption was studied. The mechanism for fluoride removal was explained by considering the interaction between the metal oxides at the surface of montmorillonite and fluoride ions. The results of the study were elucidated using isothermic and kinetic models. Desorption of the adsorbed fluoride ions was done by washing the adsorbent with sodium hydroxide solution of pH 12.

A similar study using montmorillonite was carried out by Karthikeyan *et al.* (2005). In this study fluoride adsorption was carried out at four different temperatures (30, 40, 50 and 60°C). The percentage of fluoride adsorbed increased gradually with time and maximum adsorption was reached at the 50th minute. Effect of particle size of the adsorbent on fluoride adsorption was clearly seen. Thermodynamic study showed that adsorption by montmorillonite increased at higher temperatures and that the process is endothermic reaction. FTIR studies showed the involvement of hydroxyl groups present on the surface during the adsorption interaction. The study also revealed that adsorption took place on the surface of the material and also through intra-particle diffusion.

2.5 Laterite and its use as adsorbent for fluoride removal

2.5.1 Laterite as a geomaterial

Laterite is gaining much prominence for the removal of fluoride from contaminated water and promising results are reported (Gomoro *et al.*, 2012; Wambu *et al.*, 2012; Sarkar *et al.*, 2006). However, extensive research has to be conducted in this area since laterite is not a standardized material and its composition varies with location and the

extent of laterisation (Schellmann, 1986). Laterite is a composite material of iron, aluminum and silicon. It is a material found in the tropical and subtropical countries of the world. In Ghana it is widely distributed, especially in the Upper East Region of the country where the problem with fluoride is endemic.

Laterites are formed from the leaching of parent sedimentary rocks (sandstone, clay, and limestone), metamorphic rocks (schists, gneisses, and migmatites), igneous rocks (granite, basalts, gabbros, peridotites) and mineralized proto-ores, which leaves the more insoluble ions, predominantly iron and aluminum. The leaching mechanism involves the dissolution of the host mineral lattice by acid which is followed by hydrolysis and precipitation of sulphates of iron, aluminum silica and insoluble oxides, under high temperature conditions of a humid sub-tropical monsoon climate.

One unique feature for the formation of laterite is the repetition of wet and dry seasons. Leaching of rocks involves infiltration by rain water during the wet season and the resulting solution containing the leached ions is brought to the surface by capillary action during the dry season. The resulting ions form soluble salt compounds which dry on the surface; these salts are washed away during the next wet season.

Low topographical reliefs of gentle crests and plateaus favor laterite formation because they prevent erosion of the surface cover. The reaction zone where rocks are in contact with water from the lowest to highest water table levels is progressively depleted of the easily leached ions of sodium, potassium, calcium and magnesium.

The parent rocks influence the mineralogical and chemical compositions of laterite. Laterites consist mainly of quartz, zircon, and oxides of titanium, iron, tin, aluminum and manganese, which remain during the course of weathering. Quartz is the most

abundant relic mineral from the parent rock. The factors that determine the mineral composition of laterites depend on their location, climate, depth and the extent of laterisation. Lateritic soils contain clay minerals, iron oxide minerals (goethite, hematite) and hydrated oxide of aluminum (gibbsite) even when the silica content of the laterite is poor. Bauxite is formed at the stage of laterisation. The difference between laterites and clays is that aluminum in laterite is in the form of oxides and hydroxides instead of silicates as in clays. The main host minerals for nickel and cobalt can either be iron-oxides, clay minerals or manganese oxides. Iron oxides are derived from mafic igneous rocks and other iron-rich rocks; bauxites are derived from granitic igneous rock and other iron-poor rocks. Nickel laterites occur in areas of the earth which experienced prolonged tropical weathering of ultramafic rocks containing the ferromagnesian minerals olivine, pyroxene and amphibole.

2.5.2 Laterite definition and classification

The definition of laterite is based on the definition adopted by Schellmann (1982, 1983) in cooperation with the International Geological Cooperation Programme (IGCP) No. 129. The term laterite is described to cover all highly weathered materials, strongly depleted in silica, and enriched in iron and alumina, regardless of their morphological and physical properties (fabric, colour, consistency, etc.). Laterites are products of intense sub aerial rock weathering. They consist predominantly of mineral assemblages of goethite, hematite, aluminum hydroxide, kaolinite minerals and quartz. The $\text{SiO}_2:(\text{Al}_2\text{O}_3+\text{Fe}_2\text{O}_3)$ ratio of a laterite must be lower than that of the kaolinized parent rock in which all the alumina of the parent rock is present in the form of kaolinite, all the iron in the form of iron oxides and which contains no more silica than fixed in the kaolinite plus the primary quartz. However, this definition does not factor

in the lateral transport, mineralogical composition and morphological characteristics of the laterite that give clues to its origin (Bourman and Ollier, 2002).

The composition of laterite varies with the extent of laterisation, parent rock and geographical location (Bourman and Ollier, 2002). The degree of laterisation is defined by the silica-sesquioxide (S-S) ratio ($\text{SiO}_2/\text{Al}_2\text{O}_3+\text{Fe}_2\text{O}_3$) which is calculated as the weight percent of the oxides. Soils are classified by the S-S ratio into the following categories;

An S-S ratio of 1.33 or less= laterite or laterite concretion

An S-S ratio of 1.33 to 2.00= laterite soil

An S-S ratio of 2 or greater= non-lateritic, tropical soil.

The term laterite soils refer to materials of soft rocks and fine grained solid with lower concentrations of Fe and Al oxides.

2.5.3 Chemical and mineralogical character of laterite

A feature of most laterites is the high content of the sesquioxides of iron and/or aluminum relative to the other components. These essential components are mixed in varied proportions. Some of the laterites may contain more than 80 per cent of Fe_2O_3 and little Al_2O_3 , while others may contain up to 60 per cent of alumina and only a few percent of Fe_2O_3 . In some cases, alkali and alkaline earth bases are absent but that is not an absolute criterion for laterite. In some cases, especially, some ferruginous crusts formed in alluvia and some concretionary horizons in ferruginous tropical soils may contain significant amounts.

Combined silica content is low in sesquioxide-rich laterites. This combined silica is in the form of kaolinite, the characteristic clay of most tropical formations. Although alumina is the main constituent, the sesquioxides of iron are the most common and the most frequent. Some laterites may contain manganese, titanium, vanadium and even chromium. Combined water determined by loss of ignition is always present in appreciable amounts especially in aluminous than ferruginous laterites.

2.5.4 Use of laterite in water treatment studies

The use of laterite in water treatment is gaining prominence. There are a number of studies that have focused on the use of laterite for water treatment. Laterite has proven to be an efficient adsorbent for fluoride adsorption in contaminated water (Gomoro *et al.*, 2012; Wambu *et al.*, 2012; Maiti *et al.*, 2011; Sarkar *et al.*, 2006). There have been investigations in the use of laterite to remove phosphorus from surface water (Zhang *et al.*, 2011). Also there has been investigations done to remove arsenic from water using laterite which has metal oxy-hydroxides of aluminum and iron (Glocheux *et al.*, 2013; Maiti *et al.*, 2012; Partey *et al.*, 2009; Halim *et al.*, 2008; Maji *et al.*, 2008). The laterite material is a preferred adsorbent for fluoride removal because it is readily available in the area of study and processing cost is low. Laterite only needs to be dug and transported to the laboratory and then washed and dried before further processing. Laterite consists of silica, alumina and metal oxides making it a good material for fluoride adsorption (Sarkar *et al.*, 2006). Sarkar *et al.* (2006) investigated the use of raw laterite from India as an adsorbent for fluoride removal. It was revealed in their work that the laterite material used had a chemical composition of Al₂O₃ (14.51%), Fe₂O₃ (3.70%) and SiO₂ (72.9%) and that these minerals formed the majority of the minerals present in the laterite. The X-ray diffraction (XRD) analyses showed the

presence of alumina and silica and these minerals may have contributed to the fluoride uptake. It was found that the laterite used performed well at lower fluoride concentrations, increased agitation time, smaller particle sizes, lower temperature and increased laterite dose.

Craig *et al.* (2015) also investigated laterite use in fluoride removal from contaminated groundwater in Ghana by comparing the efficiency of laterite with bauxite and alumina. In her work, the laterite used had a silica content of 70.9%, Fe_2O_3 (as goethite and hematite) content of 36.8% and alumina content was at 13.5%. The study showed that although laterite could remove fluoride from water, the efficiency was not as good as bauxite and alumina.

2.5.5 Modification of laterite for use in water treatment

The use of natural materials as adsorbents for removal of fluoride is available in detail in the literature. However, it is found that the adsorption capacities of these natural materials may be low (Osei *et al.*, 2015) and the material adsorptive surface had to be modified or activated to enhance fluoride uptake.

The work of Wambu *et al.* (2012) which involved the adsorption of fluoride ions from water using acid treated lateritic material from Kenya is of importance in this study. The adsorptive capacity of the laterite material for fluoride adsorption was enhanced by activating the material with 0.1 N HCl. It was shown in the study that acid activation of the laterite increased the fluoride adsorption from 20% for the untreated laterite to 80% after treatment with the acid. The activation with acid resulted in the

protonation of the surface sites of the material and thus increasing the overall positive charge and potential for fluoride adsorption.

Gomoro *et al.* (2012) also investigated the use of laterite for fluoride removal by thermally treating the laterite to improve the adsorption capacity of laterite for fluoride uptake. Results from the study showed an improvement in the adsorption capacity as a result of the heat treatment. The maximum adsorption was obtained for laterite samples fired at 500°C. In another study carried out by Maiti *et al.* (2011), laterite was modified by treating first with acid and followed by a base. The study revealed that the modification improved the adsorption capacity of laterite.

2.6 Adsorption mechanism and kinetic considerations

2.6.1 Adsorption models/isotherms

Adsorption isotherms are useful in obtaining information about the mechanism of adsorption. Adsorption equilibrium is established when the sorbate concentration in bulk solution is in dynamic balance with that on the liquid-solid interface (Chen and McGill, 1999). The isothermic models Langmuir and Freundlich are used to describe the equilibrium data.

The Langmuir model hypothesizes that uptake occurs on a homogenous surface by monolayer sorption without interaction between the adsorbed molecules. This empirical model assumes that each molecule has similar or unique sorption activation energy with no transmigration of the adsorbate in the plane of the surface (Liu, 2006). According to Sohn and Kim (2005), the three important premises of Langmuir isotherm are;

- (1) Monolayer coverage
- (2) Adsorption site equivalence and
- (3) Independence.

However, the second and third assumptions do not always hold because solutes will have tendency to adsorb onto more active sites where pre-adsorbed molecules could be easily displaced. According to Foo and Hameed (2010), the linear forms of Langmuir isotherm are represented as;

$$\frac{c_e}{q_e} = \frac{1}{Q_{max}b} + \frac{c_e}{Q_{max}} \quad (2.9)$$

$$\frac{1}{q_e} = \left(\frac{1}{Q_{max}b}\right)\frac{1}{c_e} + \frac{1}{Q_0} \quad (2.10)$$

$$q_e = Q_{max} - \left(\frac{1}{b}\right)\frac{q_e}{c_e} \quad (2.11)$$

$$\frac{q_e}{c_e} = bQ_{max} - bq_e \quad (2.12)$$

The sorption capacity (Q_{max}) is the amount of adsorbate at complete monolayer coverage (mg/g), it gives the maximum sorption capacity of sorbent and b (Litres/mg) is the Langmuir isotherm constant that relates to the energy of adsorption (Chen *et al.*, 2011). The respective values of Q_{max} and b are determined from the slope and intercept of the straight line plot of C_e/q_e versus C_e or a plot of $1/q_e$ versus $1/C_e$. In order to find out the feasibility of the isotherm, the essential characteristics of the Langmuir isotherm can be expressed in terms of a dimensionless constant separation factor or equilibrium parameter, R_L ;

$$R_L = \frac{1}{1+bC_0} \quad (2.13)$$

Where b (L/mg) is the Langmuir isotherm constant and C_0 is the initial concentration of fluoride (mg/L). There are four probabilities for the R_L value;

- (1) For favorable adsorption $0 < R_L < 1$

(2) For unfavorable adsorption $R_L > 1$ (3) For linear adsorption

$R_L = 1$ and

(4) For irreversible adsorption $R_L = 0$.

The Freundlich isotherm also has empirical origin, but it is extremely useful for experimentally determining the adsorption capacity, K_F .

It is expressed as;

$$q_e = K_F C_e^{1/n} \quad (2.14)$$

Where n is constant representing adsorption intensity and is always greater than unity.

The corresponding linear form of the equation is;

$$\ln q_e = \ln K_F + \frac{1}{n} \ln C_e \quad (2.15)$$

The model is useful in describing multilayer sorption and sorption on heterogeneous surfaces (Ho *et al.*, 2002).

The Freundlich isotherm is linear if $1/n = 1$ and as $1/n$ decreases, the isotherm becomes non-linear. The values of $1/n$ less than 1 show good adsorption intensity (Babaeivani and Khodadoust, 2013). The units for q_e and C_e should be consistent if parameters are to have any practical application. The units for K_F depend on the value of $1/n$ and are comparable only when their $1/n$ parameters are the same (Chen and McGill, 1999).

2.6.2 Limitations of the Freundlich and Langmuir models

According to Ayoob and Gupta (2008), these adsorption models suffer two limitations;

1. The model parameters obtained are usually unique for a particular set of conditions and that cannot be used as a prediction model for another.

2. The models are unable to provide a fundamental understanding of ion adsorption. However, the fact that the models are in continuous use shows their ability to fit a wide variety of adsorption data quite well. It is also a reflection of the appealing simplicity of the isotherm equations and the ease with which their adjustable parameters can be estimated.

2.6.3 Sorption dynamics

Sorption mechanism involving mass transport and chemical reaction processes could be understood with two types of models; reaction-based and diffusion-based models.

The prediction of the sorption kinetics is important for the design of industrial adsorption column.

2.6.3.1 Reaction-based models

The sorption mechanism of fluoride removal could be investigated using the pseudo first order and pseudo-second-order kinetic models at different experimental conditions.

A simple pseudo-first-order kinetic model according to Sundaram *et al.* (2008) is represented by Equation (2.16);

$$\log(q_e - q_t) = \log q_e - \frac{K_{ad}}{2.303} t \quad (2.16)$$

Where q_t is the amount of fluoride on the surface of the sorbent at time t (mg/g) and K_{ad} is the equilibrium rate constant of pseudo-first-order sorption. The straight line plots of $\log (q_e - q_t)$ against t for different experimental conditions will give the value of

the rate constant, K_{ad} . Linear plots of $\log (q_e - q_t)$ against t give straight line which indicates the applicability of pseudo-first order equation.

The most popular linear form of the pseudo-second-order kinetic model according to Sundaram *et al.* (2008) is;

$$\frac{t}{q_t} = \frac{1}{h} + \frac{t}{q_e} \quad (2.17)$$

Where, $q_t = q_e^2 K t / (1 + q_e K t)$, amount of fluoride on the surface of the sorbent at any time, (mg/g), K is the pseudo-second-order rate constant (g/mgmin), q_e is the amount of fluoride ion adsorbed at equilibrium (mg/g) and the initial sorption rate, $h = K q_e^2$ (mg/g min). The value of q_e (1/slope), K (slope²/intercept) and h (1/intercept) of the pseudo-second-order equation can be found experimentally by plotting t/q_t against t .

2.6.3.2 Diffusion models

For a solid-liquid sorption process, the solute transfer is usually characterized either by particle diffusion or pore diffusion control (Sundaram *et al.*, 2008).

A simple equation for particle diffusion controlled sorption process according to Meenakshi and Viswanathan (2007) is as follows;

$$\ln \left(1 - \frac{C_t}{C_e} \right) = -K_p t \quad (2.18)$$

Where K_p is the particle rate constant (min^{-1}). The value of particle rate constant is obtained by the slope of $\ln (1 - C_t/C_e)$ against t .

The pore diffusion model used here refers to the theory proposed by Weber and Morris (1964). The intraparticle diffusion equation is given below;

$$q_t = K_i t^{1/2} + C \quad (2.19)$$

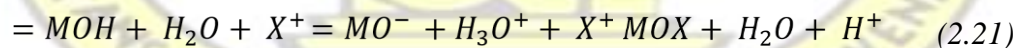
Where K_i is the intraparticle rate constant ($\text{mg/g min}^{0.5}$) and C is the thickness of the boundary layer. The slope of the plot of q_t against $t^{1/2}$ will give the value of intraparticle rate constant.

2.6.4 Mechanism for fluoride uptake

Various investigators have studied the mechanism of fluoride adsorption on various adsorption media, which among others include Sujana *et al.*, 2009; Sujana and Anand, 2010; Sujana and Anand, 2011; Mohapatra *et al.*, 2009; Bhatnagar *et al.*, 2011 and Jinadasa *et al.*, 1993. In the case of the use of lateritic materials such as bauxite and lateritic soils, the results by Sujana *et al.* (2009; 2010; 2011) and Jinadasa *et al.* (1993) are relevant. Sujana *et al.* (2009; 2010; 2011) have suggested for adsorption on Fe/Al hydroxides the mechanism for fluoride adsorption in acid media is by anion exchange that can be represented by (2.20):



They reasoned that fluoride adsorption in the basic media was controlled by van der Waals forces and could be expressed as (2.21):



Where, X^+ represents a cation such as Na^+ .

In the discussion on fluoride adsorption on goethite surfaces, Jinadasa *et al.* (1993) have suggested reactions for fluoride adsorption onto goethite, which do not only involve OH^- ion exchange:

(2.22)



Reaction (2.22) represents an ion exchange reaction, whilst reactions (2.23) and (2.24) represent adsorption due to specific surface reactions.

2.7 Analytical procedures for the determination of fluoride concentration in solutions

There are a variety of analytical methods for the determination of fluoride concentration in water. These include direct spectrophotometric methods (Yamamura *et al.*, 1962), colorimetric methods (Zhu *et al.*, 2005), ion chromatographic methods (Bayon *et al.*, 1999) and potentiometric methods using ion-selective electrodes (Thomas and Gluskoter, 1974). However, potentiometric methods using ion-selective electrodes have wider usage due to the fact that it is easy to use the electrodes and the electrodes have response to a wider concentration range. There is also the advantage of a rapid response time and not affected by colour or turbidity of the sample.

2.8 The role of Total Ion Solution Adjustment Buffer (TISAB) solutions in fluoride determination

The presence of various ions in the solution inhibits the response of the fluoride electrode. These ions include phosphate, citrate, bicarbonate and polyvalent cations. Polyvalent cations (e.g. Al^{3+} , Fe^{3+}) interfere forming complexes with fluoride which are not measured by the fluoride ion selective electrode. Aluminum–Fluoride complex ions are about ten times more stable than Iron (III) Fluoride complex ions. As the

aluminum concentration increases, more fluoride is consumed to form the metal fluoride complex. Additionally, TISAB, which contains a strong chelating agent, eliminates the interference by complexing polyvalent cations. The hydroxide ion is measured directly by the electrode. The addition of TISAB minimizes the effect of the hydroxide ion by buffering the solution at pH 5-5.5.

Sample pH is critical. At low pH values, fluoride forms bifluoride ($[\text{HF}_2]^-$) which is not detected by fluoride ion selective electrode (FISE). Again adding TISAB prevents this interference by buffering the pH. Temperature changes affect electrode potentials. Therefore, standards and samples are equilibrated at the same temperature.

CHAPTER THREE

MATERIALS AND METHODS

Described in this chapter are materials used, experimental procedures developed and adopted for the study of fluoride adsorption process on laterite. Different laterite samples were characterized for fluoride adsorption. Alumina modified laterite (AML) was synthesized and characterized for fluoride adsorption. The general analytical scheme that was followed to carry out this work is described in the scheme (Figure 3.1).

3.1 Materials

The main materials used for the study included laterite samples collected from three areas in the Bongo district of the Upper East Region of Ghana namely, Agamolga, Balungu and Dua. Commercial grade alumina was obtained from the local aluminum smelter, Volta Aluminum Company (VALCO) in Ghana.

3.1.1 Selection of laterite and sample preparation

Laterite samples were taken from burrow pits which have been excavated for road construction purposes from Agamolga, Balungu and Dua in the Bongo district of the Upper East Region of Ghana. Figure 3.2 is a map showing the places (underlined in the map) in the Bongo district where laterite materials were taken.



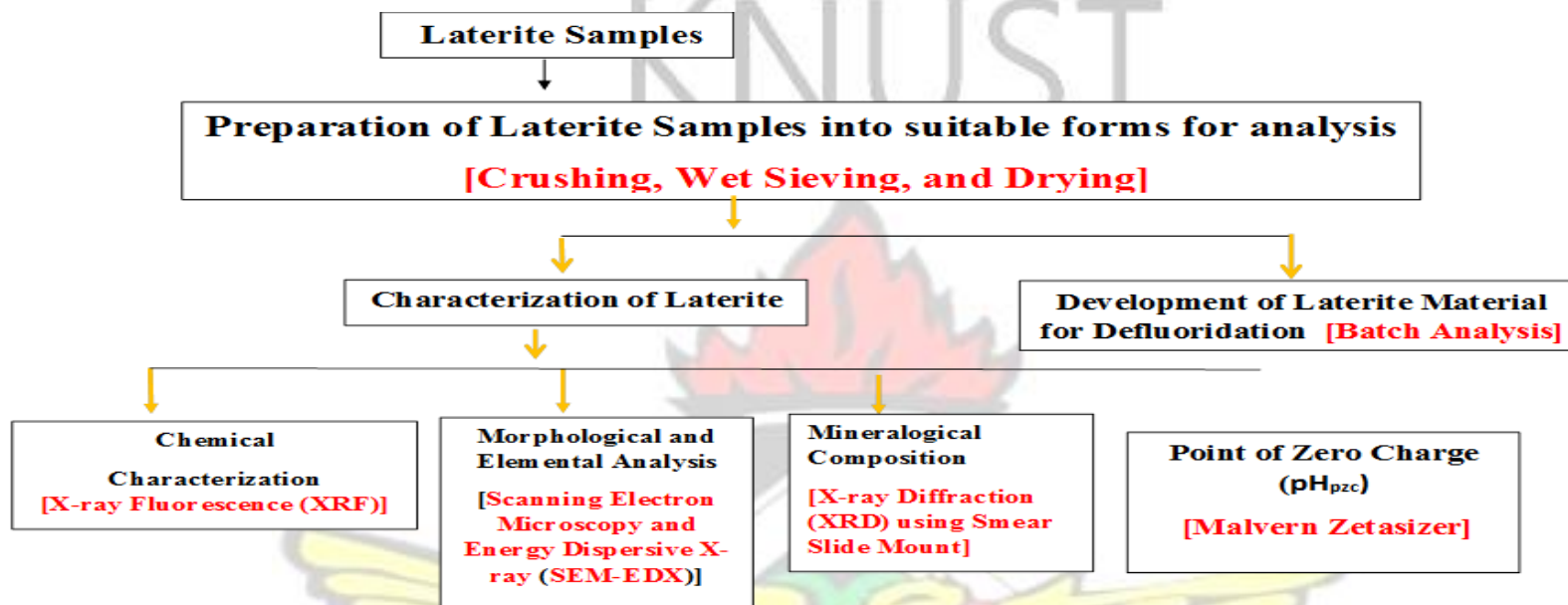


Figure 3.1: General analytical scheme.

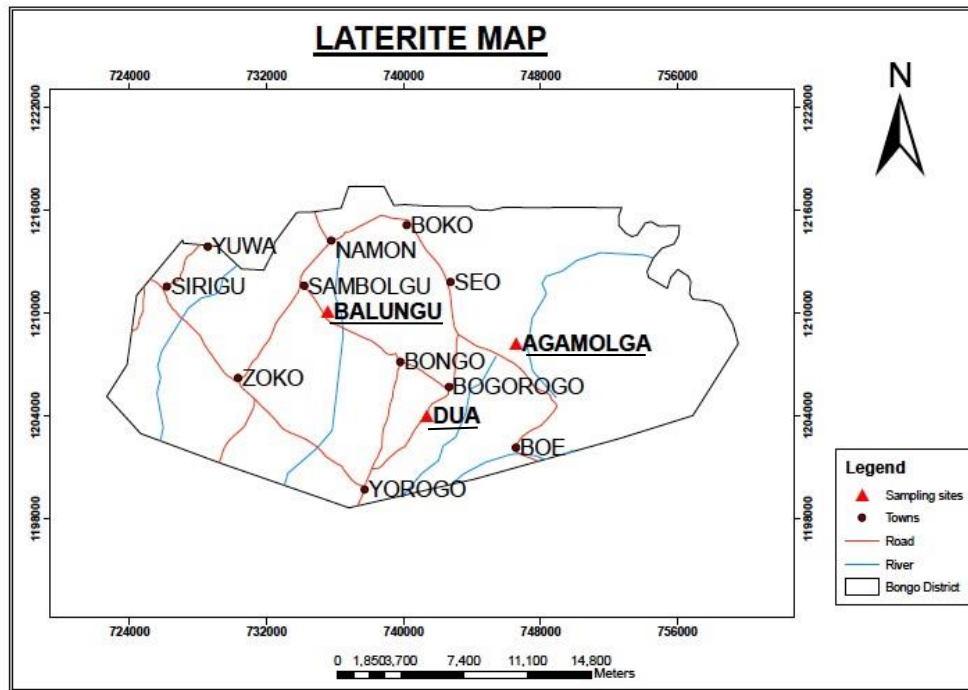


Figure 3. 2: A map showing locations (underlined) where laterite samples were collected.

The samples were sun dried, crushed, milled and wet-sieved to obtain particle size fractions <90, 90-125, 125-180, 180-500 and 500-1000 μm using appropriate sieves.

3.1.2 Alumina samples

Commercial grade alumina powder was obtained from the local aluminum smelter, VALCO in Ghana. The powder was washed with 1 M HCl and 1 M NaOH concurrently to remove possible impurities and then dried in an oven. The alumina was then further milled into fine powder and used to prepare the alumina modified laterite for fluoride adsorption.

3.2 METHODS

3.2.1 Characterization of laterite samples

The chemical and mineral compositions of the laterite samples used in this study were determined using X-ray Fluorescence (XRF) spectrometry, X-ray Diffraction (XRD) and Scanning Electron Microscopy-Energy Dispersive X-ray Spectroscopy (SEM-EDX).

3.2.1.1 XRF analysis

The chemical compositions of the different laterite samples were determined using X-ray Fluorescence (XRF) analysis. Major and minor elements in the laterites were measured using the XRF machine (Spectro-X-Lab 2000) at the Geological Survey Department in Accra and presented as oxides. About 4 g of the laterite was measured and mixed with about 0.09 g of wax to bind the laterite particles together. The mixture was pulverized in a milling machine (RETSCH Mixer miller (MM301)) into very fine powder. The pulverized sample was placed in a disc and placed under the hydraulic press (SPECAC hydraulic press). The pellet produced was placed in the Spectro X-Lab XRF machine to determine the major and minor oxides.

3.2.1.2 XRD analysis

The mineral phases of each sorbent collected from the three sites was determined using X-ray diffraction (XRD) analysis. About 5 g portions of each milled fraction were pulverized in laboratory ceramic mortar and pestle. The powders were pressed and side-loaded into specially-designed sample holders and aligned in front of the Xray

beam on a goniometer of a Siemens D5000 Advance X-ray diffractometer. The analysis included elucidation of the mineral phases of the laterite. The resulting XRD scans were viewed and interpreted using the Siemens XRD data evaluation (EVA) software. Background correction and Fourier transformation were performed on each scan before interpretation. Minerals were identified by matching to reference mineral patterns stored in the ICDD (International Centre for Diffraction Data). This analysis was done at the Materials Laboratory of KNUST, Kumasi.

3.2.1.3 SEM analysis

SEM and EDX analyses were recorded using FEI Quantus 3D FEG SEM 20kV. Samples were prepared by dispersing dry powder on double sided conductive adhesive tape and coated with 15nm platinum powder to increase conductivity and reduce charging effect in SEM for texture and elemental analysis. This analysis was done at the Mechanical Laboratory of Southern University and A.M College, Baton Rouge, Louisiana, USA.

3.2.1.4 Electrophoretic studies

The pH at which the zeta potential is zero is the isoelectric point (IEP) (Tripathy *et al.*, 2006). The IEP of the three laterite samples were determined by measuring the zeta potential using the Malvern Zetasizer Nano ZS at the laboratory of UNESCOIHE, Netherlands.

The Isoelectric points of the three laterite samples were determined in a 1 mM KNO_3 electrolyte. Laterite samples were prepared for analyses by crushing each of the samples into very fine powder. Samples in solution were prepared without settling the

particles and slightly turbid. Air bubbles inside the suspensions were removed and samples brought to room temperature before measuring with the Zetasizer. The titrants used were 0.1 M HCl and 0.1 M NaOH.

3.2.2 Heat treatment

Laterite samples were heat-treated to verify if any changes would occur in the mineralogy as a result of the heat treatment and also to determine the effect of heat treatment on fluoride adsorption. Thirty grams of laterite (<90 μm , 90-125 μm , 125-180 μm , 180-500 μm and 500-1000 μm size fractions) were each weighed into different crucibles and heat treated in a furnace at temperatures of 200, 300, 400, 500 and 600°C for 2 hours, 4 hours and 6 hours. At the end of each particular period of firing, the heat treated soil sample was removed from the furnace and kept in a desiccator to cool to room temperature before it was used for the defluoridation experiments.

3.2.3 Preparation of fluoride solution

All reagents used were of analytical grade. A stock solution (100 mgF⁻/L) was prepared by dissolving 0.221 g NaF in 1 L deionized water. All the solutions used for fluoride removal experiments and analysis were prepared by an appropriate dilution from the stock solution.

3.2.4 Preparation of TISAB

TISAB II was prepared by pouring 500 ml deionized water in a 1000 mL beaker.

About 57 mL glacial acetic acid, 58 g reagent grade sodium chloride and 4 g of 1, 2-cyclohexylenedinitrilotetraacetic acid (CDTA) were added to 500 mL deionized water in a 1000 mL beaker. The CDTA is the decomplexing agent that releases all complexed F^- into free F^- ions, which are measureable with FISE. The beaker was placed in a water bath for cooling. A calibrated pH electrode was immersed into the solution whilst slowly adding 5 M NaOH until the pH reached 5.08. Solution was cooled to room temperature and deionized water was added to make it up to the 1 L mark of the volumetric flask.

3.2.5 Analysis of fluoride solutions

Fluoride ion concentrations >0.1 mg/L were measured using a fluoride ion selective electrode (Orion 290A+) connected to a single junction calomel reference electrode (Orion model 9609BNWP ion plus sure-flow fluoride on an advanced ISE/pH/mV/ORP meter). Total ion solution adjustment buffer (TISAB II) was added to each solution before measurement. Fluoride ions are selectively adsorbed by the ISE membrane establishing a potential or voltage whose magnitude is proportional to the concentration of fluoride in the sample. This potential is compared to the constant potential of a reference electrode. By measuring the potential of known standards, a calibration curve was constructed for determining the concentration of fluoride in unknown samples. In each case, 5 mL of fluoride containing solution (standards and unknown), 5 mL of TISAB II buffer was added and fluoride concentration determined with the meter.

3.2.6 Adsorption tests with laterite

Fluoride uptake by the raw laterite samples was investigated by weighing 10 g of sample each time into a beaker. 100 mL of 10 mg/L fluoride solution prepared from the stock solution was added and stirred. Solution samples were taken at contact times of 2.5, 5, 10, 15, 20, 25, 30, and 35 minutes for fluoride analysis. The pH of the solution was determined before, during and after each defluoridation experiment. Initial tests were conducted with 180-500 μm sample fractions to determine the effect of pre-treatment temperature on adsorption. Based on the results obtained, 400°C and 2 hours pre-treatment time were selected for subsequent adsorption tests. The pH of the solutions was monitored for the heat-treated and unheated laterites from the three sites.

3.3 Alumina modified laterite (AML) material

3.3.1 Preparation of AML

To improve the adsorptive surface of laterite for fluoride uptake, laterite was coated with alumina and heat-treated. Laterite of particle size range of 180-500 μm was selected, thoroughly washed with demineralized water and air-dried before use for modification. The 180-500 μm particle size laterite was selected over smaller particle sizes to avoid clogging of columns when the material is put in a column. A weighed amount of alumina was taken and ground to very fine powder, mixed with sufficient deionized water to form a pulp. Weighed amounts of laterite at different ratios (1, 3, 5 and 7 g of alumina to 10 g of laterite) were added and mixed thoroughly. The mixture was dried in a Heraeus electric oven at 110°C until completely dried. Dried samples

were allowed to cool and then calcined in a Vecstar model furnace at a temperature of 400°C for 2 hours.

3.3.2 Characterization of AML

SEM-EDX analysis was conducted on selected AML samples for morphological as well as elemental analysis. XRD analyses were also carried out on selected material (AML) to determine whether any phase transformation had taken place.

3.3.3 Batch adsorption studies with AML

The adsorption of fluoride on AML material was studied at room temperature ($27\pm 2^\circ\text{C}$) by batch experiments. 100 mL of fluoride solution of concentration (10 mg/L) in 250 mL polyethylene bottle was shaken with 4 g of adsorbent for 35 minutes on a shaker. The bottles were capped to prevent exchange of CO_2 in order to achieve a stable pH during the experiments. At specified times (2.5, 5, 10, 15, 20, 25, 30, 35 minutes), aliquots samples were taken to analyze for fluoride with fluoride ion selective electrode. The pH was measured after each aliquot sample is taken. The pH of the blank fluoride solution (10 mg/L) was observed to be between 5.7 and 6.2. The amount of fluoride adsorbed at any time t , (q_t in mg g^{-1}) was determined as follows;

$$q_t = \frac{(C_0 - C_t)V}{W} \quad (3.1)$$

Where c_0 and c_t (mg/L) are the initial fluoride concentrations and concentrations at time t , V is the volume of solution (L) and W is the mass of the adsorbent (g). Data for adsorption isotherm was obtained by varying the initial fluoride concentration between 5 and 50 mg/L at pH 6.0-6.2.

3.3.4 Competitive uptake of anions experiments

In order to find the effect of individual co-existing ions on the adsorption of fluoride onto AML material, different concentrations of five anions (nitrate, sulphate, chloride, phosphate and bicarbonate) were selected. The sodium salts of each of the anions mentioned above was used. A 100 mL volume of each solution with an initial fluoride concentration of 10 mg/L was mixed with 4 g of AML material, and the analysis was performed similar to the batch adsorption tests.



CHAPTER FOUR

RESULTS

4.1 Tests with laterite materials

4.1.1 Chemical characterization of raw laterite samples

The chemical compositions of the different laterite samples were determined using XRF. Results from the determinations are presented as major elements in Table 4.1 and minor elements in Table 4.2.

Table 4.1: Composition of the major elements in the raw laterite samples.

Major Elements as oxide	Composition (mass %)		
	Agamolga	Balungu	Dua
SiO ₂	29.53	21.81	31.78
TiO ₂	0.55	0.50	0.40
Al ₂ O ₃	11.07	4.94	8.00
Fe ₂ O ₃	25.82	42.33	5.70
MnO	0.11	0.84	0.02
MgO	0.78	0.68	0.74
CaO	0.09	0.12	0.08
Na ₂ O	0.53	0.57	0.44
K ₂ O	0.03	0.43	4.48
P ₂ O ₅	0.16	0.15	0.12
SO ₃	0.01	0.01	0.06
Cl	0.14	0.15	0.13
<u>L.O.I</u>	<u>31.20</u>	<u>27.50</u>	<u>48.10</u>

Total	100.02	100.04	100.05
-------	--------	--------	--------

KNUST



Table 4.2: Composition of minor elements in the raw laterite samples.

Minor elements (mg/kg)	Agamolga	Balungu	Dua	Minor elements (mg/kg)	Agamolga	Balungu	Dua
V	576	796	163.3	Mo	7.8	11.6	66.5
Cr	877.3	761.7	208.7	Sb	1.5	4	3.9
Co	93.2	351	50.8	I	3.9	1.5	1.5
Ni	3.7	28.8	1.8	Cs	1.5	1.5	8.1
Cu	34.6	76.6	15.4	Ba	134.2	1273	2168
Zn	19.5	31.1	23.1	La	2	2	10.9
Ga	19	17.7	15.8	Ce	476.1	801.4	54.5
As	5	19.8	0.8	Hf	4.6	7.7	2.5
Rb	6.6	10.8	66.6	Ta	9	16	4.9
Sr	15.2	17.1	299.8	Pb	39.1	52.2	20.2
Y	6.6	13.8	6.3	Bi	1.7	1.9	8.1
Zr	174	152.4	134.5	Th	12.2	9.6	6
Nb	9.5	8.4	7.6	U	3	2.3	2

KNUST



4.1.2 Phase/mineralogical composition of the raw laterite samples

Results of XRD and SEM analyses of the Agamolga, Balungu and Dua laterite samples are presented in Figures 4.1-4.4. The pH_{pzc} of the three laterites was determined and the results are shown in Table 4.3.

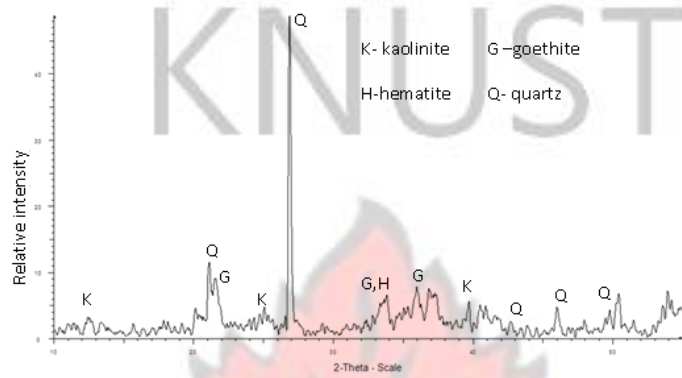


Figure 4.1: X-ray diffraction pattern of Agamolga laterite sample.

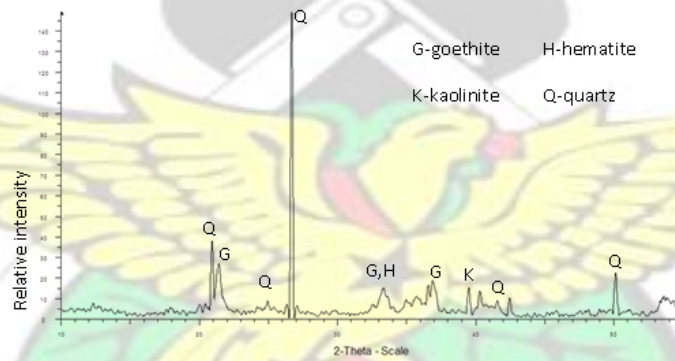


Figure 4.2: X-ray diffraction pattern of Balungu laterite sample.

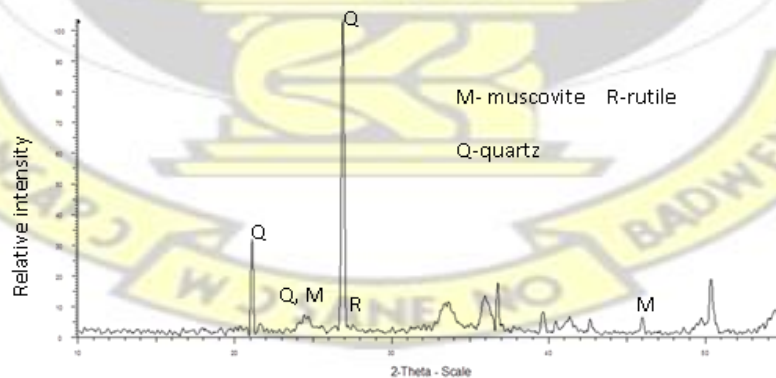


Figure 4.3: X-ray diffraction pattern of Dua laterite sample.

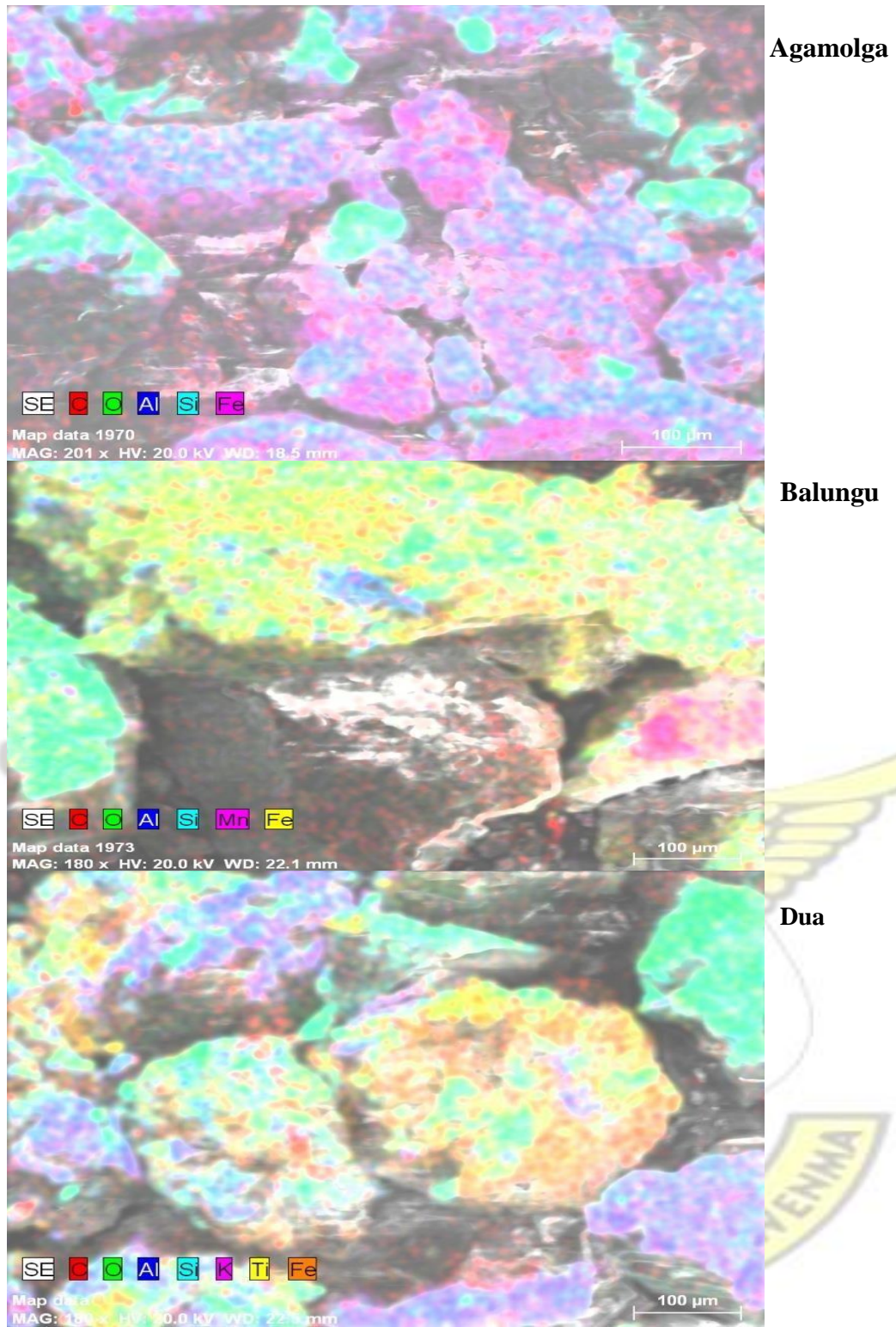


Figure 4.4 : SEM image of Agamolga, Balungu and Dua laterite.

Table 4.3: Point of zero charge (pH_{pzc}) results of Agamolga, Balungu and Dua laterite.

Laterite sample	pH _{pzc}
Agamolga	3.75
Balungu	4.36
Dua	2.99

4.1.3 Effect of particle size on fluoride uptake by Balungu laterite material

The effect of grain sizes of Balungu laterite on fluoride uptake was investigated and the results are presented in Table 4.4.

Table 4.4: Effect of particle size of Balungu laterite on fluoride adsorption.

Time (minutes)	Residual fluoride concentration (mg/L)			
	<90(μm)	90-125(μm)	180-500(μm)	>500(μm)
0	10	10	10	10
2.5	4.23	4.47	8.19	8.93
5	3.81	3.69	6.61	8.63
10	2.54	3.36	4.77	8.09
15	2.36	3.02	3.96	7.56
20	2.15	2.79	3.37	7.17
25	1.87	2.63	2.97	6.85
30	1.75	2.47	2.69	6.43
35	1.82	2.46	2.47	5.94

4.1.4 Adsorption tests with the raw and laterite heat-treated at 400°C

Agamolga, Balungu and Dua laterites were contacted with 10 mg/L of fluoride solution. Laterites of particle size fractions of 180-500 μm were used for the analysis. The results of the analysis are presented in Table 4.5 for changes in fluoride concentration and Table 4.6 for changes in pH during adsorption.

Table 4.5: Fluoride uptake by raw and heat treated (HT) laterites at 400°C.

Time(minutes)	Residual fluoride concentration(mg/L)					
	Agamolga		Balungu		Dua	
	Raw	HT	Raw	HT	Raw	HT
0	9.87	10.01	10.02	10.15	9.87	10.16
2.5	8.52	5.34	8.04	8.19	8.96	6.69
5	7.71	4.63	7.53	6.61	8.36	6.23
10	7.39	4.01	6.89	4.76	7.92	5.52
15	6.97	3.19	6.58	3.96	7.83	4.90
20	6.38	2.89	6.71	3.36	7.71	4.79
25	6.16	2.62	6.71	2.97	7.65	4.45
30	5.91	2.29	5.86	2.69	7.56	4.00
35	5.59	2.17	5.30	2.47	7.14	4.19

Table 4.6: Changes in solution pH during adsorption of fluoride by Agamolga, Balungu and Dua laterites.

Time(minutes)	pH					
	Agamolga		Balungu		Dua	
	Raw	HT	Raw	HT	Raw	HT
0	5.18	6.02	5.12	6.05	5.24	6.13
2.5	7.25	7.34	6.57	6.22	6.98	7.32
5	7.28	7.67	6.58	6.51	6.99	7.50
10	7.34	7.71	6.61	6.54	7.07	7.47
15	7.40	7.71	6.68	6.56	7.05	7.43
20	7.44	7.72	6.77	6.56	7.09	7.38
25	7.42	7.70	6.76	6.56	7.05	7.35
30	7.48	7.69	6.68	6.53	7.09	7.33
35	7.48	7.69	6.71	-	7.10	7.33

4.1.5 Effect of initial pH of solution on fluoride uptake by laterites heat-treated at 400°C

The initial pH of the fluoride solution was varied to determine the effect of pH on fluoride uptake. The results of fluoride concentration and solution pH changes are shown in Tables 4.7-4.12 for the three different laterite samples.

Table 4.7: Effect of initial pH on fluoride adsorption by Agamolga laterite

Time (minutes)	Residual fluoride concentration								
	pH6.02*	pH2	pH3	pH3.94	pH6	pH9	pH10.1	pH11	pH12
0	10.00	10.35	10.09	10.35	9.82	9.84	10.36	10.01	10.36
2.5	8.69	4.65	4.42	7.07	7.91	8.29	7.73	9.01	8.05
5	7.87	4.09	3.84	6.59	7.69	8.29	7.55	9.08	8.29
10	7.55	3.68	3.21	5.99	7.05	7.26	7.03	9.08	8.29
15	7.12	3.25	2.68	5.67	6.34	6.57	7.06	9.01	8.29
20	6.53	3.09	2.41	5.44	5.91	6.07	6.59	9.23	8.36
25	6.31	2.96	2.06	5.18	5.52	5.71	6.16	8.79	8.42
30	6.05	2.85	1.80	4.99	5.03	5.51	5.81	8.89	8.62
35	5.74	2.77	1.59	4.70	4.99	4.81	5.69	8.54	8.75

pH6.02- the pH of the fluoride solution without adding an acid or base

Table 4.8: pH changes at different time intervals after pH adjustment at varying starting pH by Agamolga laterite

Time (minutes)	pH at different time intervals after adjustment of initial pH								
	pH6.02*	pH2	pH3	pH3.94	pH6	pH9	pH10.1	pH11	pH12
2.5	6.21	2.13	3.94	5.98	6.69	7.69	8.43	10.68	11.82
5	7.25	2.13	4.08	6.14	6.86	7.58	8.34	10.54	11.69
10	7.28	2.16	4.53	6.54	6.99	7.52	8.04	10.43	11.53
15	7.34	2.29	4.68	6.73	7.11	7.51	7.92	10.3	11.47
20	7.40	2.3	4.71	6.83	7.12	7.47	7.86	10.23	11.37
25	7.44	2.3	4.87	6.92	7.14	7.47	7.82	10.13	11.28
30	7.42	2.35	4.97	6.98	7.17	7.45	7.85	10.08	11.25
35	7.48	2.36	5.06	7.01	7.24	7.42	7.84	9.98	11.20

Table 4.9: Effect of initial pH on fluoride adsorption by Balungu laterite.

Time (minutes)	Residual fluoride concentration (mg/L)								
	pH6.05*	pH2	pH3	pH4	pH6	pH9	pH9.99	pH11	pH12
0	10.02	9.99	10.09	9.99	10.00	10.04	10.23	9.92	9.87
2.5	8.04	6.05	6.65	7.76	7.29	8.02	7.35	8.64	8.33
5	7.53	5.59	6.73	7.14	7.11	7.99	7.17	8.61	8.11
10	6.89	5.29	6.22	6.12	5.64	6.96	6.45	8.37	7.94
15	6.58	5.06	5.93	5.34	4.92	6.16	5.99	7.96	7.53
20	6.71	4.86	5.39	4.97	4.53	5.43	5.59	8.08	7.47
25	6.71	4.86	4.90	4.57	4.19	4.95	5.29	7.92	7.47
30	5.86	4.73	4.60	4.43	3.59	4.50	4.65	7.71	7.36
35	5.30	4.64	4.28	4.07	3.25	4.26	4.51	7.41	7.39

pH6.05*- the pH of the solution when no acid or base has been added.

Table 4.10: Variation of solution pH during adsorption with Balungu laterite after initial pH adjustment.

Time(minutes)	pH at different time intervals after adjustment of initial pH								
	pH6.05*	pH2	pH3	pH4	pH6	pH9	pH9.99	pH11	pH12
2.5	6.57	2.12	3.54	5.97	6.36	7.45	8.45	10.36	11.87
5	6.58	2.26	3.68	6.11	6.49	7.41	8.06	10.21	11.76
10	6.61	2.37	4.25	6.35	6.57	7.32	7.60	10.17	11.61
15	6.68	2.49	4.49	6.43	6.63	7.26	7.46	10.10	11.4
20	6.77	2.61	4.53	6.50	6.67	7.26	7.36	9.87	11.35
25	6.76	2.68	4.75	6.53	6.75	7.26	7.26	9.81	11.19
30	6.68	2.80	4.83	6.57	6.79	7.26	7.17	9.66	11.10
35	6.71	2.92	5.00	6.57	6.84	7.26	7.20	9.56	11.02



Table 4.11: Effect of initial pH on fluoride adsorption by Dua laterite.

Time (minute)	Residual fluoride concentration								
	pH6.13*	pH2.01	pH3	pH4	pH6	pH9	pH10.1	pH11	pH12.02
0	10.0	10.27	10.16	10.27	10.15	10.13	10.34	9.98	10.34
2.5	9.09	4.99	5.34	7.29	7.59	9.03	7.47	8.04	7.18
5	8.48	4.47	5.22	7.12	7.69	9.22	7.17	8.04	7.23
10	8.04	4.18	5.16	6.57	6.91	8.82	7.35	7.69	6.95
15	7.95	3.66	4.73	6.46	6.79	8.46	7.21	7.60	6.86
20	7.83	3.47	4.67	6.21	6.58	8.36	7.23	7.36	6.64
25	7.77	3.47	4.52	5.86	6.39	8.09	6.92	6.74	6.69
30	7.68	3.43	4.41	5.86	6.16	8.02	6.75	7.30	6.81
35	7.26	3.34	4.34	5.75	6.01	7.92	6.59	7.66	6.75

pH6.13- pH of the solution when no acid or base has been added

Table 4.12: pH at different time intervals after pH adjustment at varying starting pH using Dua laterite.

Time (minutes)	pH at different time intervals after adjustment of initial pH								
	pH6.13*	pH2.01	pH3	pH4	pH6	pH9	pH10.1	pH11	pH12.02
2.5	6.98	2.03	3.30	5.63	6.67	7.70	8.71	10.67	11.88
5	6.99	2.03	3.34	5.94	6.83	7.64	8.58	10.56	11.88
10	7.07	2.01	3.42	6.14	6.89	7.60	8.27	10.52	11.85
15	7.05	2.00	3.43	6.22	6.93	7.57	8.10	10.44	11.79
20	7.09	2.01	3.51	6.34	6.96	7.52	7.97	10.38	11.83
25	7.05	2.01	3.59	6.43	7.02	7.49	7.93	10.35	11.84
30	7.09	1.98	3.64	6.49	7.03	7.48	7.88	10.30	11.82
35	7.10	2.00	3.66	6.57	7.06	7.40	7.83	10.24	11.82

KNUST



4.1.6 Contact time and initial fluoride concentration

The effect of contact time at various initial fluoride concentrations of solution with Balungu laterite was investigated and the results are presented in Table 4.13. The results are presented as amount of fluoride adsorbed, (q_t).

Table 4.13: Amount of fluoride adsorbed by Balungu laterite at different initial fluoride concentrations.

Time (minutes)	q_t for initial fluoride concentration (mg/g)		
	5mg/L	7.5mg/L	10mg/L
0	0.00	0.00	0.00
2.5	0.07	0.09	0.14
5	0.07	0.09	0.14
10	0.07	0.11	0.15
15	0.07	0.11	0.15
20	0.07	0.12	0.15
25	0.08	0.13	0.15
30	0.09	0.13	0.16
35	0.09	0.13	0.17

4.2 Tests with alumina modified laterite (AML)

4.2.1 Micro-structural characterisation of AML

The micro-structure of the AML material was examined using SEM EDX techniques. SEM images of AML were taken and the results are presented in Figure 4.5 for AML of composition of 10 g laterite plus 1g alumina and also for AML of composition of 10 g laterite plus 3 g alumina. In the SEM images below, red represents iron, yellow represents silicon, green is oxygen and blue is aluminum.

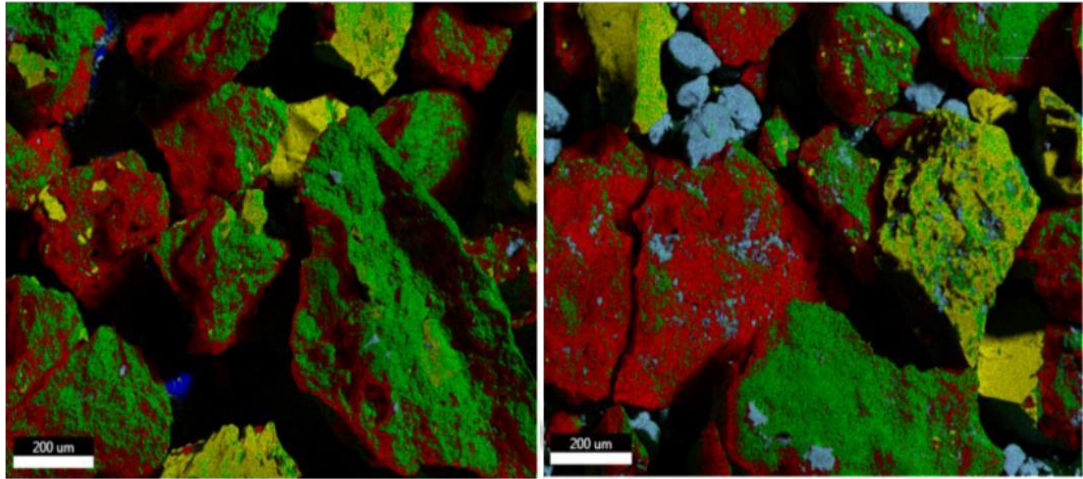


Figure 4.5: SEM image showing overlay of elements in AML of composition of (a) 10 g laterite plus 1 g alumina and (b) 10 g laterite plus 3 g alumina.

4.2.2 Adsorption responses of AML material treated at various temperatures

AML was heat treated at various temperatures and the F^- adsorption response was measured and presented as percentages of fluoride adsorption efficiency in Table

4.14. Fluoride adsorption efficiency (P) was calculated as;

$$P(\%) = \frac{C_0 - C_t}{C_0} * 100\% \quad (4.3)$$

Where P is fluoride adsorption efficiency (%), C_0 is the initial fluoride concentration (mg/L) and C_t is the fluoride concentration at time t (mg/L).

Table 4.14 Effect of heat treatment on adsorption efficiency by AML.

Time(minutes)	P (%)				
	200°C	300°C	400°C	500°C	600°C
2.5	78.88	78.44	68.12	78.29	80.96
5	87.69	87.36	83.15	87.83	86.54
10	91.38	89.82	90.56	92.04	89.82
15	92.26	91.91	94.91	93.37	90.71
20	93.02	92.91	95.16	93.99	91.56
25	93.45	93.66	95.71	94.28	91.66
30	93.89	94.20	96.04	94.32	92.33
35	94.16	94.34	97.13	94.54	93.19

4.2.3 Fluoride adsorption at different laterite-alumina ratios

Fluoride adsorption at different AML compositions is presented in Table 4.15. The values represent the rate of adsorption within 35 minutes of contact time.

Table 4.15: Effect of different ratios of alumina modified laterite on fluoride uptake.

Ratio	Rate of fluoride adsorption(mg/L.min)	
	Agamolga	Balungu
0.1	1.56	0.88
0.3	0.42	0.28
0.5	0.26	0.15
0.7	0.23	0.33

4.2.4 Fluoride adsorption at various initial solution pH

The initial pH of the fluoride solutions was adjusted by adding HCl or NaOH depending on the starting pH. AML material of composition 3 g alumina to 10 g laterite was used. 4 g of AML was contacted with 10 mg/L fluoride solution and the pH of the fluoride solution was adjusted to values between 2 and 11. The results are shown in Table 4.16 for F⁻ concentration profile during adsorption and Table 4.17 for solution pH during adsorption.

Table 4.16: Effect of initial pH of fluoride solution on fluoride uptake by AML.

Time(min)	Residual fluoride concentration(mg/L)								
	pH5.96*	pH2.04	pH3.01	pH4.03	pH5.52	pH6.04	pH9.03	pH10.04	pH11.01
0	10.00	9.99	9.99	10.01	10.13	10.00	10.10	9.98	9.99
2.5	1.83	3.35	3.62	2.09	2.27	1.66	3.64	7.06	7.99
5	1.10	3.39	3.17	1.08	1.26	1.15	2.34	6.91	8.06
10	0.75	3.45	2.47	0.63	0.86	0.77	1.71	5.57	7.99
15	0.60	3.46	1.92	0.49	0.71	0.63	1.46	5.27	7.75
20	0.56	3.34	1.53	0.49	0.62	0.60	1.36	4.79	7.81
25	0.49	3.28	1.33	0.42	0.58	0.54	1.21	4.52	7.48
30	0.33	3.36	1.13	0.39	0.56	0.52	1.13	4.47	7.25
35	0.42	3.11	0.99	0.38	0.50	0.52	1.12	4.25	7.25

pH 5.96- pH of the solution when no acid or base has been added.

Table 4.17: Solution pH during adsorption by AML in acidic and alkaline pH ranges.

Time (min)	Solution pH (mg/L)								
	pH5.96*	pH2.04	pH3.01	pH4.03	pH5.52	pH6.04	pH9.03	pH10.04	pH11.01
5	6.90	2.20	4.10	5.20	-	6.30	7.80	9.30	10.50
10	7.20	2.30	4.30	5.50	5.80	6.30	7.60	8.70	10.40
15	7.20	2.30	4.30	5.70	6.10	6.40	7.50	8.60	10.30
20	6.90	2.40	4.40	5.80	6.30	6.50	7.30	8.40	10.30
25	7.10	2.40	4.40	5.90	6.20	6.50	7.40	8.40	10.30
30	6.90	2.50	4.50	6.00	6.40	6.50	7.40	8.40	10.20
35	7.10	2.50	4.50	6.20	6.40	6.50	7.30	8.30	10.20

4.2.5 Effect of sorbent dosage and initial fluoride concentration

Using an AML composition of 3 g alumina and 10 g laterite, the dosage of AML was varied between 1 g and 10 g in a 10 mg/L F⁻ solution. The time allowed for the removal was 35 minutes. The results in percentage of fluoride removal are presented in Table 4.18.

Table 4.18: Effect of adsorbent dosage on fluoride uptake by AML.

Dosage (g/100 mL)	Percentage of Fluoride Removal (%)
1	60.72
3	88.41
4	97.13
7	96.24
10	97.47

4.2.6 Effect of initial fluoride concentration on fluoride adsorption by AML

Initial fluoride concentration of the solution was varied between 1.5-15 mg/L and tested with AML material of same composition and dosage. The adsorption data is presented in Table 4.19.

Table 4.19: Effect of initial concentration of fluoride solution on fluoride uptake by AML.

Time (minutes)	Residual fluoride concentration (mg/L)				
	1.5mg/L	3mg/L	5mg/L	10mg/L	15mg/L
2.5	0.16	0.39	0.94	3.45	5.22
5	0.12	0.25	0.45	2.46	4.43
10	0.11	0.17	0.34	1.94	3.52
15	0.10	0.14	0.26	1.68	2.80
20	0.09	0.14	0.24	1.44	2.43
25	0.09	0.14	0.24	1.43	2.22
30	0.08 0.08	0.13 0.13	0.23 0.21	1.33	2.05 2.06
35				1.30	

4.2.7 Adsorption in the presence of competing anions

There are other anions in natural water that can compete with fluoride during adsorption.

Different concentrations of five (5) anions were used. The AML material in the ratio of 3 g alumina to 10 g laterite was used in a 10 mg/L F⁻ solution. The results are shown as residual fluoride concentration (mg/L) and fluoride uptake (mg/g) in Table 4.20.

Table 4.20: Effect of other anions on F⁻ adsorption by AML.

Analyte concentration(mg/L)		Residual fluoride concentration (mg/L)	Fluoride uptake (mg/g)
Cl ⁻	0	0.2783	0.2430
	5	0.2609	0.2435
	10	0.1745	0.2456
	20	0.1899	0.2453
	30	0.2084	0.2448
	50	0.2278	0.2443
SO ₄ ²⁻	0	0.2783	0.2430
	50	0.3247	0.2419
	100	0.3234	0.2419
	150	0.2759	0.2431
	200	0.3705	0.2407
NO ₃ ⁻	0	0.2783	0.2430
	1	0.2184	0.2445
	2	0.2500	0.2437
	3	0.2038	0.2449
	5	0.2377	0.2441
	10	0.2253	0.2444
HCO ₃ ⁻	0	0.2783	0.2430
	100	0.4000	0.2400
	200	0.6667	0.2333
	300	0.9716	0.2257
	500	1.3888	0.2153
PO ₄ ³⁻	0	0.2783	0.2430
	0.2	0.2639	0.2434
	0.6	0.2069	0.2448
	0.8	0.2817	0.2429
	1	0.2038	0.2449
	10	0.2611	0.2435
	50	0.5566	0.2361
	100	2.1438	0.1964

CHAPTER FIVE

DISCUSSION

5.1 Characterization of laterite

5.1.1 Chemical characteristics of laterite

The major differences in the composition of the laterites are in the SiO_2 , Al_2O_3 and Fe_2O_3 content, which are the dominant oxides (Table 4.1) These oxides constitute about 69%, 66% and 45% for the Agamolga, Balungu and Dua laterites, respectively. The silica-sesquioxide ratios were 0.80, 0.46 and 2.32 for the Agamolga, Balungu and Dua soils, respectively. This indicates that the Agamolga and Balungu soils classify as true laterites whereas Dua soil is a non-lateritic soil according to Joachin and Kandiah (1941) classification. However, according to Schellmann (2013) the iron oxide/aluminum oxide ratio gives an indication of the parent rock type. The values for Agamolga, Balungu and Dua samples are 2.3, 8.6 and 0.7, respectively. Balungu laterite is low in SiO_2 but high in Fe_2O_3 indicating that it has its source from basic rocks. Dua sample on the other hand is low in Fe_2O_3 and high in SiO_2 , and is associated with acidic rocks. SiO_2 is not known to favour fluoride adsorption therefore adsorption performance of the Dua laterite will be affected negatively. Dua also contains a relatively high amount of K_2O coming from the presence of muscovite in the sample.

Some of the minor elements (Table 4.2) are relatively high in content, especially Cr in the Agamolga sample, V, Cr, Ba and Ce in the Balungu sample and Ba in the Dua sample. Other investigators have used oxides of these elements in the Agamolga and

Balungu laterites in preparing composite materials as adsorbents for fluoride (Biswas *et al.*, 2010; Liu *et al.*, 2010).

5.1.2 Mineralogical characteristics

A comparison of the X-ray diffraction patterns of the three samples is presented in Figure 5.1. The Agamolga laterite contains goethite, hematite, kaolinite and quartz. The minerals in Balungu laterite include mainly goethite, hematite, quartz and minor amounts of kaolinite. Dua sample contains mainly muscovite, kaolinite, rutile and quartz but with relatively small amount of goethite.

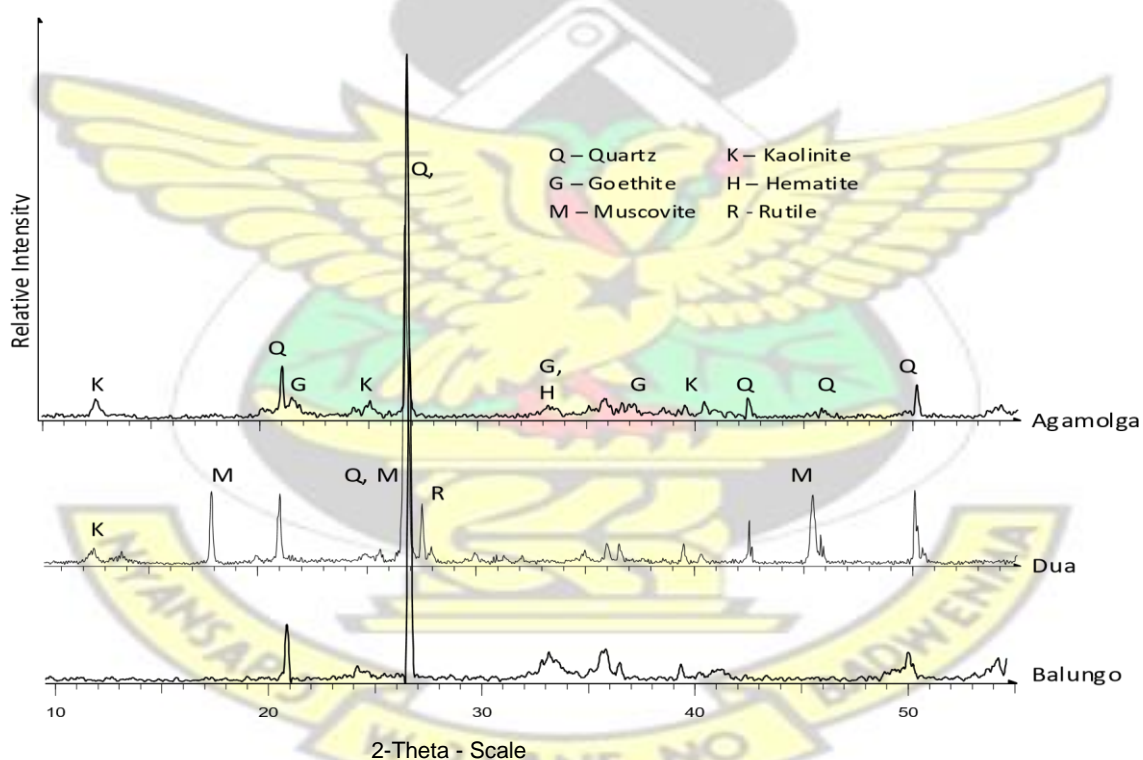


Figure 5.1: XRD pattern of the Agamolga, Balungu and Dua laterite samples.

If it is assumed that all the alumina in the Balungu and Agamolga samples come from kaolinite, it would suggest that the Agamolga laterite would have twice the amount of

kaolinite in the Balungu laterite, leaving about equal amounts of quartz in both samples. The goethite/hematite contents of the Agamolga and Balungu samples would be 25.8% and 42.0%, respectively.

The isoelectric point (IEP) values averaged 4.36, 3.74 and 2.94 for the Balungu, Agamolga and Dua samples, respectively (Table 4.3). These values are influenced by the composition of the lateritic soils. The silica and kaolinite contents, which register low IEP values, are higher in the Agamolga and Dua samples.

The data presented in Fig.5.1 shows that the three laterite samples all contain goethite/hematite, kaolinite and quartz, but in varying amounts. Dua laterite in addition contains muscovite and rutile (Figure 4.4). These will determine the efficiency of fluoride adsorption.

Combining the mineralogical and chemical characteristics, it is possible to say that fluoride adsorption will be favored in the use of the Agamolga and Balungu laterites, because of high iron oxide content. The differences in performance of these two will be the result of the iron oxide and kaolinite contents.

5.1.3 SEM analysis

Scanning electron microscopic pictures of the three samples show that apart from quartz, there seem to be intimate association of kaolinite, hematite, goethite and in the case of Dua sample, muscovite (Figure.4.4).

5.1.4 Implications of characteristics of laterite and its use as an adsorbent for fluoride removal

In this experiment, the point of zero charge or isoelectric point only represents an aggregated value and therefore may not be an influential determinant in fluoride adsorption, which position agrees with those of Sujana *et al.* (2009) and Sarkar *et al.* (2006).

The values obtained for the IEP would suggest that for most of the conditions used for the adsorption tests, the surfaces of the particles would have been negatively charged. Consequently, electrostatic attraction of the fluoride ions to the surface would not be significant. Fluoride uptake would not be dominated by exchange mechanism involving fluoride ions in solution and hydroxide ions on the particle surface. Specific adsorption will play an important role in fluoride adsorption.

5.1.5 Effect of heat-treatment on the mineralogy of laterites

The effect of heat treatment on the mineralogy of laterite was investigated using Balungu laterite. The raw Balungu laterite was treated at various heat temperatures of 300, 400 and 500°C. The XRD pattern (Fig.5.2) shows changes in the mineralogy as a result of the heat treatment. The XRD pattern showing the raw Balungu laterite gives two major goethite peaks. However, heat treatment of the laterite at 400 and 500°C seems to have resulted in the loss of one of the goethite peaks which indicates a possible phase transformation. The missing goethite peak is orthorhombic and has a space group of 62 nm and according to Bravais lattice classification, it is primitive.

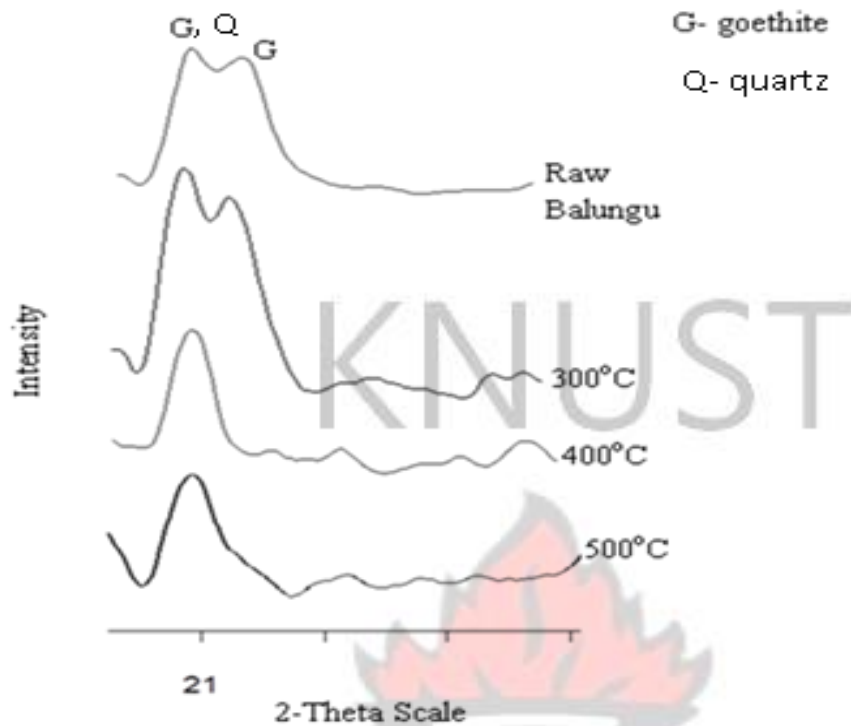
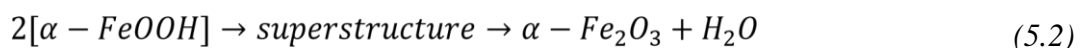


Figure 5.2: A comparison of x-ray diffraction peaks of the raw and heattreated Balungu laterite between $2\theta=20-22$.

The literature is not precise at which temperature goethite is completely transformed to hematite. In the work of Wu (2012) two temperature ranges were identified as probable temperatures at which goethite is transformed to hematite. The transformation of goethite to hematite results in a decrease in the surface area. The temperature ranges for the transformation are low temperature transformation (200-400°C) and high temperature transformation (800-1050°C). For the low temperature transformation it presupposes that there is direct transformation;



Whereas in the high temperature transformation it presupposes that there is an intermediate material formed before hematite is formed;



In the same work, Wu (2012) asserts that the goethite structure is not changed until at a heat treatment temperature of 600°C.

5.2 Fluoride adsorption tests with laterite

5.2.1 Fluoride uptake by raw and heat-treated laterites

Data set in Table 4.5 has been used to prepare Fig. 5.3 to illustrate the difference in the adsorption of the raw and heat-treated laterite. Generally, the fluoride uptake by the raw laterites was poor, with the Dua laterite being the poorest performer with a decrease of only about 2 mg/L in fluoride concentration from an initial fluoride concentration of 10 mg/L, as against about 4 mg/L for the Agamolga and Balungu laterites.

When the samples were pre-treated at 400°C for 2 hours, the performance of the laterites improved with fluoride concentrations decreasing by 3.42 and 2.83mg/L for Agamolga and Balungu samples, respectively. This result agrees with the work by Gomoro *et al.* (2012), which attributed higher performance to the de-hydroxylation of goethite and kaolinite minerals during heat treatment, increasing the surface area and thereby enhancing the adsorption properties of the laterites. The initial rapid uptake by the heat-treated Agamolga laterite as compared to the Balungu laterite was probably due to the higher kaolinite content of the Agamolga sample. The amount of kaolinite present in Agamolga and Balungu could be compared based on the aluminum content (Table 4.1).

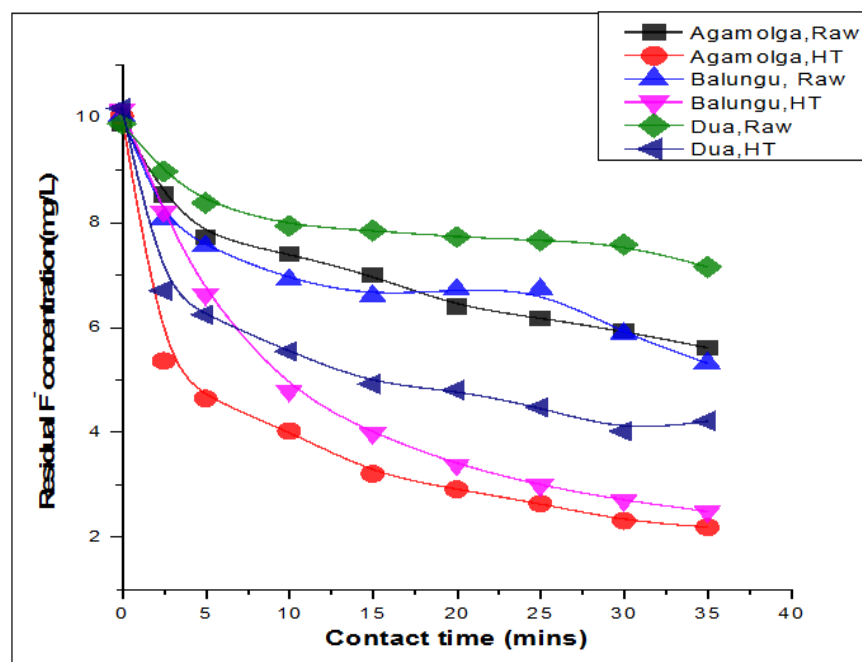


Figure 5.3: Fluoride removal from water by raw and heat-treated (HT) laterite (400°C).

Vithanage *et al.* (2012) have suggested that the fluoride ion shows more attraction towards aluminum sites than iron sites. The fluoride uptake by the Balungu laterite was initially slower than that of the other two laterites, probably due to the lower kaolinite content but approached the uptake by Agamolga in 35 minutes. It is further suggested that the presence of relatively high amounts of chromium and cerium as minor elements in the Agamolga and Balungu soils may also have contributed to the better fluoride uptake probably as lattice substitution. Biswas *et al.* (2010) used a synthetic iron (III)-aluminum (III)-chromium (III) ternary mixed oxide, while Liu *et al.* (2010) applied an Al-Ce hybrid sorbent with much success in their defluoridation tests.

5.2.2 Solution pH during fluoride adsorption

Data on changes in solution pH during fluoride adsorption presented in Tables 4.6 has been plotted in Figure 5.4 for the raw and heat-treated laterites. The increase in solution pH during adsorption corresponds to the release of OH^- ions into the solution from the exchange with F^- ions in the case of the Agamolga and Dua laterites.

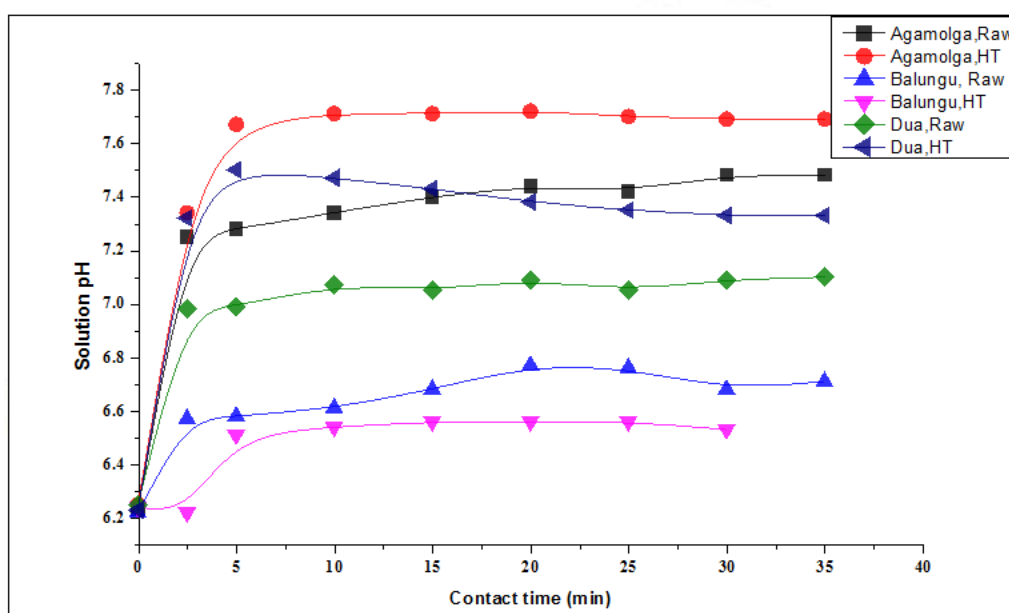


Figure 5.4: Change in solution pH during fluoride adsorption by raw and heat-treated (HT) laterites.

The Balungu sample showed a different behaviour, however, as the solution pH showed a decrease for the heat-treated sample even though the results showed higher fluoride adsorption. It appears that fluoride uptake after about 2.5 to 5 minutes involves other mechanisms such as specific adsorption instead of OH^- exchange as the pH stabilizes.

Plots of change in fluoride concentration and pH of solution during adsorption at various initial pH (Tables 4.9 and 4.10) are presented in Figure 5.5 for heat-treated Balungu laterite.

KNUST



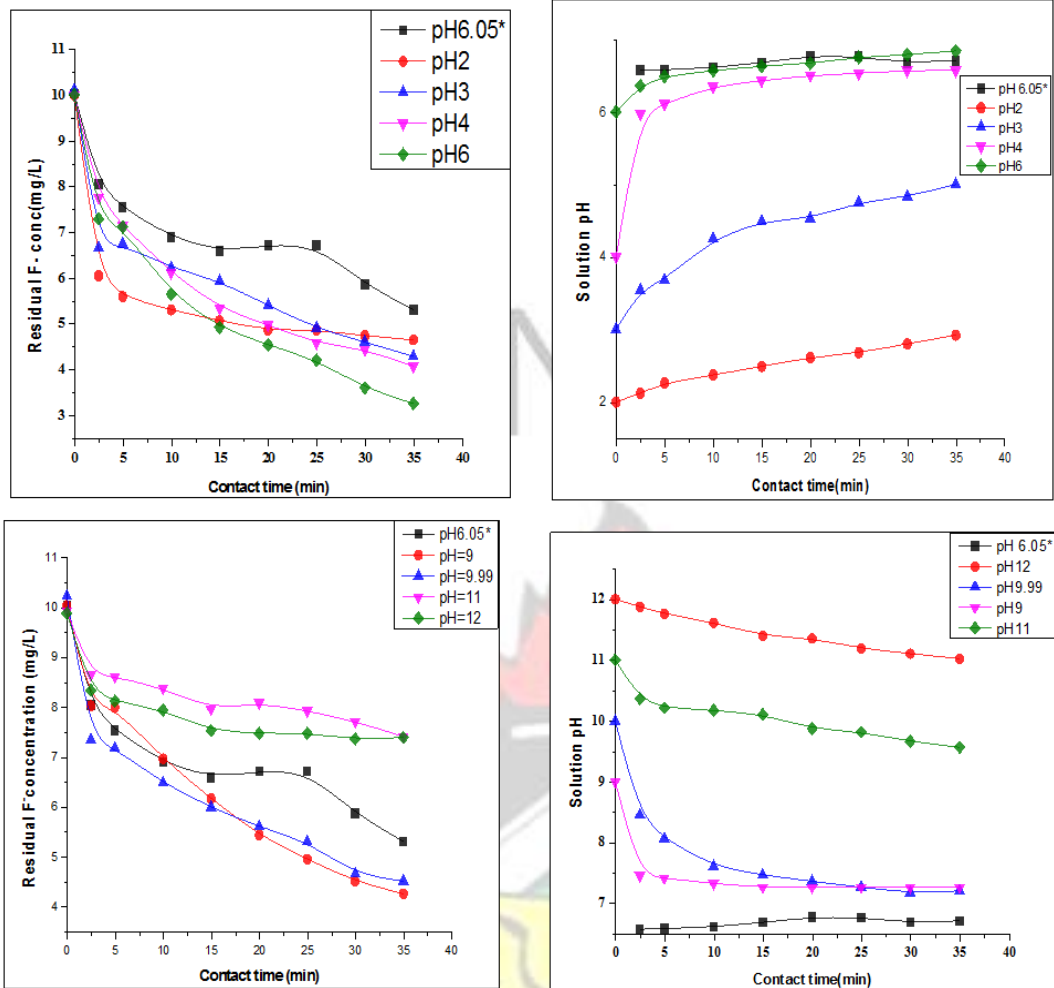


Figure 5.5: Change in fluoride concentration and solution pH during adsorption at various initial pH media for the heat-treated Balungu laterite (pH6.05* means pH of solution without adding an acid or base).

An illustration of data from Tables 4.7-4.8 for Agamolga and Tables 4.11- 4.12 for Dua are given in Figs 5.6 and 5.7, respectively.

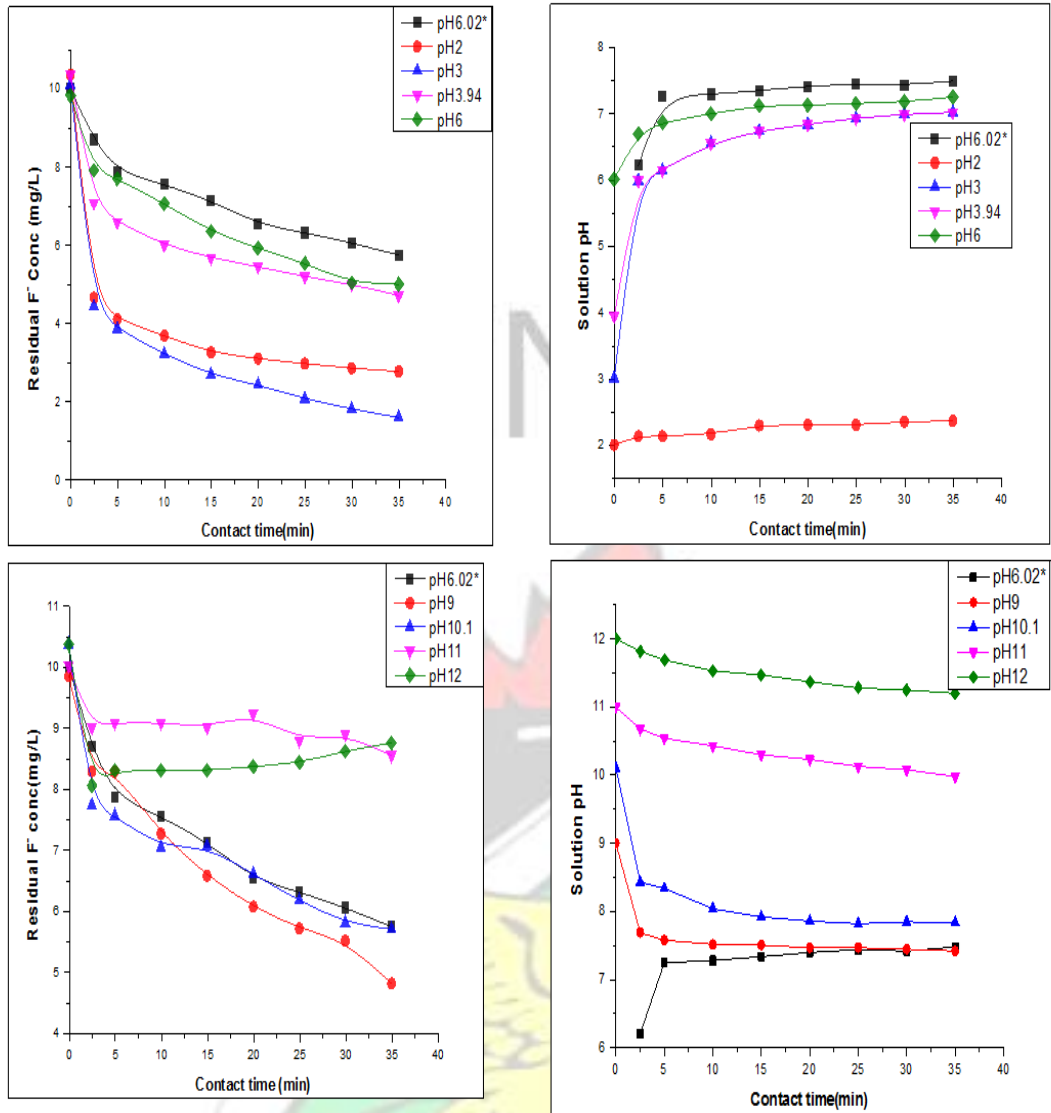


Figure 5.6: Change in fluoride concentration and solution pH during adsorption at various initial pH media for the heat-treated Agamolga laterite (pH6.02* means pH of solution without adding an acid or base).

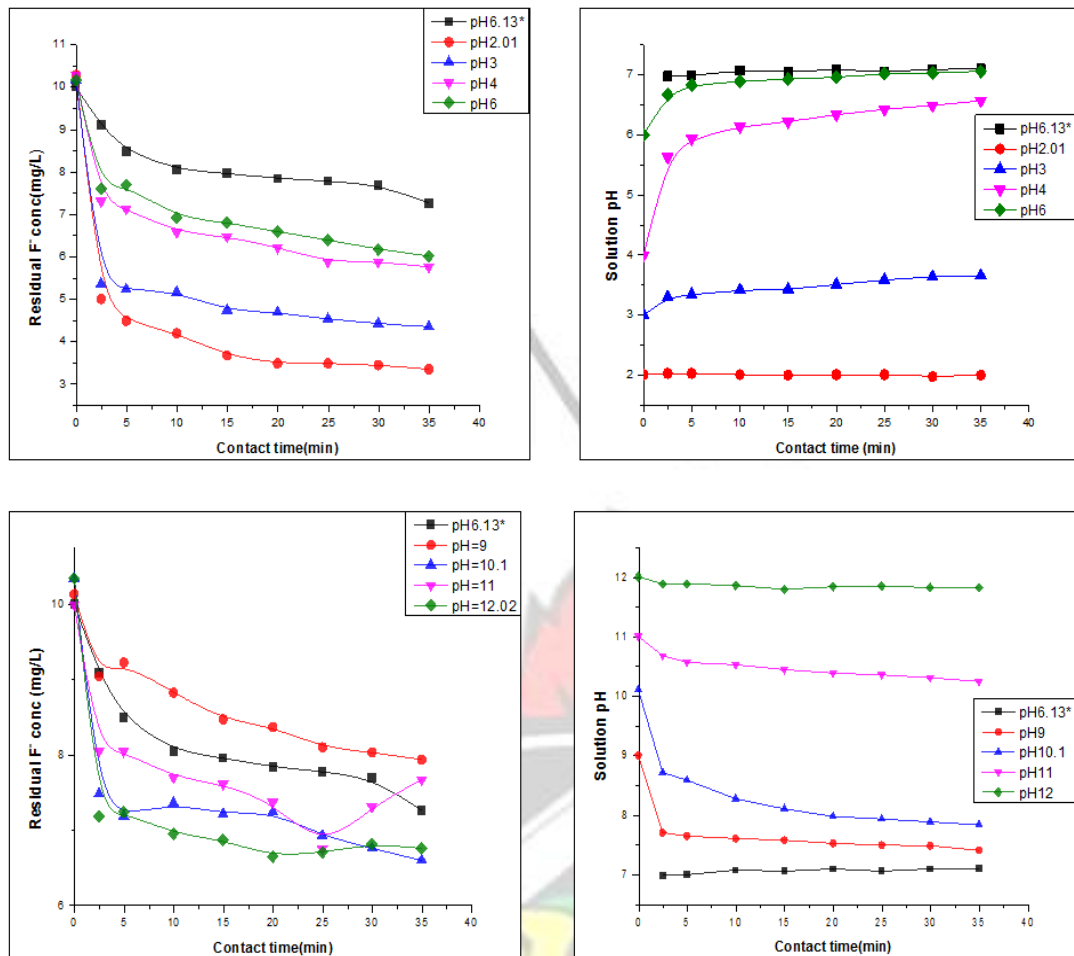


Figure 5.7: Change in fluoride concentration and solution pH during adsorption at various initial pH media for the heat-treated Dua laterite (pH6.13* means pH of solution without adding an acid or base).

These data show that fluoride adsorption took place in both acidic and basic media, with the extent of adsorption higher in acidic media, especially at the initial 2-5 minutes of contact due to the high concentration of vacant adsorbent sites and high diffusion. Increase in solution pH was observed during adsorption in acidic media, which is expected from the exchange of OH^- ions with F^- ions. In the basic media however, solution pH decreased, being more significant at pH below 11, suggesting either consumption of OH^- ions or release of H^+ ions into solution. Exchange mechanism therefore seems not to be supported in this case. This result does seem to suggest a specific adsorption of fluoride ions in solution. Additionally, there seemed

to be a gravitation of solution pH towards the value 7. Marginal pH changes for initial solution pH of 2, 3, and 12 may be due to high acidity or basicity respectively.

5.2.4 Effect of particle size on fluoride uptake

Results of adsorption tests carried out with Balungu laterite at different particle sizes (<90, 90-125, 180-500 and >500 μm) are presented in Figure 5.8. It shows that the residual fluoride was lowest (1.82 mg/L, Table 4.4). Particle size of >500 μm had the highest residual fluoride (5.94 mg/L, Table 4.4). This suggests that finer particle sizes of Balungu laterite had the highest defluoridation capacity than the bigger particle sizes.

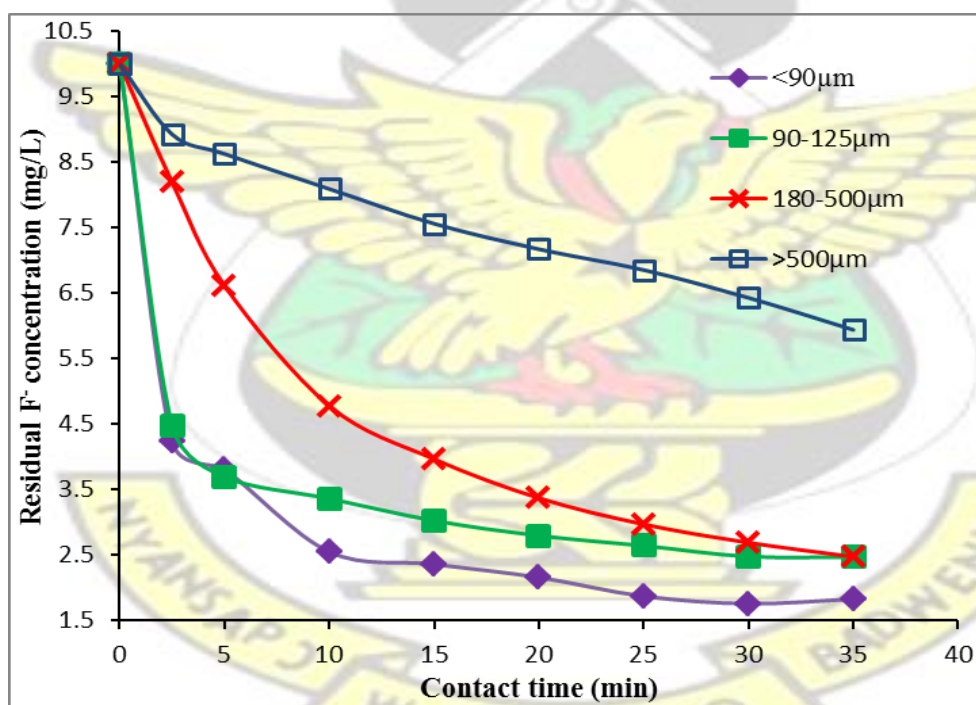


Figure 5. 8: Effect of particle size of laterite on fluoride removal.

The 180-500 μm particle size fractions was selected for further tests, keeping in mind the possible application in columns in the field application.

With finer particle sizes, the solute finds more adsorbent sites. However, finer particle sizes present operational challenges as finer particles have to be separated by filtration during batch operations.

5.2.4 Equilibrium adsorption by Balungu laterite at different initial fluoride concentrations

A plot of equilibrium fluoride adsorption at different initial concentrations (using data from Table 4.13) is presented in Fig. 5.9.

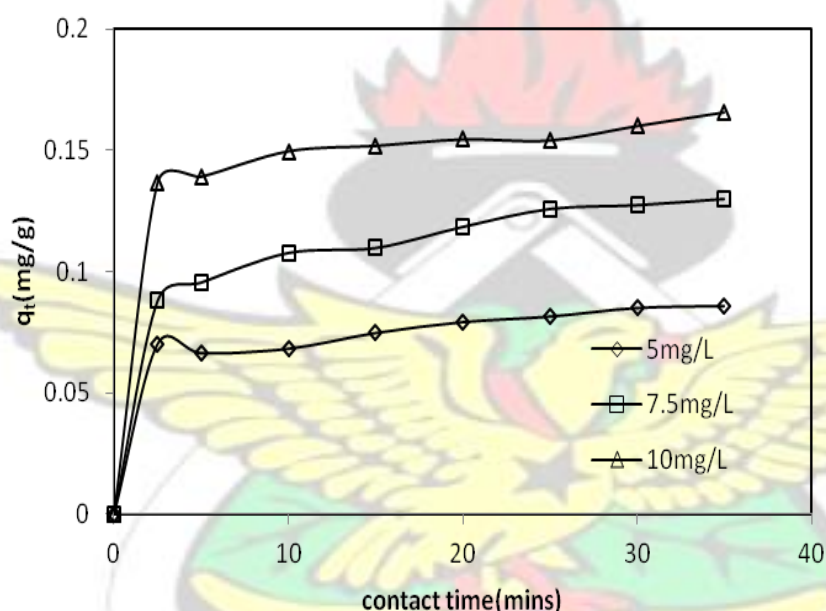


Figure 5.9: A plot of fluoride adsorption at different initial concentrations.

The initial uptake was fast and increased as the initial concentration was increased, approaching a plateau. The amount of fluoride adsorbed was proportional to the initial concentrations, increasing from 0.086 mg/g to 0.166 mg/g for 5 mg/L to 10 mg/L fluoride concentrations, respectively. A similar trend was observed by Kumar *et al.* (2009) in the removal of fluoride by granular ferric oxide.

The effect of initial concentration of fluoride on adsorption equilibrium was also studied and it could be seen on the graph that the time to reach equilibrium is not a factor of initial concentration.

5.3 Mechanism and kinetics considerations

According to Sujana *et al.* (2009; 2010; 2011), fluoride adsorption in acidic media is by anion exchange (Equation 2.20) whilst in the basic media, it is by van der Waals forces (Equation 2.21). As suggested, fluoride adsorption in the basic media leads to a decrease in pH as a result of the production of hydronium ions (see Equation 2.21). Although the equation could be used to explain the decrease in the solution pH during adsorption in the basic media, it did not account for fluoride adsorption as observed in this study. The surface of the suspended metal oxide would have been negatively charged and thereby repulsing the negatively charged fluoride ions. Data from this work as shown in Table 4.3 have indicated an isoelectric point (IEP) of 4.36, 3.75 and 2.99 for the Balungu, Agamolga and Dua lateritic soils respectively, suggesting negatively charged surface in basic media.

It is well known that HF is a weak acid ($pK_a = 3.2$) and that in solution a strong hydrogen bond occurs between F^- and the hydronium ion ($F^- \cdots H_3O^+$) to form the ion pair $H_3O^+F^-$ (Rossiter *et al.*, 2010). Modifying reaction (Equation 2.23) accordingly, will result in the release of hydronium ion from the specific adsorption of the F^- ion:



Reaction (5.3) shows that fluoride uptake could be accompanied by release of hydronium (H_3O^+ or simply H^+) into the solution, lowering the pH during adsorption, as obtained in basic media during these studies.

In summary, two mechanisms account for the fluoride adsorption behaviour on iron hydroxide-containing lateritic soil in acidic and basic solution. The adsorption is by ion exchange between hydroxide ion on laterite surface and fluoride ion in acid solution. In basic media however, fluoride uptake is by specific surface reaction involving the $\text{H}_3\text{O}^+\text{F}^-$, which leads to the release of hydronium ion into solution and thereby causing a decrease in solution pH during adsorption.

The adsorption of fluoride by laterite was investigated using Langmuir and Freundlich isotherms. The Langmuir and Freundlich plots were prepared using:

$$\frac{1}{q_e} = \frac{1}{Q_{\max}} + \frac{1}{Q_{\max} b C_e} \quad (5.4)$$

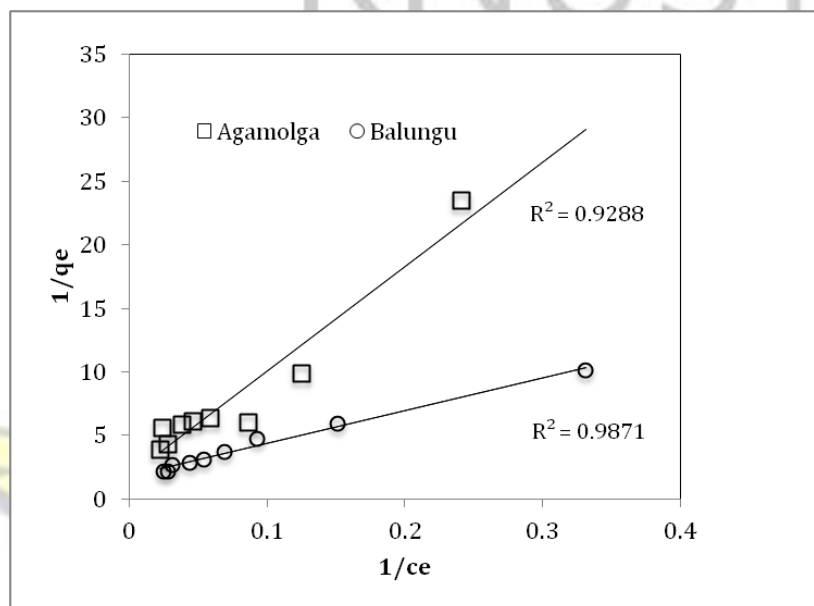
$$\log q_e = \log K_F + \frac{1}{n} \log C_e \quad (5.5)$$

respectively, where q_e is the amount of F^- adsorbed at equilibrium (mg/g), C_e is the residual F^- concentration reached at equilibrium state (mg/L); Q_{\max} is the monolayer capacity of the adsorbent and b is the Langmuir adsorption constant (Chen *et al*, 2011). K_F and n are Freundlich constants related to the adsorption capacity and the intensity of adsorption respectively. The values of $1/n$ less than 1 show good adsorption intensity (Babaeiveli and Khodadoust, 2013). The Langmuir plot was obtained by

plotting $1/q_e$ against $1/C_e$ (Appendix 1) and Freundlich isotherm by plotting $\text{Log}q_e$ against $\text{Log} C_e$ (Appendix 2).

The Langmuir and Freundlich plots for the Balungu and Agamolga laterites are presented in Fig. 5.10a and b, respectively.

(a)



(b)

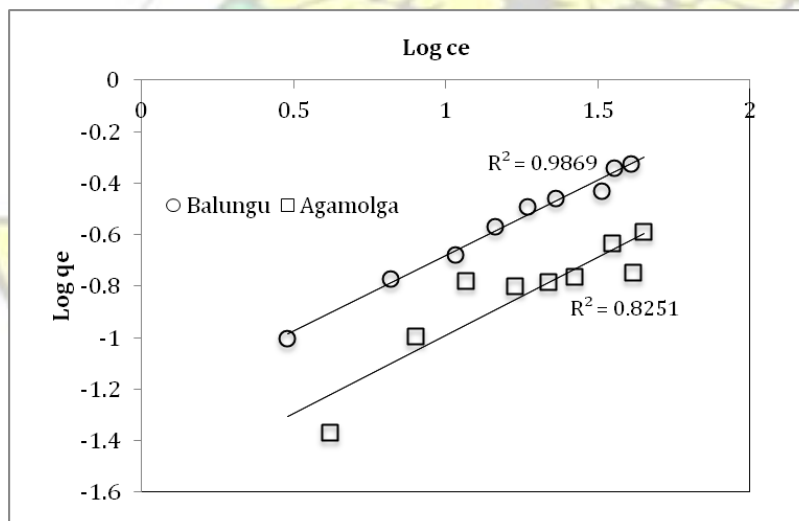


Figure 5.10: Langmuir (a) and Freundlich (b) plots of equilibrium adsorption data for Agamolga and Balungu laterites.

The plots show that adsorption data for Balungu laterite fits both Freundlich and Langmuir isotherm. Data points on both isotherms for the Agamolga sample are more

scattered. The adsorption capacity according to the Langmuir plot was 0.55 mg g^{-1} for both untreated Balungu and Agamolga laterite samples. On the other hand, the Freundlich plot gave a value of 0.055 for the Balungu and 0.025 for the Agamolga samples respectively. These values for the raw laterites are very low for any field applications.

KNUST

Adsorption kinetics experiments were done to evaluate the performance of the adsorbent and also understand the dynamics of the adsorption process. To do this, two models were employed, the Pseudo-first order and Pseudo-second order models.

According to Liu *et al.*, 2010; Kumar *et al.*, 2009 and Fan *et al.*, 2003, pseudo-first order reaction is given as;

$$\frac{dq_t}{dt} = k_1(q_e - q_t) \quad (5.6)$$

The integrated pseudo-first order rate equation is written as;

$$\log(q_e - q_t) = \log q_e - k_1 t \quad (5.7)$$

The pseudo-second order reaction is given as;

$$\frac{dq_t}{dt} = k_2(q_e - q_t)^2 \quad (5.8)$$

$$\frac{d(q_e - q_t)}{(q_e - q_t)^2} = -k_2 dt \quad (5.9)$$

Integrating Equation 5.9 at boundary conditions ($t=0$, to $t=t$ and $q_t=0$ to $q_t=q_t$) gives;

$$\frac{1}{q_e - q_t} = \frac{1}{q_e} + k_2 t \quad (5.10)$$

$$\frac{t}{q_t} = \frac{1}{k_2} \frac{1}{q_e^2} + \frac{t}{q_e} \quad (5.11)$$

where q_e and q_t represent the amount of fluoride adsorbed at equilibrium and anytime, t (mg/g of solid material). k_1 (min^{-1}) and k_2 ($\text{gmg}^{-1}\text{min}^{-1}$) are the equilibrium rate constant of pseudo-first- and second-order sorption respectively, t is the shaken time (min). k_1 is determined from the slope of the linear plot of $\text{Log}(q_e - q_t)$ against t whilst k_2 is calculated from the intercept of the plot of t/q_t against t . The results of the kinetics analysis are given in Appendix 3 as 1st order kinetics and Appendix 4 as 2nd order kinetics and they were used to plot Figure 5.11 and Figure 5.12, respectively.

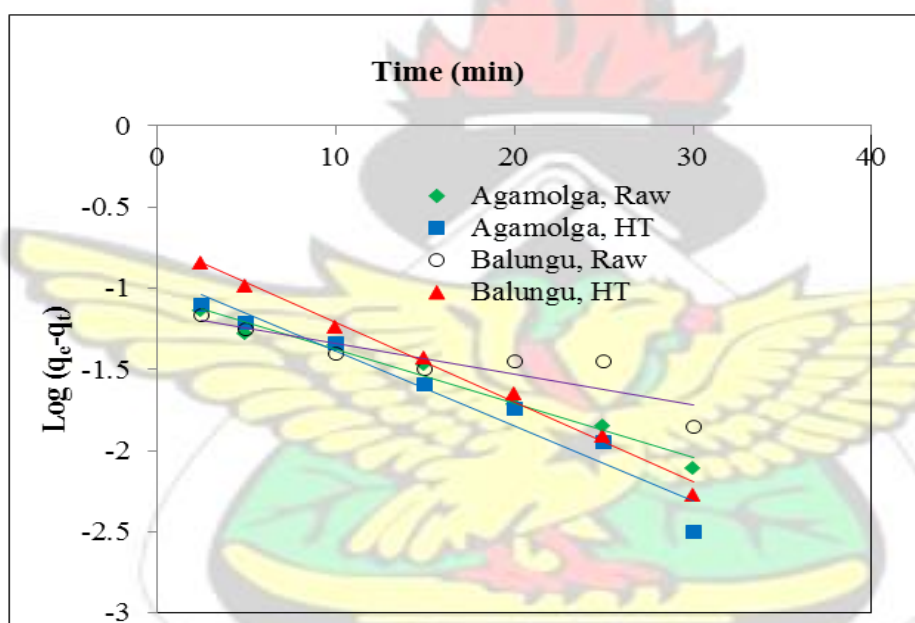


Figure 5.11: Pseudo-first order plots of adsorption data.

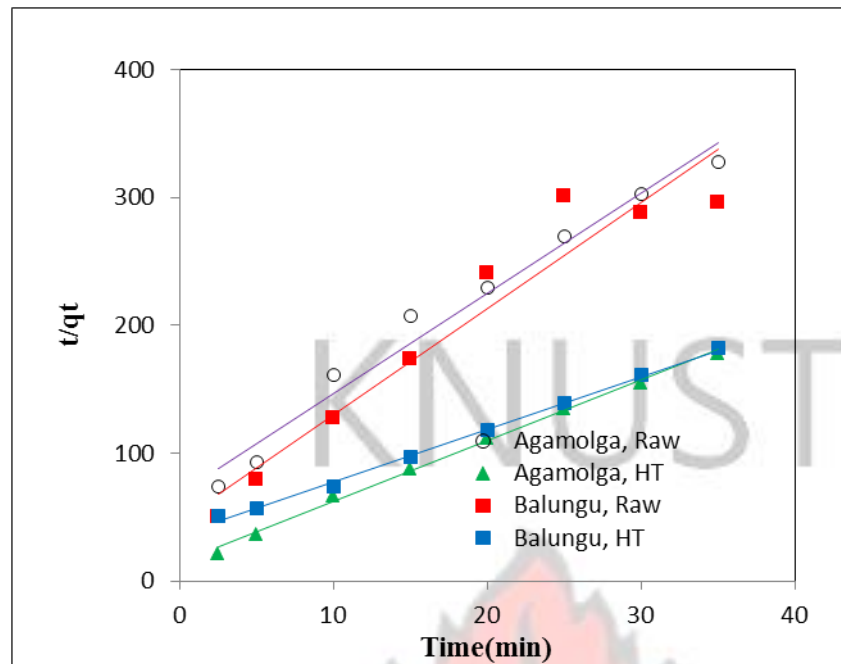


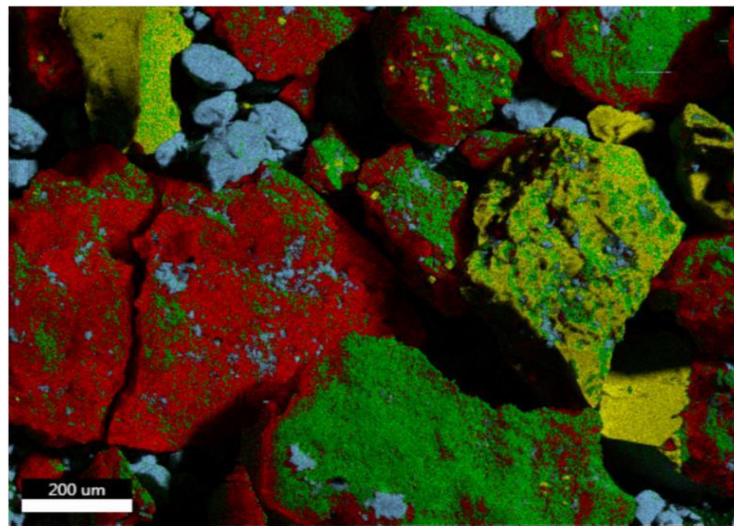
Figure 5.12: Pseudo-second-order plots of adsorption data.

The coefficient of determination (R^2) was used to evaluate the fitness of a set of data to a particular model. In this experiment, the kinetic data for Agamolga and Balungu laterites fitted to both the Pseudo-first-order and Pseudo-second-order models based on the R^2 values (Appendix 5).

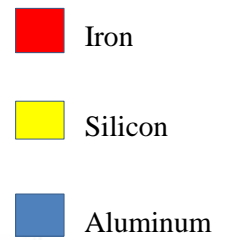
5.4 Micro-structural Characterization of AML

SEM micrographs of the 3 g alumina: 10 g laterite composite is shown in Figure 5.13. These reveal irregularly shaped particles with surface agglomerates of smaller sized particles adhering to larger particles. The EDX spectra in addition show close association of these elements in all areas. The bigger particles show a mixture of elements including Fe, Si, and Al which are closely associated (Fig. 5. 13a). Some alumina particles are found to be thinly coated on the surface of the iron particles whilst the rest of the alumina particles are seen as loose particles.

(a)



Legend



(b)

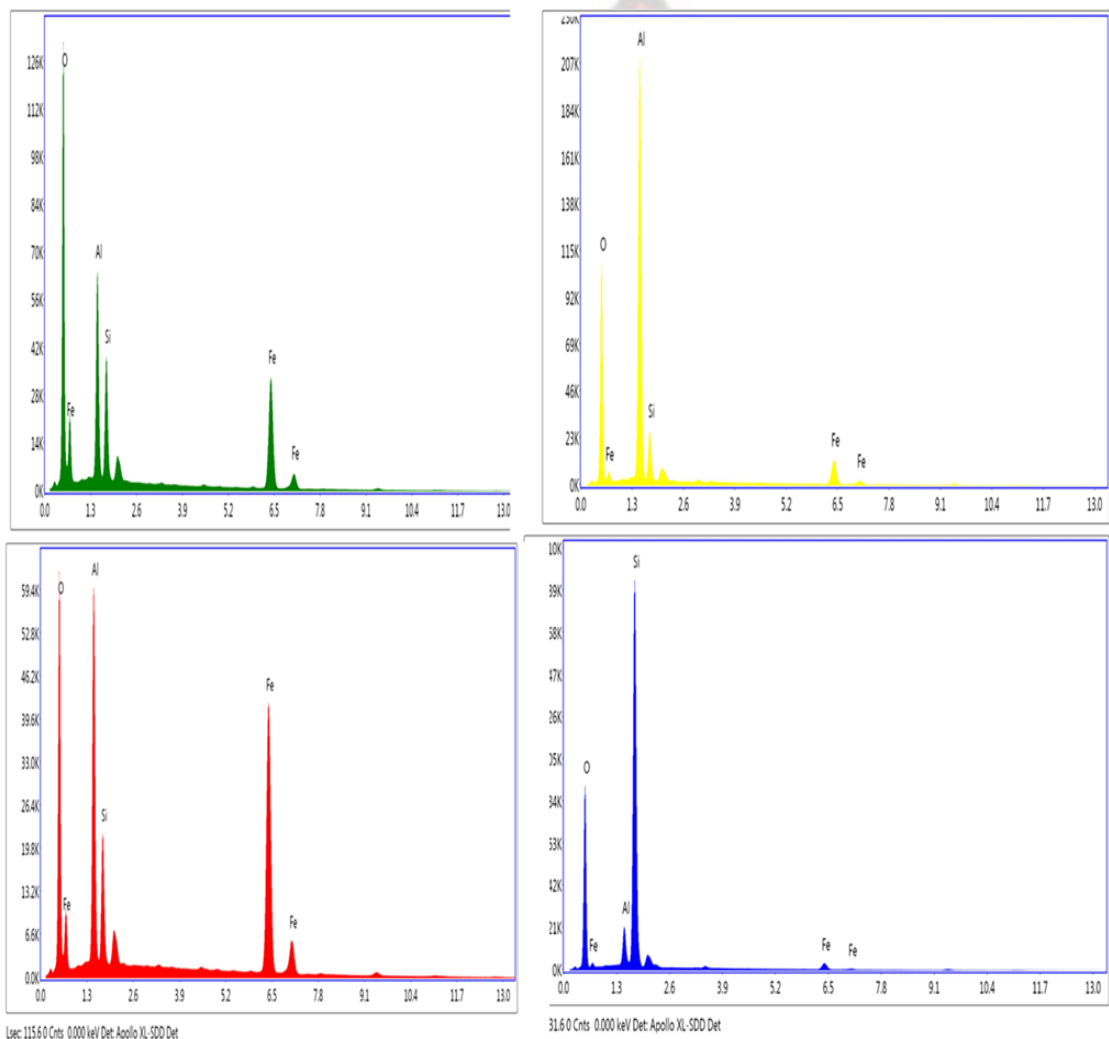


Figure 5.13: SEM image (a) and EDX spectra (b) of AML (3 g alumina: 10 g laterite) taken at different phases on the surface of the AML.

It is also proposed that in the synthesis of AML, some of the aluminum may have diffused into the lattice structure of the iron minerals, goethite or hematite (Fey and

Dixon, 1981). This is illustrated in Figure 5.14, which illustrates the process of AML synthesis. Fe^{3+} and Al^{3+} are isomorphous in character and therefore Al^{3+} can replace Fe^{3+} or vice versa in their crystal structure forming a structure of formula $(\text{Fe}_{1-x}\text{Al}_x\text{OOH})$ (Wu, 2012). The substitution is not limited to FeOOH but also occurs in Fe_2O_3 . It is suggested that aluminum in the alumina coating and iron from the surface of iron oxide particle, at the temperature of processing would diffuse across. It is known in bauxite refining that aluminous goethite is quite stable against caustic soda attack (Wu, 2012). The stability of this is important during fluoride removal from adsorbent by caustic soda, during adsorbent regeneration with caustic soda.

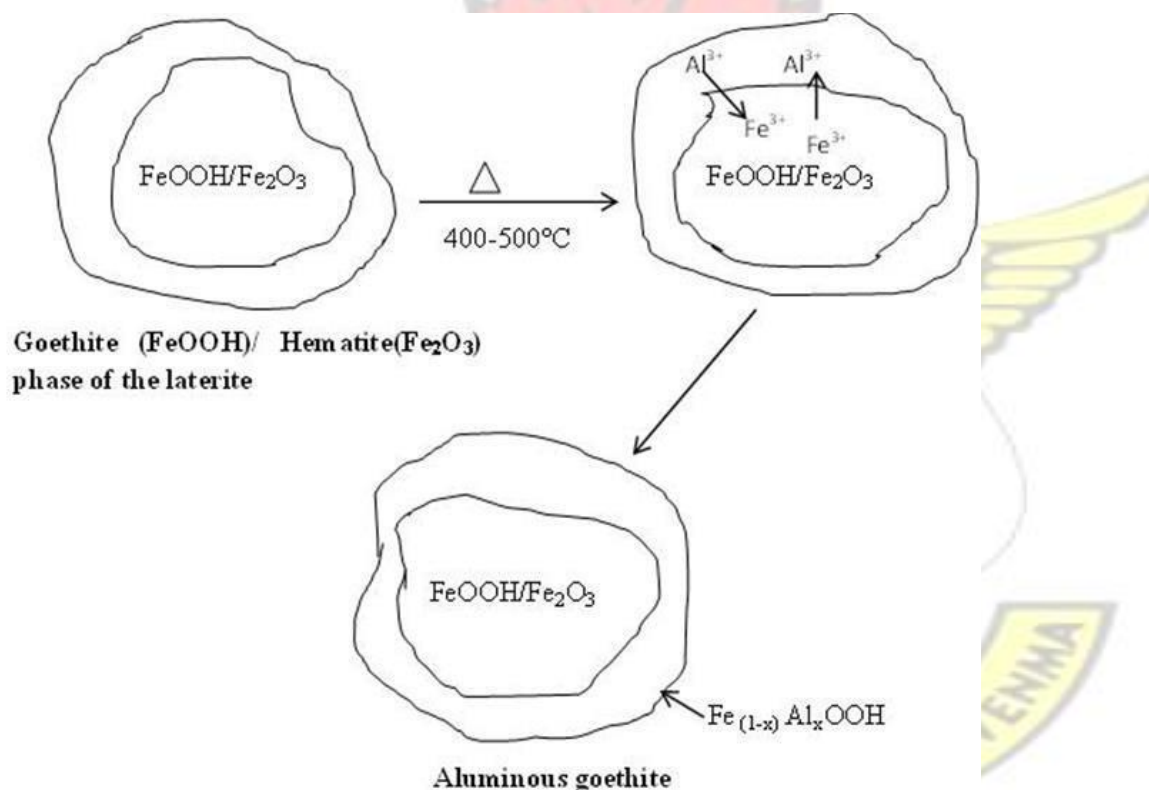


Figure 5.14: Schematics showing AML synthesis.

Figure.5.13b shows the EDX spectra of four different areas on the AML. The EDX spectra show that there are spots on the AML that have more of the alumina particles than the other. For instance, the iron particles have more aluminum on the surface than

the silica particles (Fig. 5.13 b (ii), (iii)). The SEM picture (Fig. 5.15) also shows the build-in (picture on the left) of aluminum into the surface of iron particles shown on the right. The iron phase is pictured in red. The assumption is that this build-in, as confirmed by Fig. 5.13 b (ii) is a new structure, $\text{Fe}_{(1-x)}\text{Al}_x\text{OOH}$. XRD of modified sample indicates the disappearance of Al_2O_3 in the modified material.

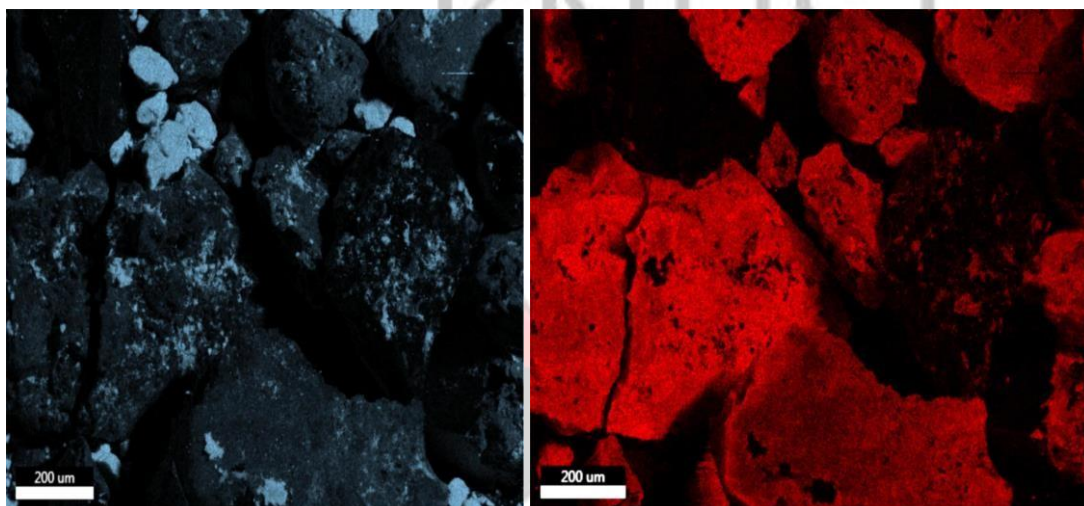


Figure 5.15: SEM image indicating aluminum build-in in the iron oxide surface.

5.5 Fluoride adsorption tests

5.5.1 Heat-treatment temperature in preparation of AML and fluoride adsorption

Data on the effect of heat treatment of AML and the ability to effectively remove fluoride from water is presented in Table 4.14 and plotted in Figure 5.17.

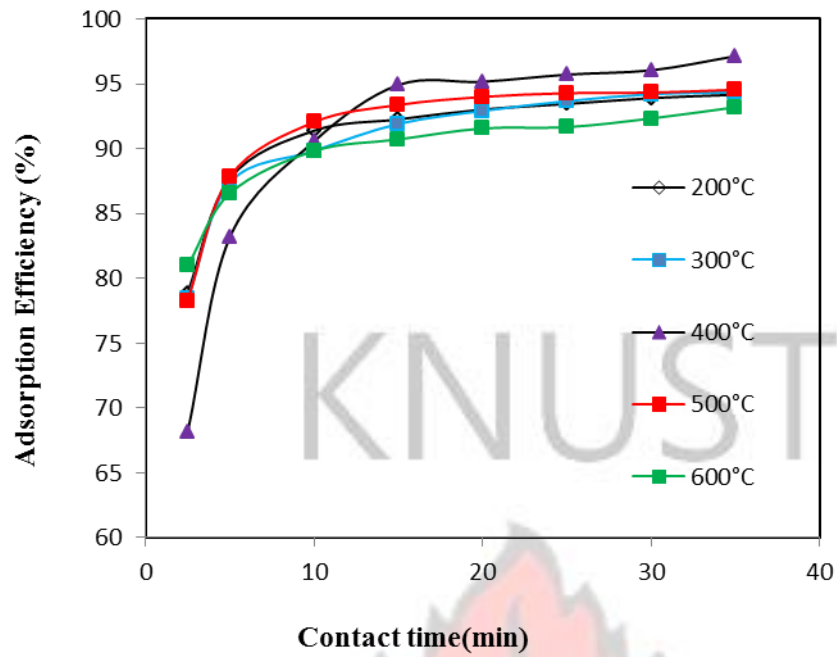


Figure 5.16: Effect of heat treatment temperature on adsorption efficiency by AML.

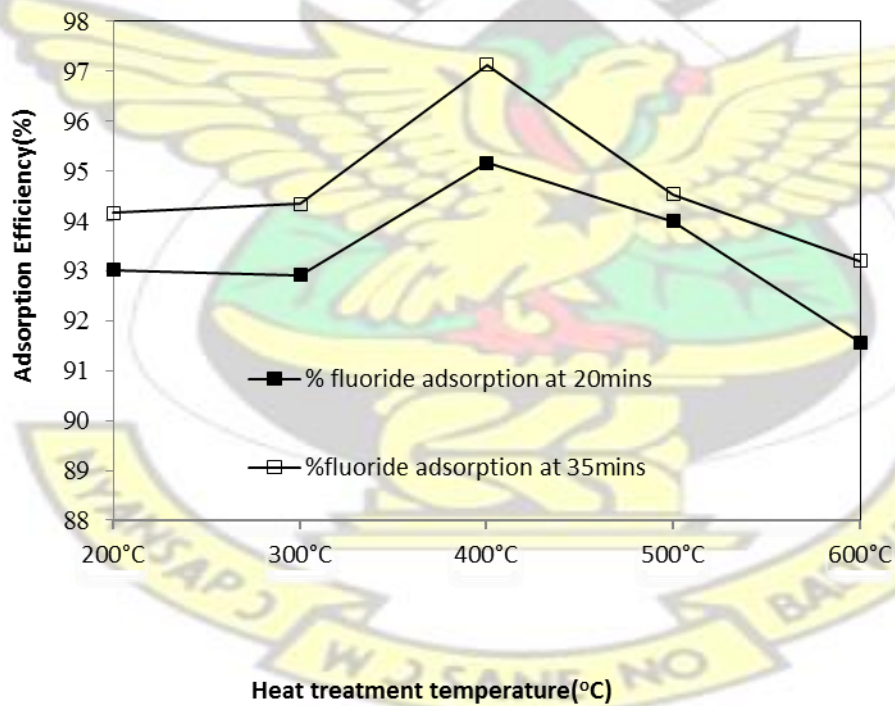


Figure 5.17: A plot of adsorption efficiency vs. heat treatment temperature at 20 and 35 minutes contact time.

The effect of heat treatment of AML on fluoride adsorption is not significant in this study (Fig. 5.17). However, a plot of adsorption efficiency vs. temperature at contact

times of 20 and 35 minutes (Fig. 5.17) shows that the best performance is at treatment temperature of 400°C.

5.5.2 AML composition and fluoride adsorption

Figure 5.18 showing the effect of different AML compositions on fluoride adsorption was prepared using data from Table 4.15. It shows that fluoride adsorption increased as the ratio of alumina used was increased. However, beyond 3 g alumina addition, the differences in fluoride adsorption were insignificant. The rate of fluoride uptake was initially higher for the Balungu laterite at low alumina addition than for the Agamolga laterite. This might be due to the different mineral phases present in the laterites. Although both laterite samples contain kaolinite, goethite and hematite phases, it could be deduced based on the chemical composition of Agamolga (Table 4.1), it contains more of aluminum in the form of kaolinite than Balungu laterite. Aluminum is present in these laterites in the form of kaolinite.

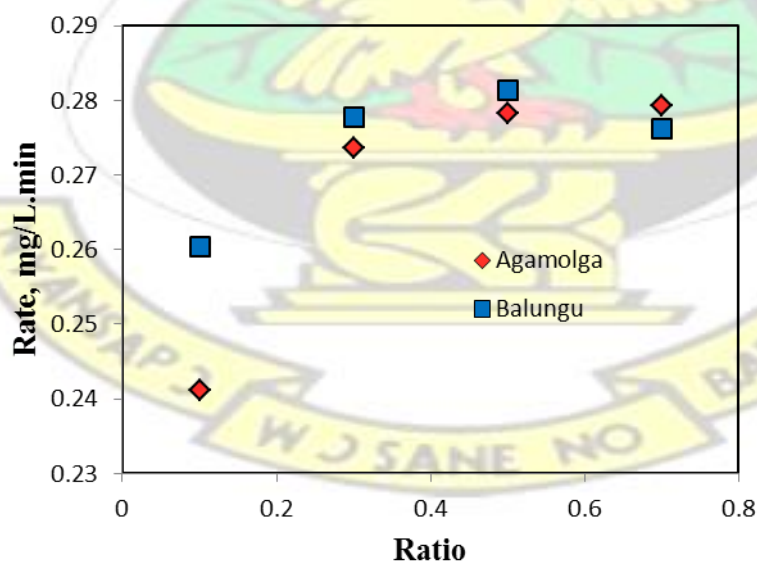


Figure 5.18: Rate of fluoride adsorption by different ratios of AML.

5.5.3 Effect of solution pH on fluoride adsorption by AML

The pH of a solution plays a vital role as it influences the surface charge in most of the solid/liquid adsorption processes. The adsorption of fluoride on AML was examined at different pH values ranging from 2 to 11. Plots of data were made for Table 4.16 for acidic media (Fig. 5.19a) and for basic media (Fig. 5.20a). The initial concentration of the fluoride solution was maintained at 10 mg/L. Data set from Table 4.17 was used for solution pH plots in acidic media (Fig. 5.19b) and in basic media (Fig. 5.20b).

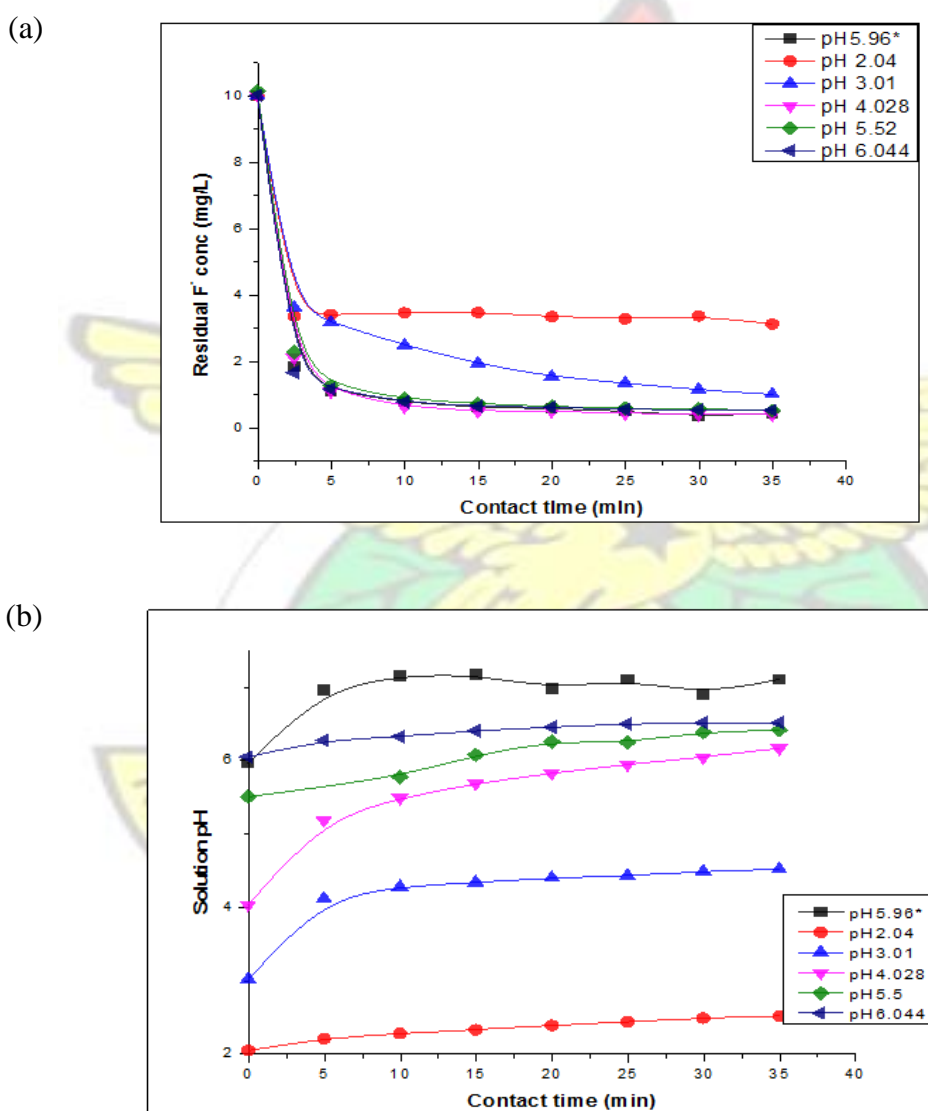
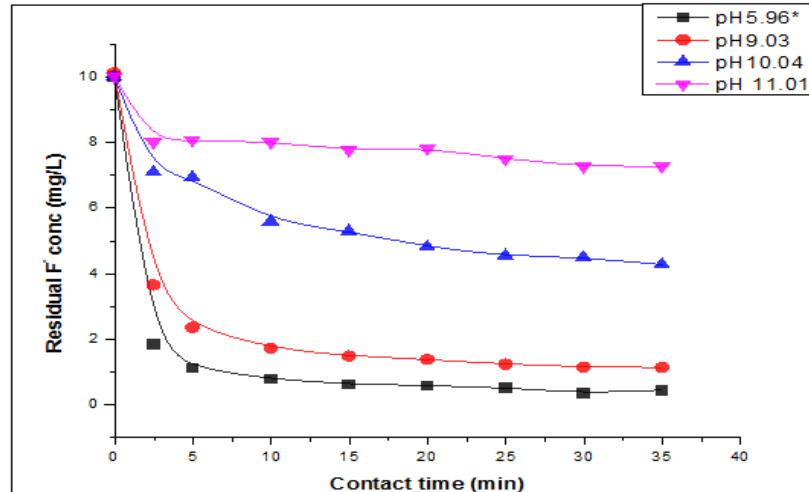


Figure 5.19: (a) Effect of initial pH on the adsorption of fluoride and (b) solution pH after adsorption by AML in acidic media.

(a)



(b)

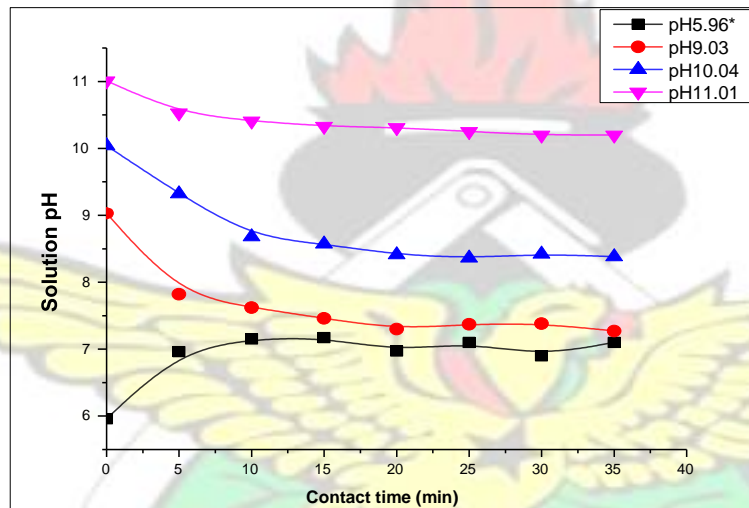


Figure 5.20: (a) Effect of initial pH on the adsorption of fluoride and (b) solution pH after adsorption by AML in basic media.

An examination of the results showed that the performance of the sorbent was best between pH 4 to pH 9 (Fig.5.19a & Fig. 5.20a).The optimal pH for fluoride removal in this experiment ranged from 4-6. However, in highly acidic medium (pH2 and pH3), the fluoride uptake by AML was relatively poorer. According to Leyva-Ramos *et al.* (2008) decrease in fluoride uptake in highly acidic media may suggest the dissolution of alumina and therefore the loss of active adsorption sites. The pH of the equilibrated solution increased when the initial pH was in the acidic pH range and decreased when

the initial pH was in the alkaline pH range. It was also noted that when the initial pH was between 4- 6, the final pH of the solution after adsorption was averagely about 6.2 (Table 4.17). It shows that the adsorbent had the capability of buffering the solution pH and keeping the adsorption system at near neutral pH during the experiments. In highly basic medium (pH>9) fluoride adsorption decreased significantly. This may also be due to dissolution of alumina at such pH.

5.5.4 Adsorbent dosage and fluoride uptake by AML

The percentage of fluoride removal was studied at different dosages (1, 3, 4, 7 and 10 g of the composite) of 3 g alumina to 10 g laterite of AML at particle size of 180-500 μm . The lowest percentage of fluoride removed (60.72%, Table 4.18) was at an adsorbent dosage of 1 g and the highest percentage of fluoride removed (97.47%) was at an adsorbent dosage of 10 g of AML.

However as seen in Fig. 5.21, the change in percentage adsorption of fluoride was insignificant after adsorbent dosage of 4g/100 mL. At higher dosage of adsorbent, there is the possibility of shielding of active adsorption sites. According to Islam and Patel (2007), there is decrease in effective surface area resulting from the conglomeration of exchanger particles when the adsorbent dosage is high.

However as seen in Fig. 5.21, the change in percentage adsorption of fluoride was insignificant after adsorbent dosage of 4g/100 mL. At higher dosage of adsorbent, there is the possibility of shielding of active adsorption sites. According to Islam and Patel (2007), there is decrease in effective surface area resulting from the conglomeration of exchanger particles when the adsorbent dosage is high.

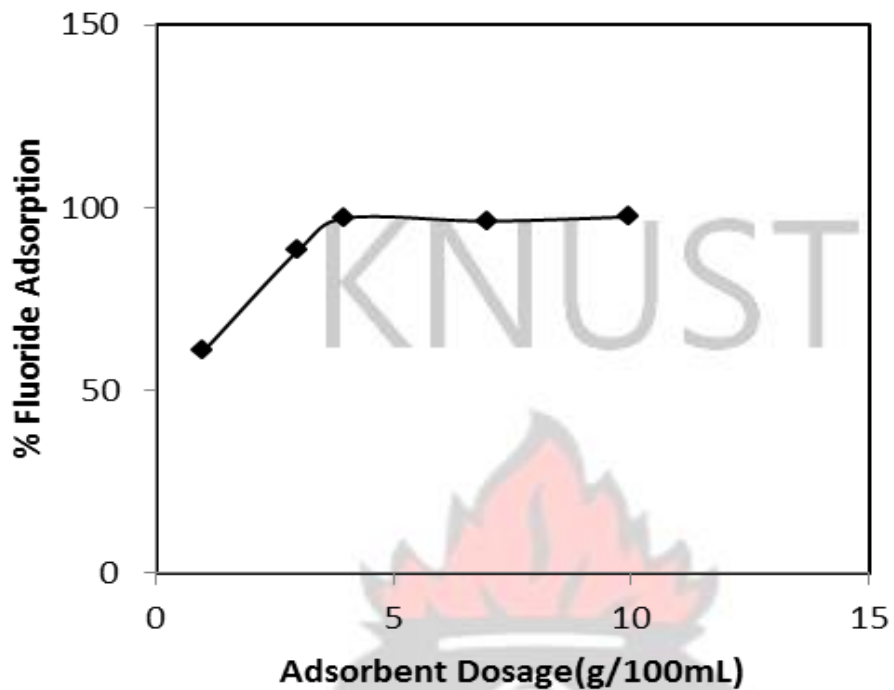


Figure 5.21: Adsorbent dosage vs. percentage of fluoride adsorption by AML (initial concentration of fluoride solution=10 mg/L).

5.5.5 Initial fluoride concentration and fluoride uptake by AML

At different initial concentration of fluoride, fluoride removal seems to be fast in the first 10 minutes of contact of AML with solution and equilibrium is almost established within 35 minutes of contact (Table 4.19).

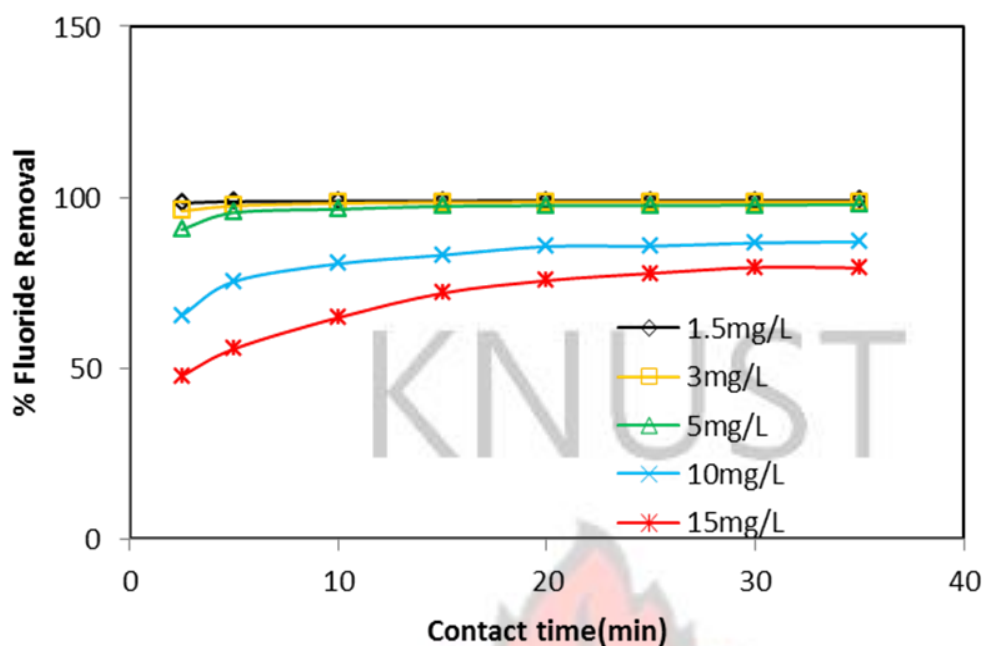


Figure 5.22: Fluoride removal by AML at various initial fluoride concentrations.

It is evident from Fig.5.22 that fluoride adsorption is maximum for concentrations between 1.5-5 mg/L, fluoride adsorption is maximum. There was a decline in the performance as concentration increased beyond 10 mg/L. In summary, AML could effectively remove fluoride from water with concentrations lower than 10 mg/L.

5.6 Equilibration isotherms and sorption kinetics

Equilibrium studies were carried out at an initial pH of 6 ± 0.2 to determine the adsorption capacity of AML. Langmuir and Freundlich models were used to fit to the experimental data. Similar to Section 5.3, the adsorption capacity of AML was determined using Equations 5.2 and 5.3. The results for the Langmuir and Freundlich data are given in the Appendix 6 and illustrated in Figure 5.23.

Both the Freundlich and Langmuir models fitted the experimental data but the Langmuir model gave a better fit to the experimental data with a correlation coefficient of 0.97 as against 0.92 for the Freundlich model (Fig.5.23).

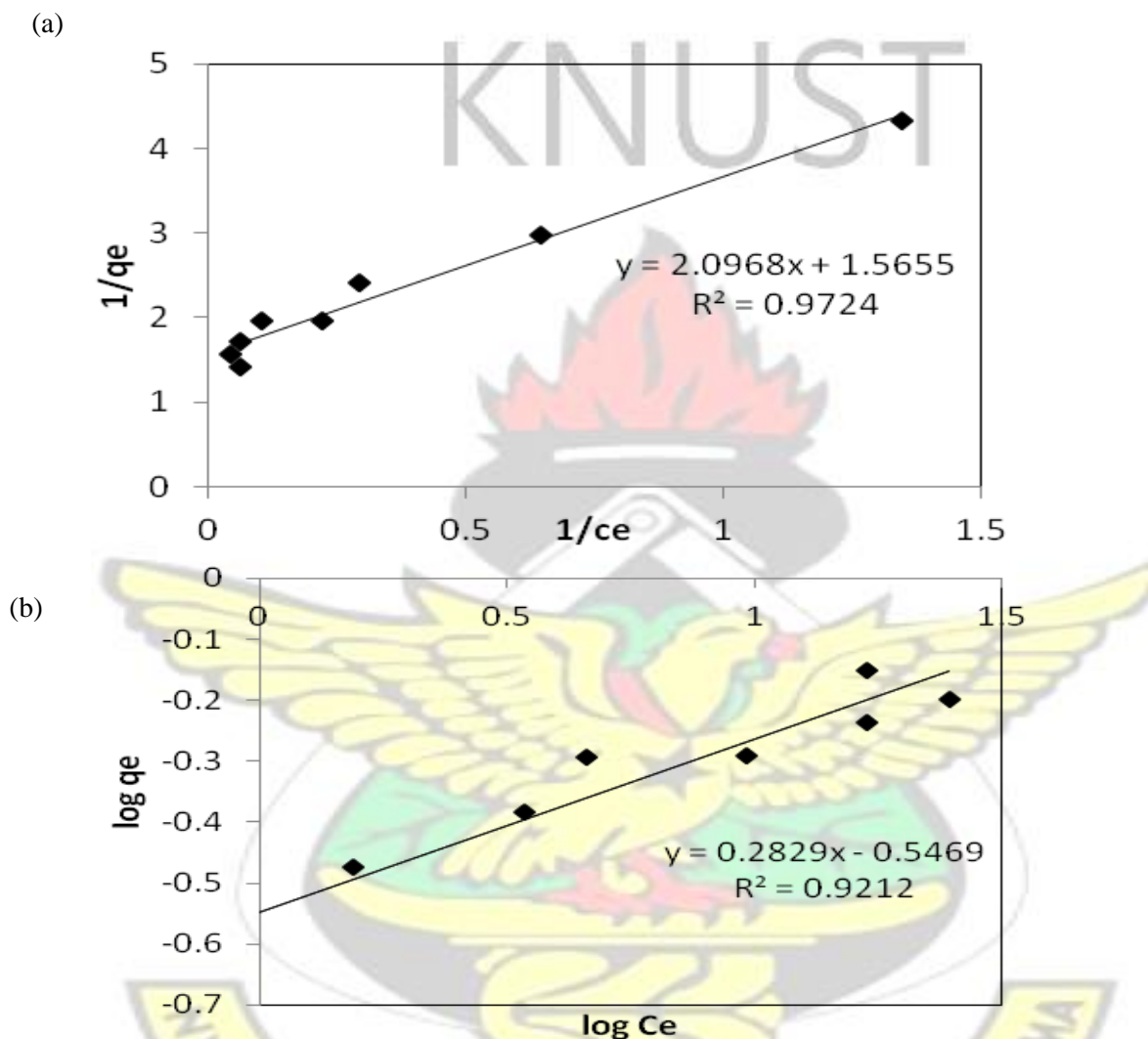


Figure 5.23: Langmuir (a) and Freundlich (b) isotherms of fluoride adsorption by AML at room temperature (adsorbent dosage= 4g/100mL, pH=6±0.2).

The favorability of fluoride adsorption process by AML was examined by the dimensionless quantity, R_L which is given as;

$$R_L = \frac{1}{(1+bC_0)} \quad (5.12) \text{ Where}$$

b is the Langmuir constant ($L.mg^{-1}$) and C_0 is the initial fluoride concentration

(mg/L). The value of $R_L < 1$ represents favorable adsorption whereas $R_L > 1$ represents unfavorable adsorption (Chen *et al.*, 2011). The value of b could be computed from the slope of the Langmuir graph (Fig.5. 23a). In this experiment, the computed values of b range from 0.03-0.15 L.mg⁻¹. It could be inferred therefore that the adsorption process is favorable.

Computing the monolayer capacity (Q_{max}) from the Langmuir graph gave a value of 0.69 mg/g. This value is an improvement over the raw laterite which gave a value of 0.55 mg/g (Osei *et al.*, 2015). It is well known that Langmuir type adsorption assumes a monolayer coverage which suggests that the adsorption of fluoride by AML is limited by surface site saturation. Satisfactory fitting of the Langmuir model to the adsorption isotherms of fluoride on different adsorbents has been reported in literature (Kumar *et al.*, 2009; Fan *et al.*, 2003).

The kinetic analysis of the adsorption data was done based on the reaction kinetics of pseudo-first order and pseudo-second order mechanisms. Following Equations 5.8 and 5.12, the data for Pseudo 1st and 2nd order kinetics were generated (Appendix 7 for 1st order kinetics and Appendix 8 for 2nd order kinetics) and plotted in Figure 5.24. As shown in Fig. 5.24(a), although pseudo-first-order kinetics describes the experimental data quite well, the correlation coefficients were relatively low especially for 3.5 mg/L and 10 mg/L fluoride concentrations (0.9 and 0.91, respectively) (Appendix 9).

Pseudo-second order kinetics describes the data perfectly well as the calculated adsorption capacities (q_2) are close to the experimental adsorption capacities ($q_{e \text{ exp}}$)

(Appendix 9) and also shows very good values for the coefficient of correlation ($R^2 > 0.99$). The linear relationship between t/q_t and t is an indication of chemisorption (Ayoob *et al.*, 2008). Similar kinetic model governed the removal of fluoride using synthetic siderite (Liu *et al.*, 2010).

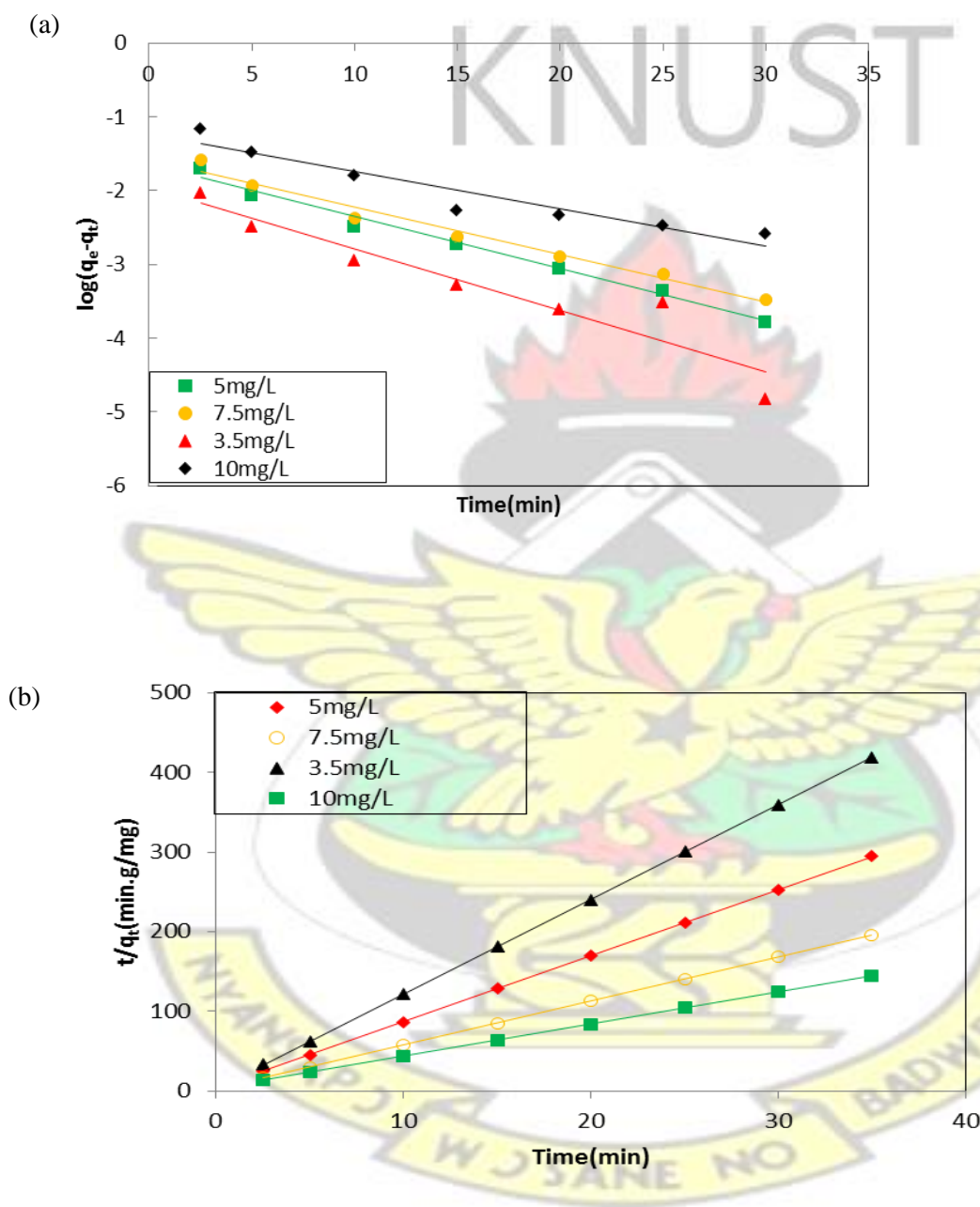


Figure 5.24: Pseudo-first-order (a) and Pseudo-second-order(b) plots of the adsorption data for AML

The application of intraparticle diffusion model in elucidating the mechanism controlling the adsorption of fluoride using AML was explored using Eq. (5.13) by

plotting the fluoride uptake (q_t) against square root of time ($t^{1/2}$) (Kamble *et al.*,2010)

as:

$$q_t = K_p t^{1/2} \quad (5.13)$$

The adsorption process is governed by intraparticle diffusion if a plot of q_t against $t^{1/2}$ gives a straight line and passing through the origin.

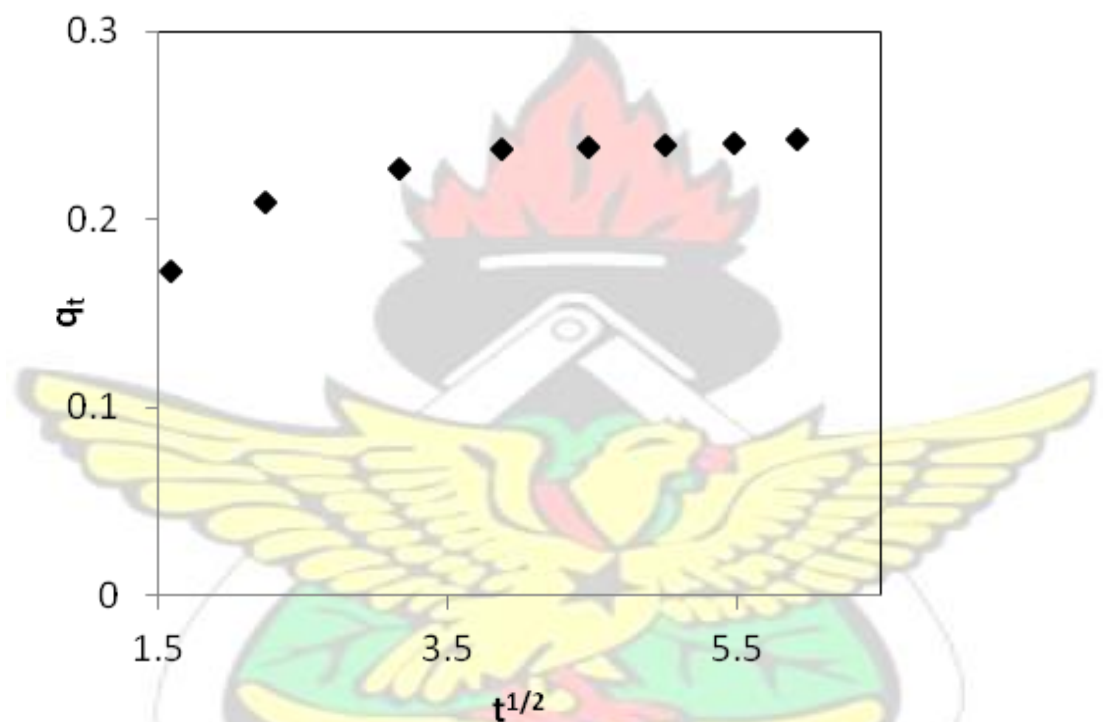


Figure 5.25: A plot of q_t against $t^{1/2}$ for (c_1 -10mg/L) by AML.

As shown (Fig. 5.25) in this experiment, a plot of q_t against $t^{1/2}$ is seen as initially curved. According to Kamble *et al.* (2010), the curved portion is a reflection of film or boundary layer diffusion. As the line did not pass through the origin is an indication that intraparticle diffusion is not the only factor but that there are other kinetic factors controlling the adsorption process (Kumar *et al.*, 2009; Liu *et al.*, 2010).

5.7 Fluoride adsorption in the presence of co-existing anions

Natural groundwater normally contains various aqueous ions that compete for sorption sites and reduce the efficiency of the sorbent to remove fluoride from water. The removal of fluoride in the presence of competing ions such as nitrate (NO_3^-), sulphate (SO_4^{2-}), chloride (Cl^-), bicarbonate (HCO_3^-) and phosphate (PO_4^{3-}) was investigated with differing concentrations of the anions depending on their recommended WHO limits in drinking water. The initial concentration of the fluoride solution was maintained at 10 mg/L at room temperature. The initial pH of the fluoride solution was 6 ± 0.2 and on adding the anions, the solution pH increased to 6.2, 8.3, 6.7, 6.1 and 8.9 for Cl^- , PO_4^{3-} , NO_3^- , SO_4^{2-} and HCO_3^- after fluoride adsorption, respectively.

Data set showing the effect of competing ions on fluoride uptake by AML at adsorbent dosage of 4 g/100mL is presented in Table 4.20. There was relatively no significant influence of Cl^- , NO_3^- and SO_4^{2-} on the fluoride uptake as shown in Figure 5.26. The influence of PO_4^{3-} on the uptake was not evident at low concentrations of phosphate (0.2-1 mg/L of PO_4^{3-}) but at concentrations >50 mg/L, it reduced the fluoride uptake (Fig. 5.26). At higher concentrations, competing anions occupied more active sites and brought about a powerful competitive adsorption which resulted in the decline of fluoride adsorption (Liu *et al.*, 2010).

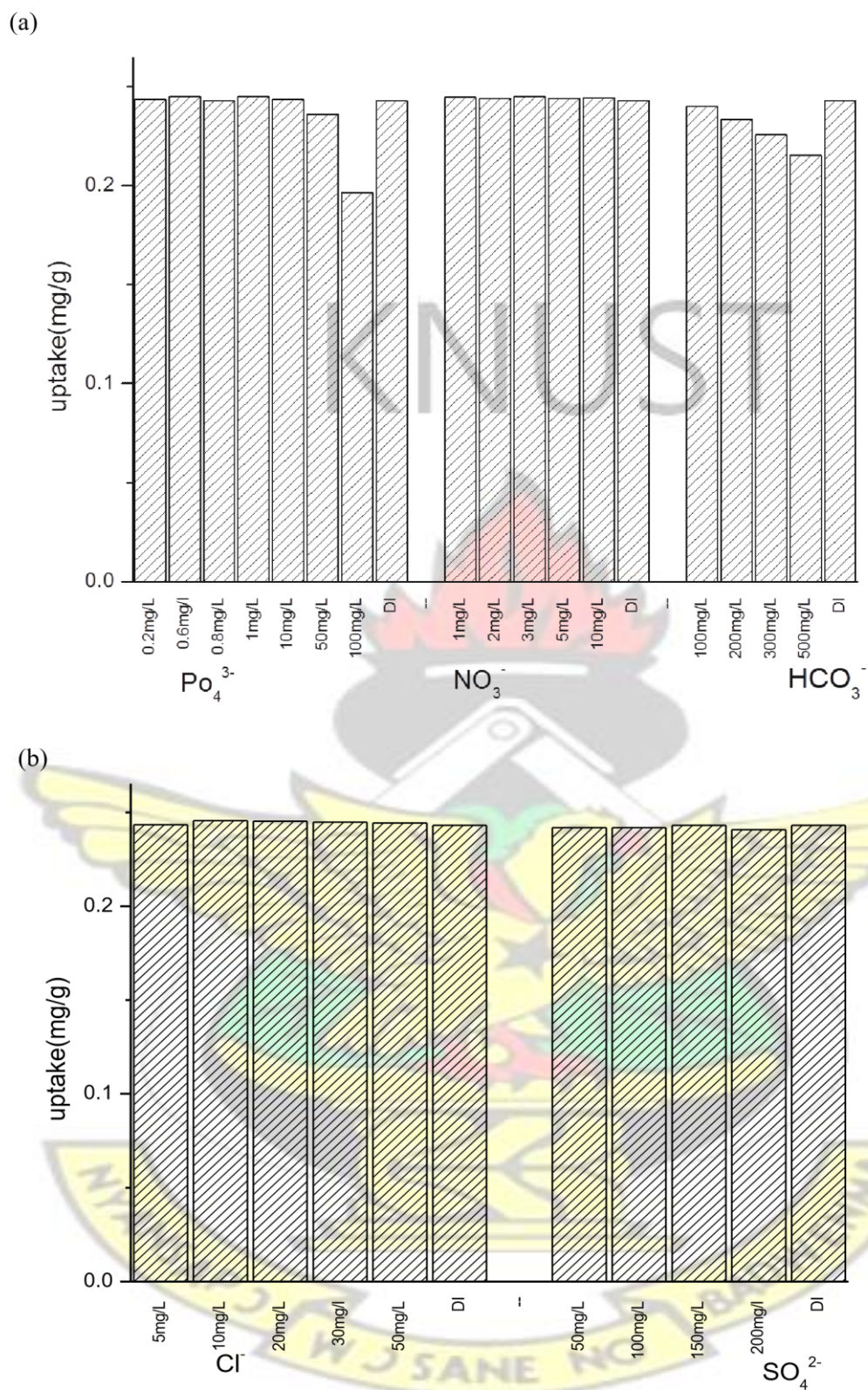
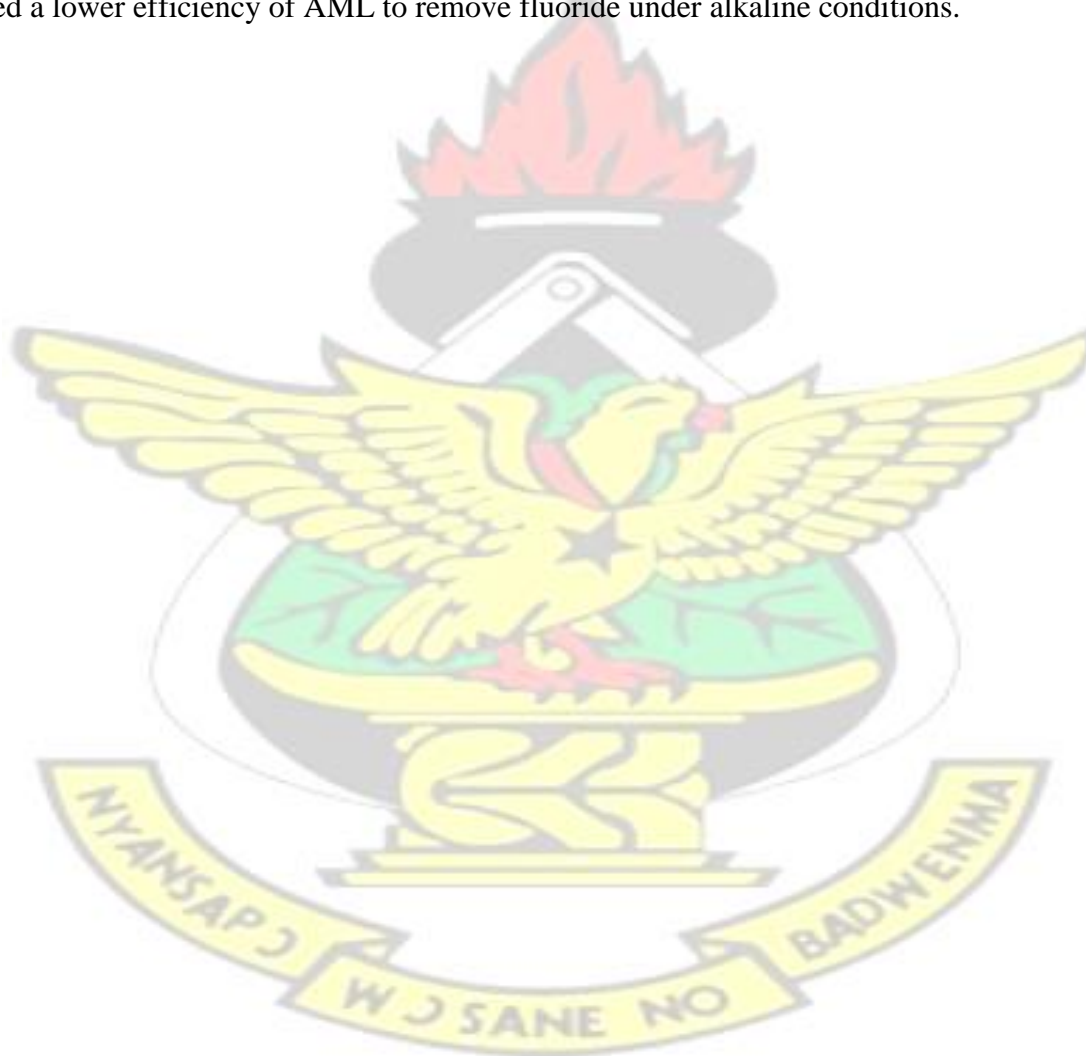


Figure 5.26: Effect of (a) PO₄³⁻, NO₃⁻, HCO₃⁻ and (b) Cl⁻, SO₄²⁻ in solution on fluoride uptake by AML.

However, phosphate is normally present in water at very low concentrations (about 1 mg/L in drinking water) (Fadiran *et al.*, 2008). The effect of bicarbonate on fluoride was clearly seen as it decreased the uptake of fluoride when the concentration was increased from 100 mg/L to 500 mg/L. Bicarbonate buffers a pH system at higher values and therefore reduce the affinity of the active sites for fluoride (Onyango *et al.*, 2004). Therefore, the effect of bicarbonate is a result of the increase in pH of the solution. This was confirmed from experiments on the effect of pH (Fig. 5.20) which showed a lower efficiency of AML to remove fluoride under alkaline conditions.



CHAPTER SIX

SUMMARY, CONCLUSIONS AND RECOMMENDATIONS

6.1 Summary

A study was carried out to evaluate the characteristics of laterite and modified laterite and the application of these materials as local adsorbent material for fluoride removal from fluoride-contaminated water. To this end laterite samples from three different areas in the Bongo district of Upper East Region of Ghana, namely Agamolga, Balungu and Dua were selected for testing.

The selected laterite materials were characterized and tested for fluoride adsorption properties. The chemical and mineral constituents of Agamolga, Balungu and Dua laterites were assessed using X-ray fluorescence, scanning electron microscopy combined with EDX and X-ray diffraction techniques. The results revealed that the laterites contained different compositions of iron oxides/hydroxides, silica (quartz) and alumina. These minerals were found to form a majority of their composition. The minerals; goethite/hematite, kaolinite and quartz were also identified as forming the mineral phases of the laterites. In addition, it was found out that Dua laterite contained muscovite and rutile. The SEM results showed an intimate association of all the minerals, which impacted on the fluoride adsorption characteristics.

As a second objective to evaluate the effect of dependent and extraneous factors on the fluoride removal characteristics of raw and heat-treated laterites, batch adsorption tests were conducted under varying experimental conditions (effect of pH,

heattreatment temperature, particle size and initial fluoride concentration) and the adsorption capacity determined using Freundlich and Langmuir isotherm models. Adsorption responses of Agamolga and Balungu under these experimental conditions were favorable but adsorption capacities were relatively low.

To improve upon the adsorption capacity, selected laterite material was modified. The composites were formed by varying the ratios of laterite to alumina with the laterite forming a larger proportion of the composite. The mineral characteristics of the composite were evaluated using X-ray diffraction and SEM-EDX techniques. Interestingly, the XRD spectra for the different ratios of AML did show alumina peaks but the SEM images and EDX spectra showed strong presence of alumina in the composite. The SEM images show alumina spread on the iron particles indicating proof of hypothesis. AML showed improved performance over untreated laterite in terms of fluoride uptake. In all cases adsorption data was tested with pseudo-first order and pseudo-second-order kinetics with very good results.

6.2 Conclusions

The following conclusions have been drawn based on the observations and results of the analyses from this study;

1. The performance of laterite as a material to remove fluoride from water depends on the chemical and mineralogical composition of the laterite. Adsorption is favoured by the presence of aluminum and iron hydroxides and not favoured by silica.

2. Performance can be enhanced by modifying the laterite by immersion in a suspension of finely ground alumina, drying and heating at 400°C.
3. Fluoride uptake by AML was better than untreated laterite as the adsorption capacity increased from 0.55 mg/g to 0.69 mg/g.
4. By modification, the surface of the iron minerals is chemically coated with alumina, which on heat-treatment leads to the formation of layer of $\text{Fe}_{(1-x)}\text{Al}_x\text{OOH}$, a stable compound that is resistant to caustic solution.
5. Fluoride uptake by both the raw laterites and AML satisfied both Langmuir and Freundlich isotherms.
6. The modification enhanced the fluoride removal property of the laterite by at least 25% (Langmuir isotherm).
7. The adsorption process was also found to be governed by both pseudo- first-order and pseudo-second-order reactions but the pseudo-secondorder model explains the adsorption process better.
8. Adsorption is not affected by the presence of other anions normally present in solution.

6.3 Recommendations

1. In the preparation of AML, it is recommended that the alumina be milled into nano particles to facilitate better coating and diffusion into the interstitial pores of the laterite.
2. Desorption tests could also be conducted to determine the regenerability of AML.
3. Column tests could be done to validate field performance.

REFERENCES

- Abugri D.A.** and Pelig-Ba K.B (2010). Assessment of fluoride in tropical surface soils used for crop cultivation. African Journal of environmental Science and Technology, **5**(9), 653-660.
- Agarwal Kailash C., Gupta Sunil K., and Gupta Akhilendra B (1999).** Development of new low cost defluoridation technology (KRASS). Water Sci. Tech, **40**(2), 167173.
- Agarwal M., Rai K., Shrivastav R., Dass S (2003).** Defluoridation of water using amended clay. J.Clean. Prod., **11**, 439-444.
- Alvarez Jenny Abanto, Rezende Karla Mayra P.C., Marocho Susana Maria Salazar, Alves Fabiana B.T., Celiberti Paula, Ciamponi Ana Lidia (2009).** Dental fluorosis: Exposure, prevention and management. Med. Oral Patol Oral Cir Bucal, **14** (2), E103-7.
- Anim-Gyampo Maxwell, Zango Musah Saeed and Apori Ntiforo (2012).**The origin of fluoride in groundwater of the Palaeozoic sedimentary formations of Ghana. A preliminary study in Gushiegu District. Research Journal of Environmental and Earth Sciences, **4** (5), 546-552.
- Apambire W.B., Boyle D.R., Michel F.A (1997).** Geochemistry, genesis, and health implications of fluoriferous groundwater in the Upper Regions of Ghana. Environmental Geology, **33** (1).
- Armienta M.A. and Segovia N. (2008).** Arsenic and fluoride in the groundwater of Mexico. Environ Geochem Health, **30**, 345-353.
- Atipoka F.A (2010).** Water supply challenges in rural Ghana. Desalination, **251**, 212-217.

Avishek Kirti, Pathak Gopal, Nathawat M.S., Jha Usha, Kumari Neeta (2010). Water quality assessment of Majhiaon block of Garwa district in Jharkland with special focus on fluoride analysis. *Environ Monit Assess*, **167**, 617-623.

Ayamsegna J.A., Apambire W.B., Bakobie N. & Minyila S.A (2008). Removal of fluoride from rural drinking water sources using geomaterials from Ghana. 33rd *WEDC International Conference*, Accra, Ghana. Access to sanitation and safe water: Global partnerships and local actions.

Ayoob S and Gupta A.K (2008). Insights into isotherm making in the sorptive removal of fluoride from drinking water. *Journal of Hazardous Materials*, **152** (3), 976-985.

Ayoob S, Gupta AK, Bhakat PB and Venugopal T Bhat (2008). Investigations on the kinetics and mechanisms of sorptive removal of fluoride from eater using alumina cement granules. *Chemical Engineering Journal*, **140**, 6-14.

Babaeiveli Kamel and Khodadoust Amid P (2013) Adsorption of fluoride onto crystalline titanium dioxide: Effect of pH, ionic strength and co-existing ions. *Journal of Colloid and Interface Science*, 419-427.

Bayon Maria Montes, Rodriguez Garcia Ana, Garcia Alonso J. Ignacio and Alfredo Sanz-Medel (1999). Indirect determination of trace amounts of fluoride in natural waters by ion chromatography: a comparison of on-line post-column fluorimetry and ICP-MS detectors. *Analyst*, **124**, 27-31.

Bhatnagar A., Kumar E., and Sillanpaa M (2011). Fluoride removal from water by adsorption- a review. *Chemical Engineering Journal* **171**, 811-840.

Biswas Krishna, Gupta Kaushik, Goswami Arijit, Ghosh Uday Chand (2010). Fluoride removal efficiency from aqueous solution by synthetic Iron (III)-Aluminum (III) - Chromium (III) ternary mixed oxide. *Desalination*, **255**, 44-51

Bjorvatn K., Bardsen A., and Tekle-Haimanot R (1997). *Defluoridation of drinking water by use of clay/soil*, in 2nd Int. workshop on fluorosis and defluoridation of water. Publ. Int. Soc. Fluoride Res., pp. 100-105.

Bourman Robert P. and Ollier Clifford D (2002). A critique of the Schellmann „ “. *C tena*, **47**, 117-131.

Bower C.A. and Hatcher J.T (1967). Adsorption of fluoride by soils and minerals. *J. Soil Sci.*, **3**, 151-154.

Brindha K. and Elango, L (2011). Fluoride in groundwater: causes, implications and mitigation measures. In Monroy, S.D. (Ed.), *fluoride properties, applications and environment management*, 111-136.

Buamah R., Asare Mensah R. and Salifu A (2013). Adsorption of fluoride from aqueous solution using low cost adsorbent. *Water Science and Technology: Water Supply*, **13**, 2.

Bulusu K.R., Nawlakhe W.G (1988). Defluoridation of water with activated alumina: batch operations. *Indian J. Environmental Health*, **30** (3), 262-299.

Camacho Lucy M., Torres Arely, Saha Dipendu, Deng Shuguang (2010). Adsorption equilibrium and kinetics of fluoride on sol-gel-derived activated alumina adsorbents. *Journal of Colloid and Interface Science*, **349**, 307-313.

Chae Gi-Tak, Yun Seong-Taek, Mayer Bernhard, Kim Kyoung-Ho, Kim SeongYong, Kwon Jang-Soon, Kim Kangjoo, Koh Yong-Kwon (2007). Fluorine geochemistry in bedrock groundwater of South Korea. *Science of the Total Environment*, **385**, 272-283.

Chen Nan, Zhang Zhenya, Feng Chuanping, Li Miao, Zhu Dirui, Chen Rongzhi, Sugiura Norio (2010). An excellent fluoride sorption behaviour of ceramic adsorbent. *Journal of Hazardous Materials*, **183**, 460-465.

Chen Nan, Zhang Zhenya, Feng Chuanping, Zhu Dirui, Yang Yinguan, Sugiura Norio (2011). Preparation of and characterization of porous granular ceramic containing dispersed aluminum and iron oxides as adsorbent for fluoride removal from aqueous solution. *Journal of Hazardous Materials*, **186**, 863-868.

Chen Z., Xing B., McGill W.B (1999). A unified sorption variable for environmental application of the Freundlich isotherm. *J. Environ. Qual.*, **28**, 1422-1428.

Chernet T., Trafi, Y., Valles, V (2002). Mechanism of degradation of the quality of natural water in the lakes region of the Ethiopian rift valley. *Water Res.*, **35**, 2819-2832.

Chidambaram S., Ramanathan, AL and Vasudevan, S (2003). Fluoride removal studies in water using natural materials. *Water SA*, **29** (3).

Craig Laura, Stillings Lisa L., Decker David L., Thomas James M. (2015). Comparing activated alumina with indigenous laterite and bauxite as potential sorbents for removing fluoride from drinking water in Ghana. *Applied Geochemistry*, **56**, 50-66.

Cumberbatch, T., Atipoka, F., Ayamgah, G., Batir, B., Berger, D., Freed, L., Momade, F., Nyarku, M., Pervez, N., Ponce, B., Rana, S., Venugopal, V., Volk, L (2008). The Development of an Indigenous Filter. EPA P3 Award: A National Student Competition for Sustainability Focusing on People, Prosperity, and Planet (2007). Cooper Union for the Advancement of Science and Art, New York.

Dey Soumen, Goswami Saswati & Ghosh Uday Chand (2004). Hydrous Ferric Oxide

(HFO) - A scavenger for fluoride from contaminated water. *Water, Air and Soil Pollution*, **158**, 311-323.

Dissanayake C.B. and Chandrajith R (2009). Introduction to Medical Geology, Erlangen Earth Conference Series. Springer- Verlag, DOI 10. 1007/978-3-64200485-8_4.

Edmunds W.M. and Smedley P.L (1996). Groundwater geochemistry and health: an overview. In: Appleton, Fuge and McCall [Eds] *Environmental Geochemistry and Health*. Geological Society special publication **113**, 91-105.

EPA (1997). Public health goal for fluoride in drinking water. California: Pesticide and environmental toxicology section office of Environmental health hazard assessment, California Environmental Protection Agency.

Fadiran AO, Dlamini SC and Mavuso A (2008). A comparative study of the phosphate levels in some surface and groundwater bodies of Swaziland. *Bull. Chem. Soc. Ethiopia*, **22**(2), 197-206.

Fan X, Parker DJ, Smith MD (2003). Adsorption kinetics of fluoride on low cost materials. *Water Research*, **37**, 4929-4937.

Fantong W.Y., Satake H., Ayonghe S.N., Suh E.C., Adelana S.M.A., Fantong E.B.S., Banseka H.S.M., Gwanfogbe C.D., Woincham L.N., Uehara Y., Zhang J (2010). Geochemical provenance of spatial distribution of fluoride in groundwater of Mayo Tsanaga River Basin, Far North Region, Cameroon: implications for incidence of fluorosis and optimal consumption dose. *Environ Geochem Health*, **32**, 147-163.

Farooqi Abida, Masuda Harue, Firdous Noushen (2007). Toxic fluoride and arsenic contaminated groundwater in the Lahore and Kasur districts, Punjab, Pakistan and possible contaminant sources. *Environmental Pollution*, **145**, 839-849.

Fawell J., Bailey K., Chilton J., Dahi E., Fewtrell L., Magara Y. (2006). Fluoride in drinking water, IWA publishing, London.

Fey Martin Venn and Dixon Joe Borris (1981). Synthesis and properties of poorly crystalline hydrated aluminous goethite. *Clays and Clay Minerals*, **29**, 91-100.

Foo K.Y. and Hameed B.H (2010). Insights into the modeling of adsorption isotherm systems. *Chemical Engineering Journal*, **156**, 2-10.

Fordyce F.M., Vrana K., Zhosvinsky E., Povoroznuk V., Toth G., Hope B.C., Iljinsky, U., Baker, J (2007). A health risk assessment of fluoride in Central Europe. *Environ Geochem Health*, **29**, 83-102.

Frencken J.E (1992). Endemic fluorosis in developing countries, causes, effects and possible solution. Publication number 91.082, NIPG-TNO, Lieden, The Netherlands.

Garcia M.G., Lecomte K.L., Stupar Y., Formica S.M., Barrionuevo M., Vesco M., Gallara R., Ponce R (2011). Geochemistry and health aspects of F-rich mountainous streams and groundwaters from sierras Pampeanas de Cordoba, Argentina. *Environ Earth Sci.*, DOI 10.1007/s 12665-011-1006-z, Special Issue.

Ghorai Subhashini, Pant, K.K (2005). Equilibrium, kinetics and breakthrough studies for adsorption of fluoride on activated alumina. *Separation and Purification Technology*, **42**, 265-271

Glocheux Yoann, Pasarin Mendez Martin, Albadarin Ahmad B., Allen Stephen J., walker Gavin M (2013). Removal of arsenic from groundwater by adsorption onto acidified laterite by-product. *Chemical Engineering Journal*, **228**, 565-574.

Gomoro Kefyalew, Zewge Felike, Hundhammer Bernd and Megersa Negussie

(2012). Fluoride removal by adsorption on thermally treated lateritic soils. Bull. Chem. Soc. Ethiop., **26** (3), 361-372.

Gunnar Jacks, Prosun Bhattacharya, Vikas Chaudhary, K.P. Singh (2005). Controls of the genesis of some high fluoride groundwaters in India. Applied Geochemistry, **20**, 221-228.

Guo Qinghai, Wang Yanxim, Guo Qinghai (2010). Hydrogeochemical genesis of ground waters with abnormal fluoride concentrations from Zhongxiang city, Hubei Province, central China. Environ Earth Sci., **60**, 633-642.

Halim M.A., Hoque Waliul S.A.M., Hossain M.K., Saadat A.H.M., Goni M.A. and Islam Saiful M (2008). Arsenic removal properties of laterite soil by adsorption filtration method. Journal of Applied Sciences, **8** (20), 3757-3760.

Harrison Paul T.C. (2005). Fluoride in water: A UK perspective. Journal of Fluorine chemistry, **126**, 1448-1456.

Hauge S., Osterberg R., Bjorvatn K., Selvig K.A. (1994). Defluoridation of drinking water: effect of firing temperature. Scand. J. Dent. Res., **102**, 329-333.

Hem J.D (1970). Study and interpretation of the chemical characteristics of natural water. Water supply paper 1473, 2nd edition, US Geological Survey, Washington, D.C., 178pp.

Ho Y.S., Porter J.F., McKay G (2002). Equilibrium isotherm studies for the sorption of divalent metal ions onto peat: copper, nickel and lead single component systems. Water, Air, Soil Pollution, **141**, 1-33.

Hu C.Y., Lo S.L., Kuan W.H., Lee Y.D (2005). Removal of fluoride from semiconductor wastewater by electro coagulation-flotation. *Water Research*, **39** (5), 895-901.

Hussain J., Hussain I., Sharma K.C (2010). Fluoride and health hazards: community perception in a fluoritic area of central Rajasthan (India): an arid environment. *Environ Monit Assess*, **162**, 1-14.

Islam M and Patel R. R (2006). Evaluation of removal efficiency of fluoride from aqueous solution using quick lime. *Journal of Hazardous Materials*, **143**, 303-310.

Jamode A.V., Sapkal V.S. and Jamode V.S (2004). Defluoridation of water using inexpensive adsorbents. *J. Indian Inst. Sci.*, **84**, 163-171.

Jayantha K.S., Ranjana G.R., Sheela H.R., Mondang Ritu and Shivananni Y.S (2004). Defluoridation studies using laterite material. *Journal of Environ. Science & Engg.*, **46** (4), 282-288.

Jha Sunil Kumar, Mishra Vinay Kumar, Sharma Dinesh Kumar and Damodaram Turkkaram (2011). Fluoride in the environment and its metabolism in humans. *Reviews of Environment Contamination and Toxicology*, 211, DOI 10.1007/978-14419-8011-3_4.

Jinadasa K.B.P.N., Dissanayake C.B., Weerasoorija S.V.R. and Senaratne A (1993). Adsorption of fluoride on goethite surfaces and implications on dental epidemiology. *Environmental Geology*, **21**, 251-255.

Joachim A.W.R and Kandiah S (1941). The composition of local soil concretions and clays. *Tropical Agriculture*, **96**, 255-358.

Johnston R., Heijnen H (2002). Safe water technology for arsenic removal. Report, World Health Organization (WHO).

Kamble Sunjay P., Deshpande Gunavant, Barve Prashant P., Rayalu Sadhana, Labhsetwar Nitin K., Malyshev Alexander, Kulkarhi Bhaskar D (2010). Adsorption of fluoride from aqueous solution by alumina of alkoxide nature: Batch and continuous operation. *Desalination* **264**, 15-23.

Karthikeyan G., Anitha Pius and G. Alagumuthu (2005). Fluoride adsorption studies of montmorillonite clay. *Indian Journal of Chemical Technology*, **12**, 263272.

Kaseva M.E (2006). Optimization of regenerated bone char for fluoride removal in drinking water: a case study in Tanzania. *Journal of Water and Health*

Kir E., Alkan E (2006). Fluoride removal by Donnan analysis with plasma-modified and unmodified anion-exchange membranes. *Desalination*, **197**, 217-224.

Ku Y., Chiou H.M., Wang W (2002). The removal of fluoride ion from aqueous solution by a cation synthetic resin. *Sep. Sci. Technol.*, **37**, 89-103.

Ku Young and Chiou Hwei-Mei (2002). The adsorption of fluoride ion from aqueous solution by activated alumina. *Water, Air and Soil Pollution*, **133**, 349-360.

Kumar Eva, Bhatnagar Amit, Ji Minkyu, Jung Woosik, Lee Sang-Hun, Kim Sun-Joon, Lee Giehyeon, Song Hocheol, Choi Jae-Young, Yang Jung-Seok, Jeon ByongHun (2009). Defluoridation from aqueous solutions by granular ferric hydroxide (GFH). *Water Research*, **43**, 490-498.

Leyva-Ramos Roberto, Medellin-Castillo Nahum A., Jacobo-Azuara Araceli,

- Mendoza-Barro - M. - (2008). Fluoride removal from water solution by adsorption on activated alumina prepared from pseudo-boehmite. *J. Environ. Eng. Management*, **18** (5), 301-309.
- Lhassani** A., Rumeau M. Benjelloun D. and Pontie M. (2000). Selective demineralization of water by Nano filtration application to the defluoridation of brackish water. *Water Research*, **35** (13), 3260-3264.
- Liu** H, Deng S, Li Z, Yu G and Huang J (2010). Preparation of Al-Ce hybrid adsorbent and its application for defluoridation of drinking water. *Journal of Hazardous Materials*, **179**, 424-430.
- Liu** Qiong, Guo Huaming and Shan Yue (2010). Adsorption of fluoride on synthetic siderite from aqueous solution. *Journal of Fluorine Chemistry*, **131**, 635-641.
- Liu** Yu (2006). Some consideration on the Langmuir isotherm equation. *Colloids and Surfaces A: Physicochemical Eng. Aspects*, **274**, 34-36.
- Lopez** M., Coca J., Rosal R., Garcia R., Sastre H (1992). Modeling and experimental behaviour of multi component anion-exchange with amberlite IRA-410. *Hung. J. Ind. Chem.*, **20**, 109-112.
- Maiti** Abhijit, Basu Jayantha Kumar, Sirshendu De (2011). Chemical treated laterite as promising fluoride adsorbent for aqueous system and kinetic modeling. *Desalination*, **265**, 28-36.
- Maiti** Abhijit, Basu Jayantha Kumar, Sirshendu De (2012). Experimental and kinetic modeling of As (V) and As (III) adsorption on treated laterite using synthetic and contaminated groundwater: effects of phosphate, silicate and carbonate ions. *Chemical Engineering Journal*, **191**, 1-12.

Maji Sanjoy Kumar, Pal Anjali, Pal Tarasankar (2008). Arsenic removal from reallife groundwater by adsorption on laterite soil. *Journal of Hazardous Materials*, **151**, 811-820.

Meenakshi and R.C. Maheshwari (2006). Fluoride in drinking water and its removal. *Journal of Hazardous Materials B*, **137**, 456-463.

Meenakshi S. & Viswanathan N (2007). Identification of selective ion-exchange resin for fluoride sorption. *J. Colloid Interface Sci.*, **308**, 438-450.

Mirna Habuda-Stanic, Maja Ergovic Ravancic and Andrew Flanagan (2014). A review on adsorption of fluoride from aqueous solution. *Materials*, **7**, 6317-6366.

Mjengera H. & Mkongo G (2003). Appropriate defluoridation technology for use in fluoritic areas in Tanzania. *Physics and Chemistry of the Earth*, **28**, 1097-1104.

Moges G., Zewge F., and Socher M (1996). Preliminary investigations on the defluoridation of water using fired clay chips. *Journal of African Earth Sciences*, **21** (4), 479-482.

Mohapatra, M., Anand, S., Mishra, B.K., Giles Dion E., Singh P. (2009). Review of fluoride removal from drinking water. *Journal of Environmental Management*, **91**, 67-77.

Mondal N.C., Prasad R.K., Saxena V.K., Singh Y., Singh V.S. (2009). Appraisal of highly fluoride zones in groundwater of Kurmapalli watershed, Nalgonda district, Andhra Pradesh (India). *Environ Earth Sci.*, **59**, 63-73.

Msonda K.W.M., Masamba W.R.L., Fabiano E (2007). A study of fluoride groundwater occurrence in Nathenje, Lilongwe, Malawi. *Physics and Chemistry of the Earth*, **32**, 1178-1184.

Naseem Shahid, Tahir Rafique, Erum Bashir, Muhammad Iqbal Bhangar, Amanullah Laghari, Tanzil Haider Usmani (2010). Lithological influences on occurrence of high-fluoride groundwater in Nagar Parkar area, Thar Desert, Pakistan. *Chemosphere*, **78**, 1313-1321.

Nath Suresh K. & Dutta Robin K (2010). Fluoride removal from water using crushed limestone. *Indian Journal of Chemical Technology*, **17**, 120-125.

Onyango Maurice S. & Matsuda, Hitoki (2006). Fluoride removal from water using adsorption techniques. *Fluorine and the Environment*, **2**. DOI: 10.1016/S 1872- 0358 (060 02001-X).

Onyango MS, Kojima Y, Aoyi O, Bernardo EC and Matsuda H (2004). Adsorption equilibrium modeling and solution chemistry dependence of fluoride removal from water by trivalent-cation-exchanged zeolite F-9. *J. Colloid Interface Sci.*, 341-350.

Osei Juliet, Gawu Simon K.Y., Schafer Andrea I., Atipoka Faustina and Momade Francis W.Y (2015). Impact of laterite characteristics on fluoride removal from water. *Journal of Chemical Technology and Biotechnology*, DOI 10. 1002.

Ozsvath David L (2008). Fluoride and environmental health: A review. *Rev Environ Sci Biotechnol*, **8**, 59-79

Partey Frederick, Norman David I., Ndur Samuel, Nartey Robert (2009). Mechanism of arsenic sorption onto laterite iron concretions. *Colloids and Surfaces A: Physicochemical and Engineering Aspects*, **337**, 164-172.

Pelig-Ba K.B (1998). Trace elements in groundwater from some crystalline rocks in the Upper Regions of Ghana. *Water, Air & Soil Pollution*, **103**, 71-89.

Reddy D.V., Nagabhushanam P., Sukhija B.S., Reddy A.G.S., Smedley P.L (2010). Fluoride dynamics in the granitic aquifer of the Wailapally watershed, Nalgonda district, India. *Chemical Geology*, **269**, 278-289.

Richards M (2010). Impact of pH on the removal of fluoride, nitrate and boron by nanofiltration/reverse osmosis. *Desalination*, **261**, 331-337

Rossiter M. . M M. Andrea I (2010). Chemical drinking water quality in Ghana: Water costs and scope for advanced treatment. *Science of the Total Environment*, **408**, 2378-2386.

Sarkar M., Banarjee A., Pramanick P.P., Sarkar A. R (2006). Use of laterite for the removal of fluoride from contaminated drinking water. *Journal of Colloid and Interface Science*, **302**, 432-441.

A.I., Rossiter H.M.A., Owusu P.A., Richards B.S., Awuah E (2009). Physico-chemical water quality in Ghana: prospects for water supply technology implementation. *Desalination*, **248**, 193-203.

Schellmann W. (1986). A New Definition of Laterite. *Geol Surv. India*, 120, 1-7.

Schellmann W., An introduction to laterite. [Online]. Available: <http://www.laterite.de/index.html>[5August 2013]

Sehn Peter (2008). Fluoride removal with extra low energy reverse osmosis membranes: three years of large scale field experience in Finland. *Desalination*, **223**, 73-84.

Shashi A., Kumar M., Bhardwaj M (2008). Incidence of skeletal deformities in endemic fluorosis. *Trop. Doct.*, **38**, 231-233.

Shier R.P., Dollimore N., Ross D.A., Binka F.N., Quigley M., & Smith P.G (1996). Drinking water sources, mortality and diarrhoea morbidity among young children in Northern Ghana. *Tropical Medicine and International Health*, **1** (3), 334-341.

Sohn Seungman and Kim Dongsu (2005). Modification of Langmuir isotherm in solution systems-definition and utilization of concentration dependent factor. *Chemosphere*, **58**, 115-123.

Srimurali M., Pragathi A., Karthikeyan J (1998). A study on removal of fluorides from drinking water by adsorption onto low-cost materials. *Environmental Pollution*, **99**, 285-289.

Stewart Theodora. Removal of fluoride from drinking water: analysis of alumina based sorption. Term paper, FS (2009). Institute of Biogeochemistry and pollutant dynamics. Department of Environmental Science, ETH, Zurich

Sujana M.G & Anand S (2010). Iron and aluminum based mixed hydroxide, a novel sorbent for fluoride removal from aqueous solutions. *Applied Surface Science*, **256**, 6956-6962.

Sujana M.G. & Anand S (2011). Fluoride removal studies from contaminated groundwater by using bauxite. *Desalination*, **267**, 222-227.

Sujana M.G., Pradhan H. K., and Anand S (2009). Studies on sorption of some geomaterials for fluoride removal from aqueous solutions. *Journal of Hazardous Materials*, **161**, 120-125.

Sundaram C. Sairam, Viswanathan Natrayasamy and Meenakshi S (2008). Defluoridation chemistry of synthetic hydroxyapatite at nano scale: Equilibrium and kinetic studies. *Journal of Hazardous Materials*, **155**, 206-215.

Sunil Kumar Srivastava & A.L. Ramanathan (2008). Geochemical assessment of groundwater quality in vicinity of Bhalswa landfill, Delhi, India, using graphical and multivariate statistical methods. *Environ. Geol.*, **53**, 1509-1528.

Tahaikt M., El Habbani R., Ait Haddou A., Achary I., Amor Z., Taky M., Alamib A., Boughriba A., Hafsi M., Elmidaou A (2007). Fluoride removal from groundwater by nanofiltration. *Desalination*, **212**, 46-53.

Tang Yulin, Guan Xiaohong, Su Tingzhi, Gao Naiyun, Wang Jianmin (2009). Fluoride adsorption onto activated alumina. Modeling the effects of pH and some competing ions. *Colloids and Surfaces A: Physicochemical and Engineering Aspects*, **337**, 33-38.

Thomas Jnr Josephus and Gluskoter Harold J. (1974). Determination of fluoride in coal with the fluoride ion-selective electrode. *Anal. Chem.*, **46** (9), 1321-1323.

Tor Ali (2006). Removal of fluoride from an aqueous solution by using montmorillonite. *Desalination*, **201**, 267-276.

Tripathy Sushree Swarupa, Bersillon Jean-Luc, Gopal Krishna (2006). Removal of fluoride from drinking water by adsorption onto alum-impregnated activated alumina. *Separation and Purification Technology*, **50**, 310-317.

United Nations (UN) Comprehensive assessment of the freshwater resources of the world, **1999** in: fluoride removal from water using adsorption techniques, Maurice S. Onyango & Hitoki Matsuda. *Fluorine and the Environment*, Chapter 1, Vol 2, DOI: 10.1016/s 1872-0358(06)02001-x.

Vithanage M, Jayarathna L, Rajapaksha A.U, Dissanayake C.B, Bootharaju M.S and Pradeep T (2012). Modeling sorption of fluoride onto iron rich laterite. Colloids and Surfaces A: Physicochemical and Engineering Aspects, **398**, 29-75.

Vuhahula E.A.M., Masalu J.R.P., Mabelya L., Wandwi W.B.C (2009). Dental fluorosis in Tanzania Great Rift valley in relation to fluoride levels in water and in „M Trona). Desalination, **248**, 610-615.

Wakgari Furi, Moumtaz Razack, Tamiru Alemayehu Abiye, Tenalem Ayenew, Dagnachew Legesse (2011). Fluoride enrichment mechanism and geospatial distribution in the volcanic aquifers of the middle Awash basin, Northern Main Ethiopian Rift. Journal of African Earth Sciences, **60**, 315-327.

Wambu Enos W., Onindo Charles O., Ambusso Willis J., and Muthakia Gerald K (2012). Fluoride adsorption onto an acid treated lateritic mineral from Kenya: Equilibrium studies. African Journal of Environmental Science and Technology, **6** (3), 160-169.

Wang W., Li R., Tan J., Luo K., Yang L., Li H., Li Y (2002). Adsorption and leaching of fluoride in soils of china. Fluoride, **35**, 12-129.

Weber W.J. and Morris J.C (1964). Equilibria and capacities for adsorption on carbon. J. Sanitary Eng. Div., **90**, 79-107.

WRC (2014). Hydrogeological and isotopic assessment of the monitoring wells in the Upper East, Upper West and Northern Regions of Ghana. WRC unpublished report.

Wu Fei (2012). Aluminous goethite in the Bayer process and its impact on alumina recovery and settling. PhD. Curtin University, Faculty of Science and Engineering, Department of Chemistry.

Wu Xiaomei, Zhang Yu, Dou Xiaomin, Yang Min (2007). Fluoride removal performance of a novel Fe-Al-Ce trimetal oxide adsorbent. *Chemosphere*, **69**, 17581764.

Yamamura S.S., Wade M.A., Sikes J.H (1962). Direct spectrophotometric fluoride determination. *Anal. Chem.*, **34** (10), 1308-1312.

Zakia A., Bernard B., Nabil M., Mohammed T., Stephan N. and Azzedine E (2001). Fluoride removal from brackish water by Electrodialysis. *Desalination*, **133**, 215-233, Elsevier Science BV.

Zevenbergen C., van Reeuwijk L.P., Frapporto G., Louws R.J., and Schuiling R.D (1996). A simple method for defluoridation of drinking water at village level by adsorption on Ando soil in Kenya. *The Science of the Total Environment*, **188**, 225232.

Zhang Liang, Hong song, He Jing, Gan Fuxing, Ho Yuh-Shan (2011). Adsorption characteristic studies of phosphorus onto laterite. *Desalination and Water Treatment*, **25**, 98-105.

Zhu Chang-Qing, Chen Jin-Long, Zheng Hong, Wu Yu-Qin, Xu Jin-Gou (2005). A colorimetric method for fluoride determination in aqueous samples based on the hydroxyl deprotection reaction of cyanine dye. *Analytica Chimica Acta*, **539** (1-2), 311-316.

Zhu J., Zhao H., Ni J. (2007). Fluoride distribution in electro-coagulation

Appendix

Appendix 1

Data for determination of isotherm models for the heat treated Agamolga laterite.

C_0 (mg/L)	Log C_e	Log q_e	$1/q_e$	$1/C_e$
5	0.6178	-1.3706	23.4734	0.2411
10	0.9022	-0.9964	9.9183	0.1253
15	1.0676	-0.7806	6.0338	0.0856
20	1.2262	-0.8006	6.3175	0.0594
25	1.3365	-0.7827	6.0633	0.0461
30	1.4244	-0.7658	5.8299	0.0376
40	1.5485	-0.6342	4.3069	0.0283
45	1.6174	-0.7494	5.6153	0.0241
50	1.6519	-0.5902	3.8919	0.0223

* C_0 = initial fluoride concentration; C_e = equilibrium fluoride concentration; q_e = adsorption capacity at equilibrium.

Appendix 2

Data for determination of isotherm models for the heat treated Balungu laterite.

C_0 (mg/L)	Log C_e	Log q_e	$1/q_e$	$1/C_e$
5	0.4798	-1.0040	10.0932	0.3313
10	0.8201	-0.7706	5.8969	0.1513
15	1.0335	-0.6779	4.7628	0.0926
20	1.1639	-0.5675	3.6942	0.0686
25	1.2679	-0.4904	3.0931	0.0539
30	1.3632	-0.4608	2.8891	0.0433
40	1.5131	-0.4311	2.6985	0.0307
45	1.5554	-0.3431	2.2036	0.0278
50	1.6082	-0.3269	2.1225	0.0246

Appendix 3

Data for Pseudo-first order kinetics (initial concentration of fluoride=10mg/L).

Time (minutes)	Log ($q_e - q_t$)			
	Agamolga, Raw	Agamolga, HT	Balungu, Raw	Balungu, HT
2.5	-1.1356	-1.101	-1.1640	-0.8446
5	-1.2771	-1.2121	-1.2536	-0.9849
10	-1.3486	-1.3386	-1.4003	-1.2396
15	-1.4631	-1.5947	-1.4951	-1.4284
20	-1.7073	-1.7416	-1.4536	-1.6495
25	-1.8486	-1.9494	-1.4536	-1.9075
30	-2.1097	-2.5046	-1.8541	-2.2701

Appendix 4

Data for Pseudo-second order kinetics (initial fluoride concentration=10mg/L).

Time (minutes)	t/q _t			
	Agamolga, Raw	Agamolga, HT	Balungu, Raw	Balungu, HT
2.5	74.2746	21.4132	50.5221	51.0796
5	92.5869	37.1282	80.3161	56.5316
10	161.2523	66.5853	127.7939	74.4269
15	207.1672	87.9221	174.3168	96.9786
20	229.3214	112.4192	241.4166	117.9597
25	269.8036	135.2815	301.7701	139.2059
30	302.8329	155.5159	288.3539	160.7771
35	327.6165	178.5397	296.5345	182.3268

Appendix 5

Comparison of Pseudo-first-order and Pseudo-second-order model parameters, calculated q_e (cal) and experimental q_e (exp) values for initial concentration of 10 mg/L.

Pseudo-first order kinetics				
C ₀ =10mg/L	q _e (exp)(mg/g)	q _e (cal)(mg/g)	K ₁ (min ⁻¹)	R ²
Agamolga, Raw	0.1068	0.0907	0.0334	0.98
Agamolga, HT	0.1960	0.1188	0.0462	0.95
Balungu, raw	0.1180	0.0710	0.0189	0.79
Balungu, HT	0.1919	0.1916	0.0493	0.99
Pseudo-second order kinetics				
C ₀ =10mg/L	q _e (exp)(mg/g)	q ₂ (cal)(mg/g)	K ₂ (g/mg.min ⁻¹)	R ²
Agamolga, Raw	0.1068	0.1274	0.9015	0.98
Agamolga, HT	0.1960	0.2099	1.5655	0.99
Balungu, Raw	0.1180	0.1207	1.4409	0.92
Balungu, HT	0.1919	0.2426	0.4662	0.99

Appendix 6

Results for determination of isotherm models for AML.

C ₀ (mg/L)	Log C _e	Log q _e	1/q _e	1/C _e
10	-0.1289	-0.6356	4.3212	1.3454
15	0.1898	-0.4733	2.9736	0.6459
20	0.5327	-0.3822	2.411	0.2933
25	0.6601	-0.2918	1.958	0.2187
30	0.9806	-0.2916	1.9572	0.1048
40	1.2235	-0.2352	1.7189	0.0598
45	1.2235	-0.1507	1.4149	0.0598
50	1.3906	-0.1969	1.5735	0.0407

Appendix 7

Data for Pseudo-first order kinetics for AML.

Time(minutes)	Log (qe-qt)			
	3.5mg/L	5mg/L	7.5mg/L	10mg/L
2.5	-2.03	-1.69	-1.59	-1.15
5	-2.48	-2.05	-1.93	-1.47
10	-2.94	-2.49	-2.38	-1.79
15	-3.28	-2.73	-2.63	-2.27
20	-3.61	-3.05	-2.89	-2.32
25	-3.51	-3.35	-3.13	-2.46
30	-4.82	-3.77	-3.48	-2.58

Appendix 8

Data for Pseudo-second order kinetics for AML.

Time(minutes)	t/qt			
	3.5mg/L	5mg/L	7.5mg/L	10mg/L
2.5	33.73	25.42	16.35	14.49
5	62.34	45.49	29.94	23.93
10	121.44	86.55	57.29	44.05
15	180.81	128.33	85.04	63.13
20	240.27	169.67	112.71	83.96
25	300.57	211.29	140.45	104.36
30	359.39	252.96	168.15	124.81
35	419.22	294.69	195.81	144.03

Appendix 9

Comparison of pseudo-first-order and pseudo-second-order models parameters and calculated $q_{e(cal)}$ and experimental $q_{e(exp)}$ values for different initial fluoride concentrations.

Pseudo-first order model				
C_0 (mg/L)	$q_{e(exp)}$ (mg/g)	K_1 (min ⁻¹)	$q_{e(cal)}$ (mg/g)	R^2
3.5	0.0835	0.0832	0.0109	0.9
5	0.1188	0.0704	0.0223	0.99
7.5	0.1788	0.0641	0.0257	0.98
10	0.2430	0.0505	0.0587	0.91
Pseudo-second order model				
C_0 (mg/L)	q_e (exp)mg/g	K_2 (g/mg.min ⁻¹)	q_2 (mg/g)	R^2
3.5	0.0842	45.2833	0.1188	1
5	0.1206	16.9434	0.1188	1
7.5	0.1809	5.5945	0.1788	1
10	0.2495	4.0750	0.2430	0.99

Appendix 10

Osei Juliet, Gawu Simon KY, Schafer Andrea I, Atipoka Faustina and Momade

F WY.: “ terite characteristics ”.

Journal of Chemical Technology and Biotechnology (2015) DOI 10. 1002.

Appendix 11

U : “An Investigation of use of Laterite-Alumina

Composite for Fluoride Removal in

F C W C ”

KNUST

